FUNCTIONAL ANALYSIS OF INTERACTIONS OF ROTAVIRUS NSP4 WITH CAVEOLIN-1, CYCLOPHILIN A, CYCLOPHILIN 40, HEAT SHOCK PROTEIN 56, AND CHOLESTEROL

A Dissertation

by

KRYSTLE ANN YAKSHE

Submitted to the Office of Graduate and Professional Studies of
Texas A&M University
in partial fulfillment of the requirements for the degree of

DOCTOR OF PHILOSOPHY

Chair of Committee, Judith M. Ball
Committee Members, Julian Leibowitz
Susan L. Payne
Friedhelm Schroeder
Head of Department, Roger Smith

December 2015

Major Subject: Veterinary Microbiology

ABSTRACT

The rotavirus enterotoxin, NSP4, is responsible for early secretory diarrhea associated with rotavirus infection and is critical for RV replication and morphogenesis. NSP4 interacts directly with caveolin-1 and cholesterol and traffics from the endoplasmic reticulum to the plasma membrane via an unconventional transport pathway for release prior to virus-induced lysis. In this study we demonstrate that NSP4 interacts with the immunophilins, cyclophilin A, cyclophilin 40, and HSP56 using co-immunoprecipitation and FRET analysis. We examined the roles of caveolin-1 and the immunophilins in NSP4 transport to the plasma membrane using silencing RNA, immunofluorescence analysis, and surface biotinylation. Cholesterol reduction was accomplished by statin inhibition of cholesterol synthesis. We found that knockdown of these cellular proteins altered the intracellular distribution of NSP4, but did not prevent NSP4 from trafficking to the PM. Cholesterol inhibition decreased the amount of NSP4 that reached the PM, indicating a role of cholesterol in NSP4 transport.

ACKNOWLEDGEMENTS

Many people are responsible for the success of this project. I could not have done any of this work without the mentorship of Dr. Judy Ball. She has been an invaluable resource in preparing my mind for research and pushing me to never give up. Dr. Becky Parr took me under her wing and taught me almost everything I know about molecular biology and has always been there in my times of need. Dr. Avery McIntosh and members of the Schroeder laboratory were instrumental in helping me with all of the imaging and providing me with lots of laughter. Dr. Megan Schroeder helped me emotionally and always supported me through the hard times. I could not have stayed the course without her.

There are many people in the wonderful department of Veterinary Pathobiology that should be acknowledged for helping me get out of bed and come to the lab every day despite the many research struggles. I also could not have done this without the people at Gold's Gym, who were always there when I needed to get out my frustrations and held me up in times of need. I have to thank my entire family and my godparents for never giving up hope and having continued patience year after year. The undergraduates that rotated through n the lab were always a welcome distraction, and they helped me continue driving forward despite the extra load of work that came with them.

Finally, my husband Zach Franklin has stuck with me through good times and bad. He was an attentive and thoughtful colleague and friend when I needed him and turned

into a loving and caring companion. I could not have done any of this without the incredible support from everyone mentioned. Thank you.

NOMENCLATURE

3AT	3-Amino-1,2,4-triazole
5FOA	5-fluorouracil
APS	ammonium persulfate
CaMKK-β	calcium dependent calmodulin kinase kinase-β
Cav-1	caveolin-1
ConA	Concanavalin A
CPE	cytopathic effect
CsA	cyclosporin A
CSM	complete synthetic media
Cy2	cyanine
Cy3	indocarbocyanine
Cy5	indodicarbocyanine
CyP40	cyclophilin 40
CyPA	cyclophilin A
DMEM	Dulbecco's modified Eagle's medium
DLP	double-layered particle
ER	endoplasmic reticulum
ERGIC-53	endoplasmic reticulum-Golgi intermediate complex 53
FBS	fetal bovine serum
FGF-2	fibroblast growth factor 2

FRET	Förster resonance energy transfer
G	glycoprotein
GAPDH	glyceraldehyde 3-phosphate dehydrogenase
h	hour(s)
HCV	Hepatitis C Virus
his	histidine
HIV	Human Immunodeficiency Virus
hpi	hours post infection
HPLC	high performance liquid chromatography
HPV	Human Papilloma Virus
HRP	horseradish peroxidase
HSP56	heat shock protein 56
IP	intraperitoneally or immunoprecipitation
LB	Luria-Burtani
leu	leucine
LSCM	laser scanning confocal microscope
LTR	long terminal repeat
NFDM	non-fat dry milk
MDCK	Madin-Darby canine kidney
MEM	minimum essential medium
MeOH	methanol
MOC	Mander’s overlap coefficient

MOI	multiplicity of infection
mTOR	mechanistic target of rapamycin
MWCO	molecular weight cutoff
NSP4	non-structural protein 4
QMA	quaternary methylamine anion
QS	quantity sufficient
P	protease-sensitive protein
PAGE	polyacrylamide gel elctrophoresis
PB	Pacific Blue™
PBS	phosphate buffered saline
PDI	protein disulfide isomerase
pfu	plaque-forming units
PM	plasma membrane
PMSF	phenylmethanesulfonyl fluoride
PPIase	peptidyl prolyl isomerase
RV	rotavirus
SDS-PAGE	sodium dodecyl sulfate polyacrylamide gel electrophoresis
Sf9	*Spodoptera frugiperda* 9
shRNA	short hairpin RNA
siNT	non-targeting silencing RNA
siRNA	silencing RNA
trp	tryptophan

TLP	triple-layered particle
UPR	unfolded protein response
VSV	Vesicular Stomatitis Virus
Y2H	yeast two-hybrid

TABLE OF CONTENTS

Page

Page

Page

Page

LIST OF FIGURES

FIGURE Page

LIST OF TABLES

1. INTRODUCTION: AN OVERVIEW OF ROTAVIRUS, NSP4, CAVEOLIN-1, CYCLOPHILIN A, CYCLOPHILIN 40, HEAT SHOCK PROTEIN 56 AND UNCONVENTIONAL PROTEIN TRANSPORT

1.1 Rotavirus

Enteric pathogens remain one of the most deadly, and therefore one of the most important groups of pathogens in the world. Diarrheal diseases caused by enteric pathogens are responsible for approximately 2 million deaths annually worldwide (Boschi Pinto, 2009), with 1.3 million deaths in children under the age of 5 (Black et al., 2010). Viruses are the most common causal agents of diarrheal disease (Estes, 2013), with rotaviruses (RV) as the most dangerous, responsible for ~450,000 deaths annually (Parashar et al., 2009). Through the use of the RV vaccines, Rotarix® and RotaTeq®, infant deaths due to dehydration and associated symptoms of RV infection have been significantly decreased in the western world despite possible problems associated with the vaccines themselves, such as limited protective ability against new viral strains and the possibility of intussusception. However, RV infection remains a tremendous problem in developing nations due to vaccine cost and availability (Hyser and Estes, 2009).

RV is spread through the fecal-oral route, usually in water, person to person, and by improperly heated food; therefore, countries with little or no water sanitation have the highest prevalence of infant death due to RV infection. Although RV infects much of the population, generally children under the age of 5 are most symptomatic. The high

rate of death in young children is due to the combination of secretory and malabsorptive diarrhea, which is caused primarily by the RV enterotoxin, nonstructural protein 4 (NSP4) and destruction of absorptive enterocytes, respectively (Ball et al., 2005). Other mechanisms of diarrhea have been noted, including activation of the enteric nervous system, villus ischemia, and mild inflammation (Lundgren et al., 2000).

Although children are most commonly affected by RV infection, it is also a problem in the elderly and immunocompromised (Liakopoulou et al., 2005; Ziring, 2005). RV type B has been connected to large outbreaks in China and other parts of Asia (Fang et al., 1989; Kelkar and Zade, 2004). In the US and Europe, RV outbreaks have occurred in long-term care facilities, such as nursing homes and extended stay hospitals (Cubitt and Holzel, 1980; Halvorsrud and Orstavik, 1980; Marrie et al., 1982). Nevertheless, most adult infections are asymptomatic (Estes, 2013) and the number of adult deaths due to RV symptoms remains low.

1.2 Vaccines

The two RV vaccines currently in use in the US are not as protective in underdeveloped countries, due to a variety of circulating strains. RV is classified into 7 distinct groups (A-G), but only A, B, and C are important for human infection. Group A RVs are grouped into serotypes by the circulating P and G types, which denote the presence of antibodies against VP4 (protease-sensitive protein, P) and VP7 (glycoprotein, G). To date, there are 27 G types and 35 P types. The most important types for humans worldwide are G1P[8], G2P[4], G3P[8], G4P[8] and G9P[8] (Santos and Hoshino, 2005). Currently, type G1P[8] is the most common Group A RV

circulating in the United States (Jain et al., 2014). However, in India and China, types G2P[6], G3P[6], G12P[8], G12P[6] and G9P[6] are more common, and are not protected by Rotarix or RotaTeq.

Before the vaccine program was introduced in the US, RV infection followed a seasonal pattern and was at its peak in winter and spring (Patel et al., 2013). It infected millions of children per year and was responsible for nearly 1 million deaths per year. After vaccination was introduced in the United States, disease incidence went down considerably and RV is now responsible for only 20-30 deaths annually in the US as opposed to about 200. In addition, the seasonality of the virus became less noticeable after introduction of the vaccine in the US (Staat et al., 2010). Although the two RV vaccines on the market are specific for the strains circulating in the Americas, they are still somewhat effective in Asian and African developing countries, although not as protective as they are in the US.

Currently, there are several vaccines in use in various countries around the world. Many countries in Central and South America and several countries in Western Europe vaccinate children with Rotarix and RotaTeq and achieve efficacies similar to that seen in the US (Estes, 2013). In China, a vaccine derived from a lamb RV strain, LLV (G10P[12]) is effective in up to 81% of children under the age of 12 months (He et al., 2013). The recent Rotashield vaccine (RV4) is being reformulated and tested in many African countries, and the new formulation is providing more protection in phase III trials than previously noted (Estes, 2013). Finally, in India, there is a strain 116E (G9P8[11]) that is undergoing testing and is proving to be highly immunogenic

(Bhandari et al.). There are several other candidates for vaccines in these countries, so the incidence of RV infections is declining worldwide, but still has proven to be a major problem in young children and the elderly.

1.3 Structure

RV is a non-enveloped, icosahedral, double stranded RNA virus, with a genome consisting of 11 double stranded RNA (dsRNA) segments. The virion consists of three concentrically arranged protein layers surrounding 11 dsRNA segments and several viral proteins. The outer layer is composed of 260 trimers of VP7, with 60 protruding spikes consisting of structurally asymmetric dimers of VP4. The middle layer is composed of 260 trimers of VP6, and the innermost layer consists of 60 dimers of VP2 (**Figure 1.1**). The proteins located within the inner VP2 core include a RNA-dependent RNA polymerase (VP1), a protein required for replicase activity (VP2), and a guanylyltransferase and methyltransferase (VP3). Rotavirus also encodes an eIF-4G interacting protein (NSP3) involved in the preferential translation of RV mRNA transcripts in the cell, a helicase (NSP2), a phosphoprotein with kinase activity (NSP5), a RNA binding protein (NSP1), and a NSP5 binding protein (NSP6) (Estes, 2013; Jayaram et al., 2004).

To gain entry into the cell, RV VP4 binds to one or more strain-dependent receptors and coreceptors, including sialic acid containing molecules, such as the GM1 ganglioside, several integrin types, histo-blood group antigens, HSP70, and the more recently discovered JAM-A (Huang et al., 2012; Isa et al., 2006; Isa et al., 2004; Torres-

Flores et al., 2015). Although it is not an absolute requirement, the VP4 spikes of most RV strains undergo trypsin cleavage to produce VP5* and VP8*, which enhances

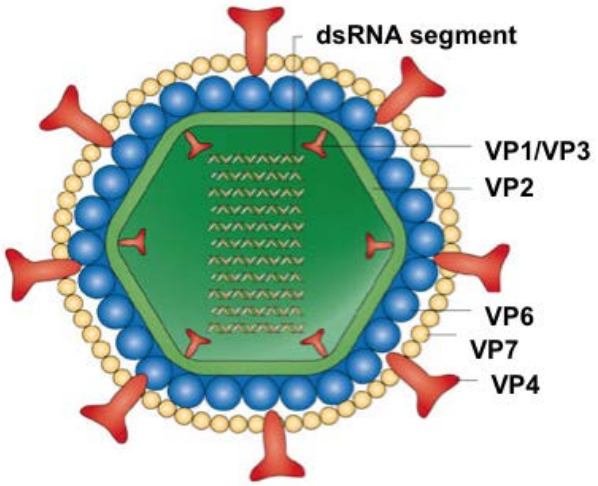

Figure 1.1 Depiction of rotavirus triple layered particle (Estes, 2013).

infectivity (Arias et al., 1996; Estes et al., 1981), stabilizes the virion and aids in receptor recognition (Crawford et al., 2006; Jayaram et al., 2004). RV entry currently is thought to be a multistep process involving sequential binding of receptors and coreceptors, resulting in conformational changes in the virion that allow cellular penetration via an unknown mechanism (Estes, 2013). There is evidence that receptor-mediated endocytosis may be involved (Arias et al., 2015; Gutierrez et al., 2010; Silva-Ayala et al., 2013), but other evidence points to direct entry (Estes, 2013). Once the virion enters the low Ca^{2+} environment of the cytosol, the calcium-dependent, outer VP7 layer is dismantled with the VP4 spike (Ruiz et al., 2000), and the double layered particles (DLPs) undergo a conformational shift to align and open 12 channels, allowing for entry

of nucleotides and hydrolysable ATP into the inner VP2 core (Jayaram et al., 2004; Spencer and Arias, 1981). Transcription of viral RNA is performed exclusively through the use of viral enzymes housed within the inner core of the intact DLP (Estes, 2013). The resulting 5' capped, but not polyadenylated viral mRNA exits through the channels into the surrounding cytoplasm (Patton et al., 2004). The ability of RV to contain the dsRNA inside of the core is an effective way to avoid cellular detection of dsRNA and induction of IFN.

The capped viral mRNAs are transported to ribosomes and translated by host cellular machinery (Jayaram et al., 2004). NSP3 serves to increase translation of viral mRNA by binding to the 3' end of the viral mRNA (Poncet et al., 1993), and then outcompeting binding of cellular poly-A binding protein to eIF4G (Piron et al., 1998). This not only preferentially increases viral mRNA translation, but also inhibits cellular mRNA translation (Padilla-Noriega et al., 2002). NSP3 may also be involved in recruitment of viral mRNAs into the electron-dense viroplasm located near the ER for secondary replication (Jayaram et al., 2004; Suguna and Rao, 2010). Most of the proteins are translated by free ribosomes with the exception of NSP4 and VP7, which are synthesized by ER bound ribosomes and co-translationally inserted into the ER membrane for late viral assembly (Estes, 2013).

During RV infection, electron-dense viroplasms ("virus factories") form adjacent to the ER and contain RV proteins VP2, NSP2, NSP5, and NSP6, and VP6 (Gonzalez et al., 2000; Petrie et al., 1984). The genomic dsRNA segments are replicated in the viroplasm and associate with some of the viral proteins before they are loaded into the

DLPs (Gallegos and Patton, 1989). There is an interaction between VP6 in the outer coat of the DLPs and the cytoplasmic C-terminus of NSP4 that facilitates the budding of the DLP into the lumen of the ER (Maass and Atkinson, 1990; Taylor et al., 1996). As the DLP enters the ER it acquires a transient envelope that is lost before the addition of the outer protein layer (Petrie et al., 1984; Tian et al., 1996). The outer layer consisting of VP7 is assembled within the Ca^{2+} rich ER, and the intact triple layered particles leave the ER and travel to plasma membrane (PM) lipid microdomains for release (Cuadras and Greenberg, 2003; Huang et al., 2004; Isa et al., 2004). It is controversial whether the RV spike protein, VP4, associates with the triple layered particles (TLPs) in the ER or is assembled at the PM. There is evidence that VP4 associates with lipid microdomains on the PM independently of TLPs (Delmas et al., 2004). It also has been shown that VP4 co-localizes with β-tubulin and is associated with peroxisomes via a peroxisomal targeting sequence (Mohan et al., 2002). Peroxisome association and accumulation of VP4 at the PM could be a mechanism for recruitment of the TLP to the PM for release, but the route of how the TLP gets from the ER to the PM remains unclear.

1.4 NSP4

RV NSP4, is a viral RNA synthesis modulator, an intracellular viral receptor, is integral to viral particle maturation, and plays an important role in pathogenesis. NSP4 is an 175 amino acid protein with a single transmembrane domain (residues 24-44) that overlaps the second hydrophobic domain (H2), 3 N-terminal hydrophobic domains, 2 N-terminal, N-linked glycosylation sites at residues 8 and 18, and several C-terminal

protein binding domains (Ball et al., 2005; Bergmann et al., 1989). The long cytoplasmic tail contains a coiled-coil amphipathic alpha helix (residues 93-137) (Bowman et al., 2000), which overlaps several protein binding sites, two of the four antigenic sites (Mori et al., 2002), the enterotoxic domain, and the oligomerization domain (**Figure 1.2**) (Ball et al., 1996; Bowman et al., 2000; Parr et al., 2006). NSP4 resides in the ER membrane and has been localized to several additional locations in the cell, as well as extracellularly (Berkova et al., 2006; Xu et al., 2000; Zhang et al., 2000). The pathways by which NSP4 traffics to these alternate locations and eventually out of the cell are largely unknown. We propose to elucidate these mechanism(s) as this knowledge will contribute to the development of therapeutics and future vaccine strategies for RV infection.

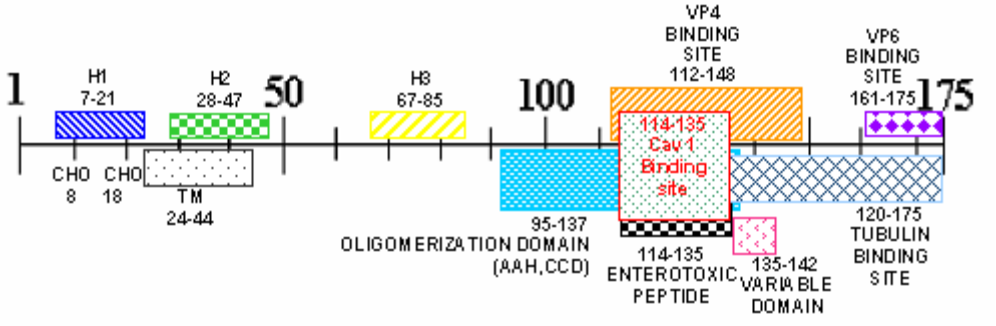

Figure 1.2. NSP4 structure and binding sites (Parr et al., 2006). H1-H3 represent the hydrophobic domains; CHO represents the glycosylation sites; TM represents the ER transmembrane domain; AAH is the amphipathic alpha-helix; CCD is the coiled-coil domain

The C-terminus of NSP4 functions as a receptor to bind VP6 and recruit DLPs into the ER (Taylor et al., 1992; Taylor et al., 1996), but its role in viral particle maturation does not end there. Silencing of NSP4 using targeted silencing RNA (siRNA) leads to a 75-80% reduction in the amount of infectious progeny released from cells, an accumulation of empty viral particles in the viroplasm and cytoplasm, an intracellular redistribution of several viral proteins, and an increase in viral RNA transcription (Cuadras et al., 2006; Lopez et al., 2005; Silvestri et al., 2005). When NSP4 is silenced, NSP2, NSP5, VP2, and VP6 are dispersed throughout the cytoplasm, rather than residing in the viroplasm (Lopez et al., 2005). Silencing of NSP4 also causes a 64% reduction of VP4 accumulation at PM lipid rafts (Cuadras et al., 2006). In addition, NSP4 is thought to play a role in the removal of the transient envelope upon DLP entry into the ER (Tian et al., 1996). Taken together, NSP4 is essential for RV particle maturation.

In addition to acting as a regulator of viral particle maturation and trafficking, NSP4 functions as an enterotoxin, and is thought to be a major contributing factor to the early secretory diarrhea during RV infection (Ball et al., 1996). The toxin alone, or a peptide (residues 114-135) corresponding to part of the enterotoxic domain, induces diarrhea in rodent pups, induces an increase in intracellular calcium (Dong et al., 1997; Tian, 1995), and causes chloride secretion across unstripped mouse intestinal mucosa without causing morphological change (Ball et al., 1996).

RV NSP4 interacts with a number of host proteins, including calnexin, caveolin-1, and tubulin, and has been shown to influence the concentration and intracellular distribution of several more, including cofilin, BiP, endoplasmin, β-coatamer protein,

and ERGIC53 (Berkova et al., 2007; Mirazimi et al., 1998; Parr et al., 2006; Xu et al., 1998, 2000). Each of these molecules plays a role in some type of cellular transport mechanism, whether involved in protein folding, vesicular transport, or cytoskeletal rearrangement. By interacting with, or affecting levels or cellular distribution of these proteins, NSP4 is able to traffic through the cell to specific loci and to the PM via an unconventional transport route.

Full length NSP4 remains endoglycosidase H sensitive and Brefeldin A resistant, indicating that it does not travel through the Golgi to undergo oligosaccharide processing (Bergmann et al., 1989; Ericson et al., 1983; Taylor et al., 1992). NSP4 production and glycosylation is not affected in RV-infected HT29 cells treated with Nocodozole or Cytochalasin D, which disrupt microtubule and actin filament polymerization, respectively; however, secretion of the $NSP4_{112\text{-}175}$ cleavage product is abolished upon addition of these agents to infected cells (Zhang et al., 2000). Also, NSP4 expression in Cos-7 cells blocks classical transport of the vesicular stomatitis virus glycoprotein (VSV-G) from the ER to the Golgi and redistributes endoplasmic reticulum-Golgi intermediate complex protein 53 (ERGIC-53) to dispersed cytoplasmic structures, suggesting that NSP4 has an inhibitory effect on transport from the ERGIC to the Golgi (Xu et al., 2000). NSP4 also co-localizes with ERGIC-53 in Cos-7 cells, but the co-localization was dependent on the C-terminal tubulin-binding domain of NSP4 (Xu et al., 2000). Another study shows NSP4 traffics via a Golgi-independent pathway and co-localizes with autophagasomal marker LC3 in HEK 293 cells (Berkova et al., 2007; Chwetzoff and Trugnan, 2006; Cuadras et al., 2006; Jourdan et al., 1997).

NSP4 localizes to the PM, and has been isolated with purified-caveolae fractions using a novel non-detergent PM isolation method (Storey et al., 2007). NSP4 also traffics to the PM with cell type-dependent transport kinetics (Gibbons et al., 2011). Together, these findings strongly suggest that NSP4 is being transported via a Golgi-independent pathway, but it remains to be determined if NSP4 follows a vesicular or soluble route from the ER to the PM. We propose that transport is not only cell-type dependent, but that NSP4 is likely using both vesicular and soluble routes to reach the PM.

1.5 Unconventional Protein Transport

Conventional protein transport of secreted proteins begins by translation and translocation of the protein into the rough ER. The proteins often contain a signal sequence that directs them to their final destination. Once folded properly, the proteins traffic from the ER, through the ER-Golgi intermediate compartment (ERGIC) to the tiered Golgi apparatus. The different compartments of the Golgi have specialized functions that process oligosaccharides on the proteins and direct them to their final destination.

In recent years, several proteins have been shown to traffic via unconventional protein trafficking mechanisms, either bypassing the Golgi on the way from the ER to the PM, reaching the PM in a COPII vesicle-independent manner from the ER, or bypassing the ER completely due to the lack of an ER signal peptide or other unconventional pathways (Nickel and Rabouille, 2009). Proteins that follow unconventional trafficking have several common characteristics, such as

endoglycosidase H sensitivity, Brefeldin A insensitivity, lack of a signal peptide, and rapid transport to the PM (Nickel and Rabouille, 2009). Nickel proposed 4 models as to how proteins lacking signal peptides may reach the PM and the extracellular space by an unconventional route: 1) Direct translocation across the PM from the cytosol to the extracellular space 2) lysosome-dependent secretion 3) secretion via multivesicular body (MVB)-derived exosomes, and 4) secretion via membrane blebbing/microvesicular secretion (Nickel and Rabouille, 2009). These mechanisms export proteins that function strictly extracellularly, such as FGF-2 and galectin-1, as well as those that have both intracellular and extracellular functions, including interleukin-1β (IL-1β) and caspase-1. It is likely that NSP4 follows one or more of Nickel's proposed mechanisms or a new mechanism to reach and traverse the PM.

In addition to trafficking via unconventional mechanism(s), translocation of these proteins across the PM is not well defined. Fibroblast growth factor 2 (FGF-2) has been studied by Walter Nickel's group, and is one of the best-characterized proteins that follows an unconventional trafficking pathway. FGF-2 is a soluble protein that contains an amphipathic α-helix and bypasses the Golgi for transport directly from the ER to the PM. FGF-2 likely is first recruited to the PM via an interaction with the phosphoinositide phosphatidylinositol-4,5-bisphosphate (PtdIns(4,5)P2), but it is unclear whether it is transported via a membrane transporter, by direct insertion into the PM, or by formation of a pore (Nickel and Seedorf, 2008). NSP4 contains an amphipathic α-helix, as well as three hydrophobic domains that have the potential of inserting directly into membranes, which may play a part in the translocation of NSP4 across the PM.

NSP4 deletion constructs and mutants have been used to show that the transmembrane domain and a cluster of lysine residues near the amphipathic alpha helix are responsible for formation of a pore in the ER membrane called a viroporin (Hyser et al., 2010). A model has been proposed for the direct membrane insertion, but it is unknown if it plays a role at the PM.

1.6 Immunophilins and Caveolin-1

A previously identified protein/cholesterol complex termed the Caveolin Chaperone Complex has been described and was thought to be involved in transport of de novo synthesized cholesterol from the ER to the PM (Uittenbogaard et al., 2002; Uittenbogaard and Smart, 2000; Uittenbogaard et al., 1998). Recently, the studies describing this complex have been retracted (Office of the Secretary, 2012), but the proteins have been shown to interact in other ways intracellularly. The proposed complex consisted of the chaperone proteins cyclophilin A (CyPA), cyclophilin 40 (CyP40), heat shock protein 56 (HSP56, FKBP4), caveolin-1 (Cav-1), and cholesterol (Uittenbogaard et al., 1998). Direct interaction of NSP4 with Cav-1, raft-like model membranes, and cholesterol have been shown in our laboratory (Huang et al., 2004; Parr et al., 2006; Schroeder, 2009). In addition, NSP4 is associated with the CyPA and CyP40 as evidenced by co-immunoprecipitation and FRET experiments (Yakshe, et al. in preparation). Mutagenesis and yeast two-hybrid (Y2H) protein interaction studies mapped the Cav-1 binding site to NSP4 residues 112-140, and later to 3 hydrophobic residues (Huang et al., 2004; Parr et al., 2006). These data indicate that the NSP4-Cav-1 interaction is due to three hydrophobic residues, leaving the charged face of the

amphipathic helix free to interact with the negative phosphates of the membrane. Despite this evidence, it remains unknown if the association of these protein components influences intracellular transport of NSP4.

Cav-1 is a scaffolding protein that is expressed in the Golgi or PM of cells, and assists in formation of caveolae on the cell surface and contributes to cell signaling. CyPA and CyP40 are both chaperone proteins with peptidyl prolyl isomerase (PPIase) activity and are commonly complexed with viral proteins (Fischer et al., 2010). HSP56 is a heat shock protein that is known to complex with several chaperone protein and also contains PPIase activity (Davies and Sanchez, 2005). Both CyP40 and HSP56 are known to be HSP90-binding immunophilins and are complexed with a nuclear steroid receptor complex (Ratajczak et al., 2009). These immunophilins also have been described as binding dynein and assisting with retrograde transport of receptor complexes (Galigniana et al., 2002; Galigniana et al., 2001). In addition, CyPA binds dynein, but has not been found in association with CyP40 or HSP56 in this capacity.

1.7 Autophagy

Autophagy is a degradation pathway used to dispose of and recycle intracellular components. A common initiator of autophagy is ER stress and this process can be inhibited by mechanistic target of rapamycin (mTOR). Autophagy starts when a complex of proteins, Atg101/FIP200/ULK1/Atg13, that combine and inhibit mTOR suppression of autophagy (Crawford et al., 2012; Mizushima et al., 2011). This complex initiates membrane formation and another complex consisting of Atg5/Atg12/Atg16 combine and act similarly to an E3 ubiquitin ligase, which contributes to removing and

recycling the amino acids of unfolded or incorrectly folded proteins. The Atg5/Atg12/Atg16 complex regulates ethanolamine addition to LC3 resulting in maturation to LC3-II. LC3-II, in turn, positively regulates autophagy vesicle double membrane formation. Once the autophagy vesicles are mature, they are transported to lysosomes, where they fuse and the cellular contents are degraded (Mizushima et al., 2011).

It is known that NPS4 traffics to multiple intracellular sites and co-localizes with autophagy protein, LC3 (Berkova et al., 2006). Recently it has been shown that NSP4 can initiate autophagy, and that autophagy initiation is required for viral maturation (Crawford et al., 2012). Autophagy is initiated after NSP4 forms a viroporin in the ER membrane, releasing calcium into the cytoplasm. The increased cytoplasmic calcium activates a calcium dependent calmodulin kinase kinase-β (CaMKK-β), which initiates autophagy. Interestingly, RV NSP4 prevents the fusion of the autophagosome to lysosomes (autophagy maturation), which may play a role in viral maturation.

This work uses siRNA directed toward the host-cell immunophilins and Cav-1 proteins to dissect the functional roles of these proteins in the transport of RV NSP4 from the ER to the PM. We reveal that although NSP4 does associate intracellularly with each of the host proteins, they are not responsible for the transport of NSP4 from the ER to the PM. Hence, NSP4 is using another means to traffic to the PM, likely a vesicular pathway, rather than a soluble one.

2. NSP4 INTERACTIONS WITH AND FUNCTIONAL STUDIES OF CAVEOLIN-1, CYCLOPHILIN A, CYCLOPHILIN 40, HEAT SHOCK PROTEIN 56, AND CHOLESTEROL

2.1 Introduction

Rotavirus (RV) infects infants and young children worldwide and is responsible for up to 450,000 deaths annually (Tate et al., 2012). The current live vaccines, Rotateq® and Rotarix®, are reported to provide significant protection against infant deaths due to dehydration and associated symptoms of RV infection, but do not prevent all symptoms or spread of the virus. They offer limited protection against emerging RV strains, and may be associated with intussusception (Angel et al., 2007). The high mortality rate in young, unvaccinated children results from a combination of secretory and malabsorptive diarrhea due to the activity of the RV enterotoxin, non-structural protein 4 (NSP4), and destruction of absorptive enterocytes, respectively (Ball et al., 2005).

RV is composed of 3 concentric capsids that enclose 11 double-stranded, RNA genome segments that encode 12 proteins, 6 structural and 6 non-structural. Viral transcription occurs within the inner capsid of the double-layered particle (DLP). Most of the viral proteins travel to a unique structure near the endoplasmic reticulum (ER), the viroplasm, where replication and initial assembly occur (Fabbretti et al., 1999). The mRNAs that encode NSP4 and VP7 are synthesized by ER-bound ribosomes and co-translationally are inserted into the ER membrane (Berkova et al., 2007). The short, hydrophobic N-terminus of NSP4 initially resides in the ER lumen, followed by a

transmembrane domain and a C-terminus that extends into the cytoplasm (Bergmann et al., 1989).

NSP4 is a multifunctional glycoprotein that localizes to several areas in the cell. Some of its functions include RV particle maturation, viral transcription, and induction of Ca^{2+}-mediated signaling events resulting in Cl^- secretion and diarrhea. NSP4 has been identified in the cytosol, ER, caveolae (Storey et al., 2007), and LC3 positive autophagosomes (Berkova et al., 2006), and directly binds host-cell molecules including tubulin (Xu et al., 2000), calnexin (Mirazimi et al., 1998), caveolin-1 (Cav-1) (Parr et al., 2006), laminin-ß3, fibronectin (Boshuizen et al., 2004), and cholesterol (Schroeder, 2009). Native NSP4 is sensitive to endoglycosidase H, resistant to brefeldin A, fails to co-localize with Golgi proteins (Prudovsky et al., 2008; Zhang et al., 2000), and lacks a signal peptide (Mirazimi et al., 1998). Thus, NSP4 traffics to the plasma membrane (PM) via an unconventional transport pathway.

Association of NSP4 and the autophagosomal marker, LC3, depends on the presence of a hydrophobic NSP4 membrane-interacting domain (Hyser et al., 2010). Autophagic vesicles can fuse with several cellular components of the endocytic pathway, including multi-vesicular bodies and lysosome-associated bodies, both of which are associated with unconventional transport (Chua et al., 2011; Nickel, 2010). The co-localization of NSP4 with autophagosomes and the punctate intracellular staining of NSP4 (Berkova et al., 2006) also support an unconventional vesicular pathway. Gibbons, et al. has described differential transport kinetics of NSP4 in two cell lines, HT29.f8 and MDCK,

and showed NSP4 can use both soluble and vesicular pathways to travel from the ER to the PM (Gibbons et al., 2011).

Cyclophilins are a large family of immunophilins that possess peptidyl prolyl isomerase activity and accelerate protein folding by catalyzing the initial folding steps in proline-containing proteins (Fischer et al., 1989). Cyclophilin A (CyPA) is the major cytosolic cyclophilin while cyclophilin 40 (CyP40) is expressed primarily in the mitochondria (Fruman et al., 1994). Both of these cyclophilins bind tightly to cyclosporin A (CsA), an immunosuppressant drug (Fischer et al., 2010). The cyclophilin family associates with viruses. For example, CyPA assists in viral uncoating in HIV infection, regulates replication of VSV and HCV, and interacts with influenza M1 protein, while cyclophilin B plays a role in oncogenic HPV infection (Fischer et al., 2010). Heat shock protein 56 (HSP56, also known as FKPB52) is an immunophilin that contains rotamase activity and binds ATP and GTP (Ratajczak et al., 2009). CyP40 is important for initiation of starvation-induced autophagy as part of the mitochondrial permeability transition pore (Carreira et al., 2010). Together, these proteins are active in protein folding and protein transport, thus contributing to many cellular processes (Walsh et al., 1992).

The focus of our laboratory has been dissecting the intracellular transport of NSP4 by examining NSP4-host cell protein interactions. Our previous studies show a direct interaction of NSP4 with Cav-1 and cholesterol (Parr et al., 2006; Schroeder, 2009), but the function of these interactions was not explored. In this study, we examined the interactions of NSP4 with the immunophilins, Cav-1, and cholesterol in both MA104

and the cloned human intestinal, HT29.f8 (Mitchell and Ball, 2004), cell lines using a variety of imaging and biochemical techniques. To explore the function(s) of the interactions, siRNA or small-molecule inhibitors were employed. The affect(s) on both NSP4 and the host cell were monitored post silencing. NSP4 transport to the PM was altered only by inhibition of HMG-CoA reductase, indicating that cholesterol is a key player in NSP4 transport from the ER to the PM.

2.2 Materials and Methods

2.2.1 Cells and Viruses

African green monkey kidney cells MA104 (ATCC, Manassas, VA), a cloned human intestinal HT29.f8 cells from parental HT29 cells (Mitchell and Ball, 2004), and Madin-Darby canine kidney (MDCK) cells (ATCC) were cultured in Dulbecco's modified Eagle's media (DMEM; CellGro, Manassas, VA) supplemented with 10% fetal bovine serum (FBS; Caisson Labs, North Logan, UT), 0.1 mM non-essential amino acids (NEAA; Gibco, Grand Island, NY), 1 mM sodium pyruvate (Gibco), and 2 mM L-glutamine (Lonza, Basel, Switzerland) at 37°C with 5% CO_2 in a humidified environment. Penicillin-streptomycin was not used in the culture mixture to prevent perturbing cell-signaling pathways. RV SA11 clone 4F (SA11.4F; gift from Mary Estes, Baylor College of Medicine, Houston, TX) was expanded in MA104 cells (Yakshe, 2015) and stored at -80°C.

2.2.2 Infection

Cells were serum starved by incubation in serum-free DMEM for 14 hours before infection, except in the case of siRNA-treated cells. Cells were infected with SA11.4f at

a multiplicity of infection (MOI) of 2 for imaging, and a MOI of 5 for surface biotinylation studies. In brief, virus was thawed on ice and sonicated using a cuphorn attachment with ice for 5 min using a Misonix sonicator 3000 at 45W (Misonix, Inc., Farmingdale, NY). Virus then was activated in serum-free DMEM with 1μg/ml trypsin (Worthington Biochemical, Lakewood, NJ) at 37°C for 30 min. The activated virus was added to cells diluted in serum-free DMEM supplemented with 1μg/ml trypsin at the specified MOI and rocked at 37°C with 5% CO_2 in a humidified environment for 1 h. The viral inoculum was removed, cells were washed with media to remove unbound virus, and serum-free DMEM was added for various times of infection as indicated in the results section.

2.2.3 Antibodies

Primary antibodies to NSP4-specific peptides were generated in mice, rabbits and rats as previously described (Storey et al., 2007) and included mouse anti-$NSP4_{150-175}$, rabbit anti-$NSP4_{150-175}$, rabbit anti-$NSP4_{112-140}$, and rat anti-$NSP4_{150-175}$. Purchased primary antibodies included rabbit anti-Cav-1 (ab18199, Abcam, Cambridge, MA), rabbit anti-CyPA (ab42408, Abcam), mouse anti-CyPA (ZC001, Zymed, Calsbad, CA), rabbit anti-CyP40 (ab3562, Abcam), rabbit anti-HSP56 (ab97306, Abcam), mouse anti-sodium-potassium ATPase (ab96292, Abcam), rabbit anti-giantin (Covance, Emeryville, CA), mouse anti-protein disulfide isomerase (PDI; Stressgen, Ann Arbor, MI), mouse anti-glyceraldehyde-3-phosphate dehydrogenase (1A10A10, BioChain Institute, Newark, CA), and rabbit anti-lamin A (Poly6135, BioLegend, San Diego, CA). Purchased secondary antibodies included $F(ab')_2$ fragments of goat anti-rabbit IgG

(H+L) conjugated to indocarbocyanine (Cy3) (Jackson Immunoresearch, West Grove, PA), F(ab')$_2$ fragments of goat anti-rabbit IgG (H+L) conjugated to cyanine (Cy2) (Jackson Immunoresearch), F(ab')$_2$ fragments of goat anti-mouse IgG (H+L) conjugated to indodicarbocyanine (Cy5) (Jackson Immunoresearch), and goat anti-rabbit IgG-Pacific Blue™ (Invitrogen) for imaging; and goat anti-mouse IgG (H+L) conjugated to horse radish peroxidase (HRP) (Zymed) and goat anti-rabbit IgG (H+L)-HRP (Thermo Fisher) for Western blot.

2.2.4 Generation and Labeling of Anti-NSP4$_{150\text{-}175}$ F(ab)$_2$ Fragments

NSP4-specific peptide antibodies were affinity purified against the immunizing peptide before use in confocal microscopy, and F(ab)$_2$ fragments were generated for fluorescent resonance energy transfer (FRET) analyses to reduce the distances of the fluorophores from the target proteins. Rabbit anti-NSP4$_{150\text{-}175}$ was affinity purified on an NSP4$_{150\text{-}175}$ peptide column prepared with pre-activated cyanogen bromide Sepharose 4B beads by following the instructions of the manufacturer (Pharmacia Biotech, Piscataway, NJ) (Axen et al., 1967). The bound peptide-IgG was eluted by altering the elution buffer pH to 4 and then 2 while reading absorbance on a UV detector.

The ImmunoPure F(ab)$_2$ preparation kit (Pierce, Rockford, IL) was utilized, and the recommended protocol was followed to produce peptide-specific F(ab)$_2$ fragments (Wines and Easterbrook-Smith, 1991). Briefly, the peptide-specific IgG was added to the immobilized pepsin tube provided with the kit. The resin separator was placed inside the tube above the mixture and the tube was incubated with shaking at 37°C for 4 h. The resin was separated from the digested mixture by pressing the resin separator to the

bottom of the tube. The digested mixture was run on an immobilized Protein A column to remove Fc fragments and the $F(ab)_2$-containing mixture was collected for dialysis. The $F(ab)_2$ fragments were dialyzed against 3 changes of 50 mM ammonium bicarbonate (2 L) in a 50,000 MW cutoff dialysis bag (Spectrum Laboratories, Rancho Dominguez, CA). The dialyzed $F(ab)_2$ was shell frozen in 1:1 ethanol:dry ice and lyophilized until dry. A small sample of the $F(ab)_2$ fragments was separated on an SDS-PAGE gel and stained with GelCode Blue (Thermo Fisher) to verify successful generation and purification of the fragments.

Cy3 or Cy5 monofunctional reactive dye was conjugated to the affinity-purified $NSP4_{150\text{-}175}$ $F(ab)_2$ to produce aliquots of Cy3 and Cy5 $NSP4_{150\text{-}175}$ $F(ab)_2$ for FRET exactly as described by the manufacturer (Amersham Bioscience, Piscataway, NJ). Briefly, 1.0 mg Cy3 or Cy5 dye was reconstituted in 500 µL of 0.2 M sodium bicarbonate. The lyophilized $F(ab)_2$ fragments were reconstituted by diluting 0.65 mg of $F(ab)_2$ in 350 µl of 1X PBS. An equal volume (350 µl) of reconstituted dye was added to the reconstituted $F(ab)_2$ fragments and incubated at room temperature for 20 min. The dye-conjugated $F(ab)_2$ fragments were dialyzed in an iCON™ concentrator with a 20 kD cutoff (Fisher Scientific) two times with 1X PBS. After concentration, the final volume (750 µl) was adjusted to 900 µl by adding 150 µl of 2 mg/ml BSA and incubating at room temperature for 20 min. The conjugated antibody was aliquoted and stored at -20°C.

2.2.5 Laser Scanning Confocal Fluorescent Microscopy (LSCM)

Cells were plated on #2 German borosilicate Labtek well coverslips (Nalge Nunc International, Naperville, IL). At various time points, the medium was removed, cells were washed with ice-cold PBS and fixed and permeabilized with ice-cold methanol:acetone (1:1, vol/vol) for 20 min at -20°C. The fixed and permeabilized cells were prepared for immunofluorescence using a modification of a previously described method (Storey et al., 2007). Briefly, fixed cells were blocked with 3% non-fat dry milk (NFDM; Carnation, Wilkes-Barre, PA) in PBS and incubated with primary antibodies (**Table 2.1**) diluted in 0.5% NFDM in PBS for 3 h at 27°C. After the cells were washed three times with PBS the secondary antibodies (**Table 2.2**) were diluted in 0.5% NFDM, and incubated for 1 h at room temperature in the dark. Primary and secondary antibody controls were included to exclude non-specific reactivity of the antibodies. Cells were washed as above in the dark and the fluorescent images were captured with a MRC-124MP BioRad LSCM system (BioRad) using a Zeiss inverted Axiovert microscope (Carl Zeiss, Inc., Thornwood, NY), a 63X Zeiss oil apochromat objective, and the 488-, 568- or 647-nm excitation lines of an argon/krypton ion laser source or the 405 nm line of a Ti:Sapphire diode laser. Fluorescence emission from the labeled cells cultured on coverslips was detected using 405-nm excitation with a bandpass emission filter for the Pacific Blue™ fluorophore (ex=410 nm, em=455 nm) (blue channel), 488 nm excitation with a HQ530/40 band-pass emission filter for Cy2 fluorophore (ex =492 nm, em=510 nm) (green channel) and 568 nm excitation with a HQ598/40 band-pass emission filter for Cy5 fluorophore (ex=650nm, em=670) (red channel). LaserSharp 3.0 (BioRad) and

Image J (public domain Java image-processing program inspired by NIH Image) were used to capture the pixilated photomultiplier tube (PMT) data, convert the image data to .tiff format, and adjust for contrast curves to construct the final images.

Table 2.1. Primary Antibodies Used in LSCM

Primary Antibody Target	Host Animal	Antibody Dilution	Comments
Caveolin-1	Rabbit	1:100	caveolae structural protein
Cyclophilin A	Rabbit	1:50	chaperone; cytoplasm localized peptidyl-prolyl isomerase
Cyclophilin 40	Rabbit	1:200	chaperone; mitochondrial localized peptidyl-prolyl isomerase
Heat Shock Protein 56	Rabbit	1:75	chaperone; heat shock protein
Golgin-97	Mouse	1:50	Trans-Golgi complex marker
Lamin A	Rabbit	1:100	Nuclear lamina protein; positive control
Protein Disulfide Isomerase	Mouse	1:50	Endoplasmic Reticulum marker
Sodium-Potassium ATPase	Mouse	1:50	Exofacial plasma membrane marker
Rotavirus NSP4	Rabbit	1:100	Peptide fragment; residues 112-140
Rotavirus NSP4	Rabbit	1:100	Peptide fragment; residues 150-175

Table 2.2 Secondary Antibodies Used in LSCM

Secondary Antibody Target	Host Animal	Antibody Dilution	Comments
Mouse IgG (H+L)	Goat	1:100	Cy5 conjugated
Rabbit IgG (H+L)	Goat	1:100	Cy5 conjugated
Rabbit IgG (H+L)	Goat	1:100	Cy3 conjugated
Rabbit IgG (H+L)	Goat	1:100	Cy2 conjugated
Rabbit IgG (H+L)	Goat	1:100	Pacific Blue™ conjugated

2.2.6 Co-localization

Cells were infected and treated as above, incubated with antibodies targeting the immunophilins and a secondary antibody labeled with Pacific Blue™ with Cy-5 labeled rabbit anti-$NSP4_{150\text{-}175}$ together. Images were collected on a Zeiss LSM 780 NLO

multiphoton confocal microscope. The extent of co-localization of the pixels in the confocal images were calculated with the Image J Coloc 2 plugin using the overlap coefficient (MOC) according to Manders (Manders, 1993),

$$\mathrm{MOC} = \frac{\sum_i (R_i \times G_i)}{\sqrt{\sum_i R_i^2 \times \sum_i G_i^2}}$$

where R_i and G_i represent the intensity values of the red and green channels, respectively, in a given pixel, i (Manders et al., 1992).

2.2.7 Co-immunoprecipitation

Aliquots of soluble protein fractions derived from RV infected cells were subjected to co- immunoprecipitation reactions with antibodies to select immunophilins. The soluble protein fractions were incubated with either rabbit anti-CyPA or rabbit anti-CyP40 for 1 h at room temperature with rotation. The mixtures containing anti-CyPA or anti-CyP40 were incubated with protein A sepharose (Pierce, Rockford, IL.) for 2 h at room temperature and pelleted at 2,500 x g for 5 min. The bound protein A beads were washed with RIPA buffer 3 times and boiled with SDS-loading buffer, and the released proteins were separated by SDS-PAGE and detected by Western blot. Controls were treated the same way using normal rabbit serum instead of epitope-specific antibodies. The primary antibodies used in Western blot analyses were generated in mice so that non-specific signals created by the secondary antibodies were avoided.

2.2.8 FRET by Acceptor Photobleaching

FRET by acceptor photobleaching was selected because of the ease of analysis. FRET is non-radiative energy transfer from a donor fluorophore to an acceptor

fluorophore when they are in close proximity (1-100 nm) to each other. In FRET by acceptor photobleaching, the acceptor fluorophore (Cy5) is bleached and the subsequent increase in the intensity of the donor fluorophore (Cy3) is measured (Karpova et al., 2003). The Cy3 and Cy5 fluorophores have overlapping emission and excitation wavelengths, respectively, and the photon released upon the emission of Cy3 will excite Cy5, as long as the fluorophores are within 10 nm of each other. Infected cells were fixed, permeabilized, and reacted with epitope-specific antibodies directed against the immunophilins followed by the addition of secondary antibodies, Cy3-conjugated $F(ab)_2$ fragments against IgG. NSP4 was directly labeled with Cy5-conjugated $F(ab)_2$ fragments against $NSP4_{150\text{-}175}$. Images were collected by exciting the fluorophores at 568 nm and 647 nm prior to photobleaching of the Cy5 fluorophore. The 647 nm line was set to 100% power for 3 min for photobleaching. An increase in the 568 nm signal was measured following photobleaching to determine if there was a positive FRET reaction. For each protein, a minimum of 3 fields was analyzed. Two areas outside of the photobleached area served as an internal control, while 2 areas inside the photobleached area served as the sample measurement. Percent FRET was calculated by subtracting the Cy3 signal post-photobleaching from the Cy3 signal pre-photobleaching and dividing it by the Cy3 signal post-photobleaching: $((Cy3_{pre} - Cy3_{post})/Cy3_{pre})$. Image analyses were performed using Image J software by NIH Image.

2.2.9 Silencing

Silencing RNAs (siRNAs) directed against Cav-1, CyPA, CyP40, and HSP56 were purchased from Dharmacon (Thermo-Fisher, Pittsburgh, PA). SMARTpool siRNA was

used from the siGENOME collection. For each protein, the pooled siRNA mixture consisted of four individual siRNAs of 19 base pairs each (**Table 2.3**). The siRNA was diluted to 5nmol in 200µL of sterile ultrapure dH_2O for a working stock of 20µM siRNA.

Table 2.3. siRNA Sequences in SMARTpool siGENOME Silencing Mixtures

Silenced Protein	siRNA Sequences
Caveolin-1	• CUAAACACCUCAACGAUGA • GCAGUUGUACCAUGCAUUA • AUUAAGAGCUUCCUGAUUG • GCAAAUACGUAGACUCGGA
Cyclophilin A	• UCCUAGAGGUGGCGGAUUU • AGAAUUAUUCCAGGGUUUA • GGAAUGGCAAGACCAGCAA • AGACAAGGUCCCAAAGACA
Cyclophilin 40	• UAAGAUACGUGGACAGUUC • GGAUGCGGAUAUAGAUUUA • GAAUAUUGGUGCUUGUAAA • GAGCCAAGCUGCAACCUAU
Heat Shock Protein 56	• GCGGUGAAGGCUAUGCUAA • GCUCUAUGCCAAUAUGUUU • GAGAACAUUCCAUCGUGUA • AGGGAGAAGAUCUGACGGA

Cells were transfected using a reverse transfection method adapted from the method provided by Dharmacon (Gutierrez et al., 2010) and Life Technologies (Protocol # MAN0007825 Rev.1.0). Briefly, for MA104 cells, Lipofectamine RNAiMax (Life Technologies, Grand Island, NY) was added to serum free DMEM at a concentration of 60 µl/ml and incubated for 10 min at room temperature to allow for equilibration. The mixture was added to a 24-well tissue culture plate containing the siRNA diluted to 2.0 µM in serum free DMEM to allow for incorporation of siRNA into the Lipofectamine

liposomes. After incubation for 5 min at room temperature, 2.0×10^5 MA104 cells or 5.0 x 10^5 HT29.f8 cells were added to the 24-well tissue culture plate containing the transfection mixture, and the cells were incubated at 37°C with 5% CO_2 in a humid environment. Serum was added to the cells to a final concentration of 10% FBS at 4 h post transfection and cells were incubated for a total of sixty h post transfection to allow for silencing. To infect, the transfection mixture was removed and the cells were washed twice with serum-free DMEM and infected with rotavirus as described above.

2.2.10 Surface Biotinylation and Recovery of Exofacial Plasma Membrane Proteins

Silenced, infected cells plated in 24-well tissue culture plates were surface biotinylated as described previously (Gibbons et al., 2011). Briefly, at 6 hpi, cells were washed with ice-cold PBS-CM (1X PBS supplemented with 0.1 mM $CaCl_2$ and 1 mM $MgCl_2$) three times to remove unbound extracellular material. A solution of 6 mg/ml membrane-impermeable EZ Link® Sulfo-NHS-SS-Biotin (Pierce-Thermo) in ice-cold PBS-CM was added to the cells at a 10 mM concentration, and was incubated with rocking for 30 min at 4°C. Excess biotin was quenched by adding cold DMEM supplemented with 10% FBS for 10 min at 4°C. Protease inhibitor cocktail (1.2mM AEBSF, 0.46μM Aprotinin, 12.3μM E-64, 14μM Bestatin, 112μM Leupeptin and 1.16μM Pepstatin; Amresco, Solon, OH) and 0.2 mM phenylmethylsulfonyl fluoride (PMSF; Sigma, St. Louis, MO) were added to SDS-free RIPA lysis buffer (150 mM NaCl, 50 mM Tris-base, 10% NP-40, 0.5% DOC, pH=8.0) and immediately added to the cells for 20 min at 4°C. The cell lysates were transferred to sterile microcentrifuge tubes,

to which 30 μL of streptavidin-agarose slurry (Pierce-Thermo, Rockford, IL) was added per 1 ml of lysate. The mixture was incubated with rotation at 4°C for 16 h.

The biotinylated proteins were collected by pelleting the bound streptavidin-agarose at 2500 x g for 5 min to pellet the streptavidin-agarose. The supernatant was collected and saved for analysis of the protein silencing experiments, and the pellet was washed three times in ice-cold SDS-free RIPA lysis buffer with protease inhibitors. The biotinylated proteins were removed from the streptavidin-agarose beads by suspending them in sample reducing buffer (Laemmli, 1970) (62.5 mM Tris pH=6.8, 10% glycerol, 2% SDS, 5% 2-mercaptoethanol, and 0.001% bromophenol blue) and boiling for 10 min. The beads were centrifuged for 5 min at 2500 x g, and the sample reducing buffer supernatant containing biotinylated exofacial plasma membrane proteins was collected for electrophoretic analysis. To ensure that there was a lack of non-specific binding to the streptavidin-agarose beads, mock-biotinylated samples were analyzed as controls.

2.2.11 Cyclosporin A Treatment

MA104 and HT29.f8 cells were plated in 12-well tissue culture plates and grown until ~80% confluent. Cells were treated with 120 μg/ml cyclosporine A (CsA) in methanol (MeOH) for 24 h. Control cells were treated with the same volume of MeOH only. After 24 h of treatment, cells were infected with SA11.4f at a MOI of 2.0. Cells were then surface biotinylated for analysis of NSP4 transport to the exofacial PM.

2.2.12 SDS-PAGE and Western Blotting

Western blotting was used to confirm the extent of silencing of each of the silenced proteins and to determine the presence of NSP4 at the plasma membrane. Briefly, equal

amounts of samples were dissolved and dissociated in sample reducing buffer, loaded and resolved on a 12% or 15% SDS-polyacrylamide gel (NEXT GEL; Amresco). The proteins were electroblotted to a 0.45 μM-pore size nitrocellulose membranes (Bio-Rad, Hercules, CA) as per the manufacturer's instructions (Mini-Protean II and Trans-Blot, Bio-rad). The nitrocellulose membranes were blocked in 10% (wt/vol) NFDM in PBS for 1 h at room temperature. The membranes then were incubated with primary antibodies diluted in 2.5% NFDM in PBS for 3 h at 27°C with rocking. The membranes were washed once with PBS, twice with PBS-Tween-20 (0.5%), and again with PBS. Secondary antibodies were diluted in 2.5% NFDM in PBS, added to the membranes, and incubated with rocking for 1 h at 27°C. The membranes were washed as above and reacted with Immobilon Western Chemiluminescent HRP Substrate (Millipore, Billerica, MA) per the manufacturer's instructions. The protein-specific bands were visualized using the ImageQuant LAS 4000 gel imager (GE Healthcare Life Sciences, Pittsburgh, PA), and densitometric analyses were performed using ImageJ.

2.2.13 Densitometry

Gel images were analyzed via ImageJ using the gel analysis function. Briefly, the intensity of each protein band was given a value for the silenced protein and for the glyceraldehyde-3-phosphate dehydrogenase (GAPDH) control in the same lane. Each band was background subtracted and measured within the linear range. The intensity value of the protein band was divided by the intensity value of the GAPDH control band to obtain a ratio of the protein amount to protein loading control (GAPDH band intensity). The non-targeting siRNA (siNT) control ratio was set to 0% silencing. The

ratio in silenced cells was divided by the ratio in siNT cells, subtracted from 1, and multiplied by 100 to obtain the percentage of silencing:

$$\%\ silencing = \ 1 - \left(\frac{\frac{silenced\ protein}{GAPDH}}{\frac{protein\ in\ NT\ cells}{GAPDH}} \right) x\ 100$$

The experiments were performed in triplicate and the standard error was calculated using:

$$SE = \sqrt{\frac{\sum (X - M)^2}{n - 1}}$$

where *X* is the sample value, *M* is the mean, and *n* is the number of experimental replicates.

2.2.14 Lovastatin Treatment

MA104 and HT29.f8 cells were plated in 25-cm^2 tissue culture flasks at a density of 2.8 x 10^6 and 5 x 10^6, respectively. The cells were grown until ~80% confluent and treated with 5 μg/ml lovastatin (from a 5 mg/ml lovastatin in ethanol stock) for 24 h at 37°C. 'Untreated' control cells were treated with the same amount of pure ethanol for 24 h at 37°C. Cells were infected as described above but incubated with serum-free DMEM containing no lovastatin during the adsorption period. After adsorption, cells were washed to remove unbound virus and replaced with serum-free DMEM containing 5 μg/ml lovastatin. Cells were incubated for 6 h and surface biotinylated as described above. To avoid interaction of the lysis buffer components with the subsequent cholesterol assay, cells were lysed mechanically by scraping in PBS with protease inhibitors (Roche) and PMSF, homogenized with a microcentrifuge tube pestle, passed

through a 22 g needle 10 times, and sonicated at 45 W for 10 min on ice. Biotinylated proteins were pulled down with streptavidin agarose as described above and supernatants were saved for cholesterol analysis.

2.2.15 Cholesterol Quantification

Cholesterol was quantitated with the Wako Cholesterol E kit (Wako Diagnostics, Richmond, VA), which measures total cholesterol, using a modified protocol (Martin et al., 2015). Briefly, cells were lysed via mechanical lysis as described above in PBS. Standards were prepared to measure the cholesterol concentration from 0-4 mg/ml. Each standard (20 µl) was placed in a borosilicate glass test tube and 20 µl of each sample was placed in a separate borosilicate glass test tube. The Color Reagent was mixed with the Buffer Solution, both provided in the kit, and 2 ml of the mixture was added to each test tube. The color was allowed to develop for 5 min at room temperature. Two-hundred µl of the developed solution was added to a 96-well microplate and the absorbance was read using an BMG Labtech FLUOstar Omega microplate reader at 600 and 700 nm. The cholesterol concentrations of the samples were determined from the standard curve.

2.3 Results

2.3.1 NSP4 Co-localized with CyPA, CyP40, and HSP56

It is known that NSP4 directly binds Cav-1 and cholesterol (Parr et al., 2006; Schroeder, 2009). Our goal was to determine the extent of co-localization of NSP4 and the immunophilins. MA104 cells were infected with RV SA11.4f (MOI=2) for 6 hours, fixed, permeabilized and labeled with antibodies against caveolin-1 or the immunophilins followed by Pacific Blue™-conjugated secondary antibodies. NSP4 was

labeled with a peptide specific Cy5-conjugated anti-NSP4$_{150\text{-}175}$. Uninfected controls were labeled with either primary or secondary antibodies only. Images were collected and analyzed via the Coloc2 plugin from Image J. We calculated the Mander's Overlap Coefficients (MOCs) for the two proteins, which indicates co-occurrence of two signals in one pixel. The MOC in an image with two signals shows high overlap between the signals when it approaches 1 and little overlap between the signals as it approaches 0 (Dunn et al., 2011). The MOCs are displayed in **Figure 2.1**. CyPA, CyP40 and HSP56 all show substantial co-localization with NSP4 in all images. NSP4 and CyPA display MOCs of 0.878 ± 0.02 and 0.841 ± 0.03, NSP4 and CyP40 display MOCs of 0.830 ± 0.04 and 0.780 ± 0.05, and NSP4 and HSP56 display MOCs of 0.971 ± 0.01 and 0.903 ± 0.02 (n=10). A graphical representation of the MOCs are shown in intensity histograms with the NSP4 signal plotted on the y-axis and the immunophilin signal plotted on the x-axis. The high Mander's coefficients suggest that NSP4 resides within close proximity of the immunophilins intracellularly.

2.3.2 NSP4 Co-immunoprecipitated with Chaperone Proteins

Since NSP4 co-localized intracellularly with CyPA, CyP40, and HSP56, we wanted to further demonstrate an association of NSP4 with immunophilin proteins CyPA and CyP40 using a biochemical assay. We were unable to find a precipitating antibody that recognized HSP56. Co-immunoprecipitations of the cyclophilins were performed on the soluble fraction of SA11.4f RV-infected HT29.f8 cells (MOI=2). Infected cells were lysed with RIPA buffer, and the soluble fraction collected via high-speed centrifugation.

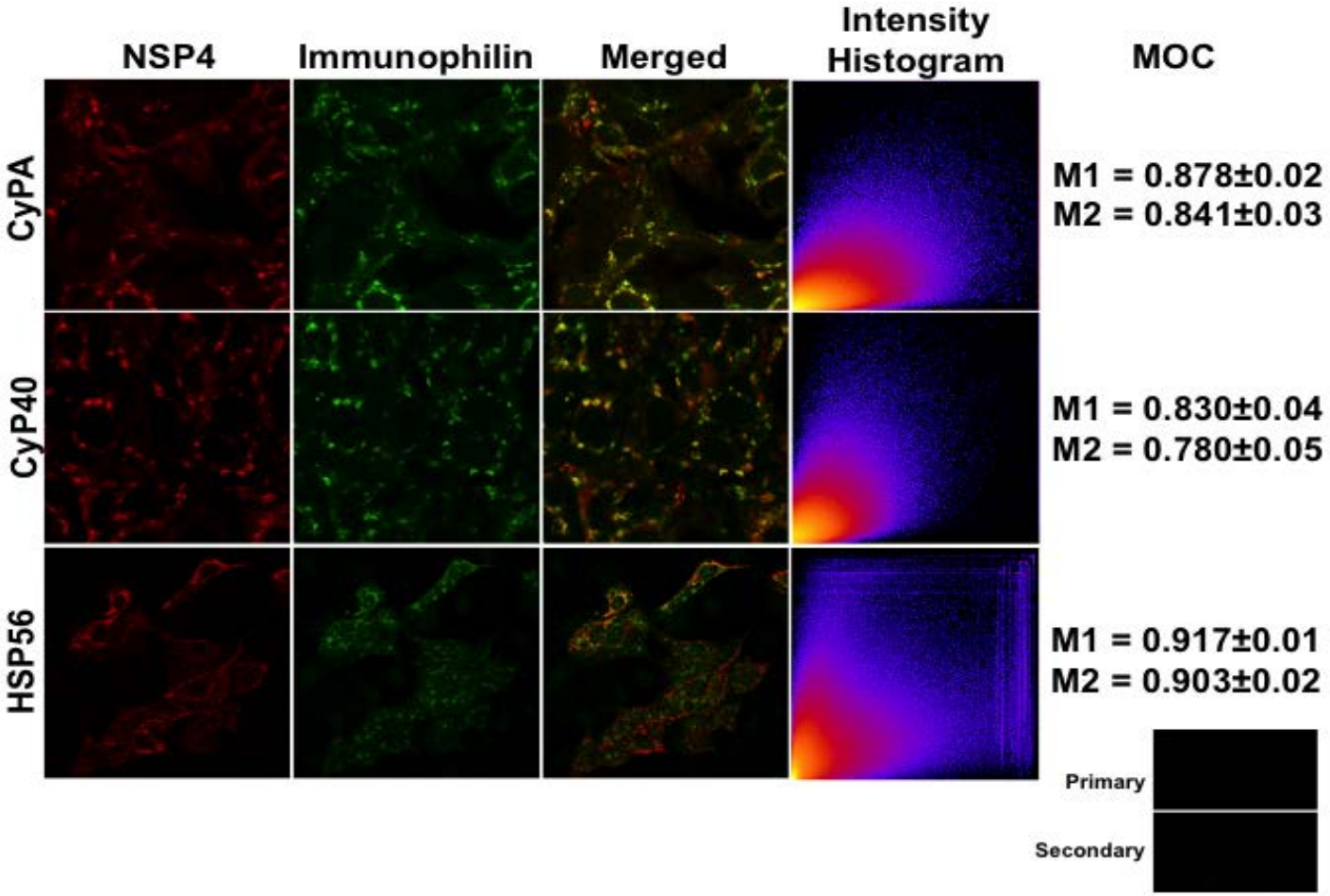

Figure 2.1 Co-localization analyses of CyPA, CyP40, and HSP56 with RV NSP4 in MA104 cells. MA104 cells were infected with RV SA11.4f for 6 h. Cells were fixed and permeabilized, and labeled with antibodies directed against the immunophilins (green) or NSP4 (red). Primary and secondary antibody controls are shown in the bottom right panel. Intensity histograms are shown in the fourth column. The Mander's Overlap Coefficients (MOC's) were calculated for each signal and are depicted in the last column.

Proteins were immunoprecipitated with Protein A-conjugated rabbit anti-CyPA or rabbit anti- CyP40. A control was immunoprecipitated with normal rabbit antisera. The immunoprecipitated proteins were released from the bound antibodies by boiling in SDS sample loading buffer and subjected to SDS-PAGE, transferred to a nitrocellulose membrane, followed by Western blot with anti-$NSP4_{150-175}$ antibody. Both anti-CyPA and anti-CyP40 bound NSP4 upon precipitation of the protein A beads, indicating a direct or indirect interaction between NSP4 the cyclophilin proteins (**Figure 2.2**). The blots were also probed with anti-CyPA and anti-CyP40 to ensure the immunophilins were reactive with their respective antibodies. Controls displayed no co-immunoprecipitation with the cyclophilins or with NSP4 (**Figure 2.2, lanes 2**). Co-immunoprecipitation with rabbit anti-HSP56 was performed, but neither NSP4 nor HSP56 were detected in the western blot (data not shown), indicating a lack of reactivity with the antibody.

2.3.3 NSP4 Was Resolved to Within 10 nm Intracellularly Using FRET

To verify that NSP4 directly interacts with the chaperone proteins intracellularly, FRET by acceptor photobleaching experiments were performed using $F(ab)_2$ fragments directed against peptide $NSP4_{150-175}$ and antibodies directed against one of three immunophilin proteins, CyPA, CyP40, or HSP56. FRET by acceptor photobleaching allows for measurement of protein proximity, by bleaching the donor fluorophore and measuring the recovery of the acceptor fluorophore if the proteins are within 10 nm of each other when using Cy3 and Cy5. MDCK cells were infected with RV SA11.4f at an MOI of 2 for 7 h. Cells were fixed, permeabilized, and stained with antibodies or $F(ab)_2$

fragments conjugated to either Cy3 or Cy5. Cy5 was photobleached and recovery of the Cy3 signal was assessed as a percentage of initial fluorescence intensity (%FRET = ($Cy3_{post}$-$Cy3_{pre}$)/$Cy3_{post}$). All three immunophilins displayed a positive FRET, indicating that NSP4 associates with these three proteins intracellularly within a distance of 10 nm (**Figure 2.3**). In each panel, 4 areas are depicted post-photobleaching (A-D): Two areas in which Cy5 was not photobleached, and where NSP4 is densely or sparsely stained (A and B), and 2 areas in which Cy5 was photobleached, and where NSP4 is densely or sparsely stained (C and D).

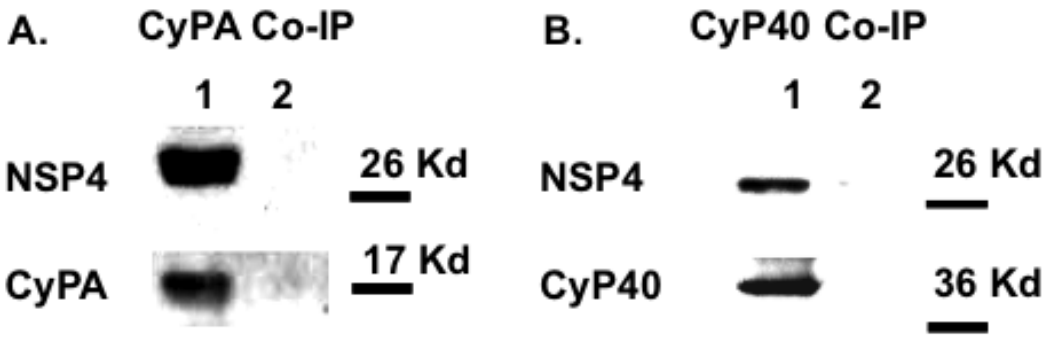

Figure 2.2 Co-immunoprecipitation of NSP4 and cyclophilin A and NSP4 and cyclophilin 40. Cyclophilin A (A) and Cyclophilin 40 (B) were precipitated from aliquots of soluble post-nuclear supernatants (PNS) of RV infected HT29.f8 cell lysates. The precipitated samples (lanes 1) and the controls precipitated with normal rabbit sera (lanes 2) were subjected to SDS PAGE and transferred to nitrocellulose. Molecular weight markers are indicated to the right of the blots. Both samples were blotted with mouse anti-NSP4 and either CyPA or CyP40. Reprinted with permission (Gibbons, 2007).

The percent FRET varied from 37.2% with HSP56 to 73% with CyPA and is indicated to the right of each row (**Figure 2.3**). Use of the donor and acceptor pair, Cy3

and Cy5 with $F(ab)_2$ fragments places the interacting proximity of these immunophilins with NSP4 within 10 nm in distance. Proteins located this closely to each other generally

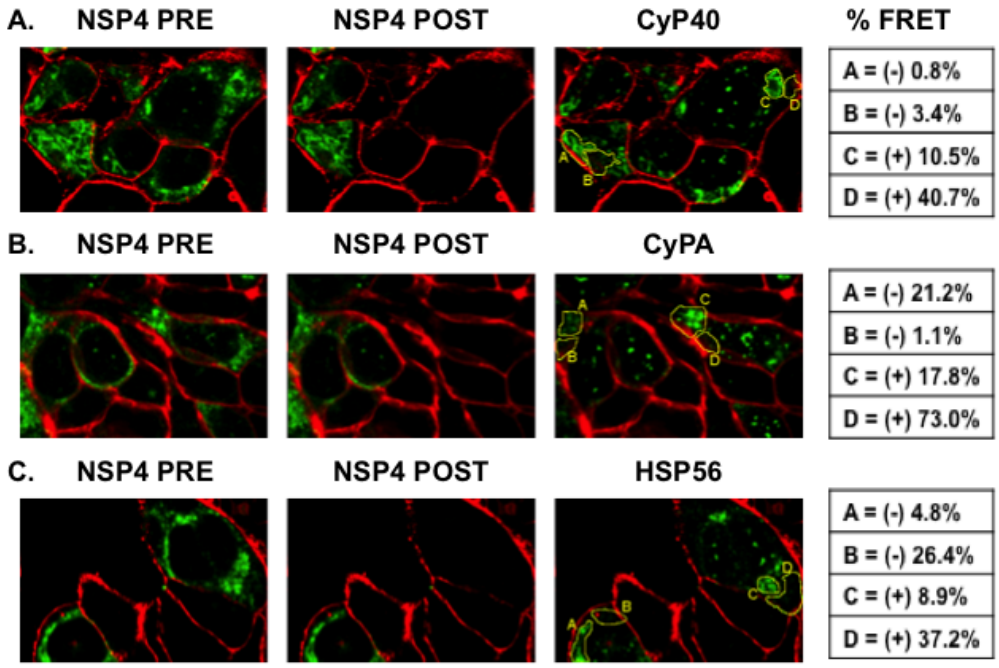

Figure 2.3. FRET analysis of NSP4 and immunophilins by acceptor photobleaching. Each row depicts pre- and post-bleaching of Cy5-NSP4 (left and center panel respectively), while the right panel shows the respective Cy3-immunophilin signal post bleaching of NSP4. The PM was biotinylated and labeled with Cy2-streptavidin. **A** shows the NSP4/CyP40 FRET, **B** shows the NSP4/CyPA, and **C** shows the NSP4/HSP 56 FRET. In the last column, A-D are indicated and were used to determine % FRET. A: Areas with intense staining but little FRET; B: Areas with minimal staining and little FRET; C: Areas with intense staining and positive FRET; and D: Areas with minimal staining and positive FRET. Areas (B) and (D) serve as the internal controls. Biotinylated PM proteins are depicted in red. Reprinted with permission (Gibbons, 2007).

are considered to be directly interacting or interacting within a multi-subunit protein complex. Akin to the co-localization data, all 3 immunophilins tested showed an intracellular interaction with NSP4 via FRET.

2.3.4 NSP4 Expression Increased Expression of CyPA, CyP40, and HSP56

Co-localization studies revealed that there is a different expression pattern of the immunophilins in RV-infected and uninfected cells. To determine if this expression pattern was altered in the presence of NSP4 only, MA104 cells were transiently transfected with a plasmid expressing full length NSP4. In transfected MA104 cells NSP4 expression increases expression of the immunophilins (**Figure 2.4A**). MA104 cells transfected with a V5-chloarmphenicol acetyltransferase fusion protein as a control, which exhibited no increase in expression heat shock protein 56 (**Figure 2.4B**). Therefore, NSP4 expressed in the absence of RV is able to increase expression of the immunophilins, which intracellularly distribute in a pattern similar to that of NSP4.

2.3.5 Silencing Cav-1, CyPA, and CyP40 Altered Intracellular Distribution of NSP4

To begin to examine the functional link between NSP4 and the immunophilins or Cav-1, siRNA was transfected into MA104 cells or HT29.f8 cells using Lipofectamine RNAiMax (Invitrogen), and reduction of expression was verified by Western blot using GAPDH as a loading control (**Figure 2.5**). Protein expression of all silenced proteins was decreased by at least 57%. HSP56 was not detected in cell lysates and could not be measured by Western blot because of limited antibody reactivity by Western blot. As shown in **Figure 2.6**, silenced cells infected with RV SA11.4f at an MOI of 2 were fixed and permeabilized at 8 hours post infection (hpi) for confocal microscopy. The fixed

cells were labeled with antibodies directed against one of the immunophilins or Cav-1 and NSP4 followed by imaging via LSCM. NSP4 has been localized to the ER (Berkova et al., 2006) , in distinct cytosolic pools (Berkova et al., 2007), in caveolae on the PM

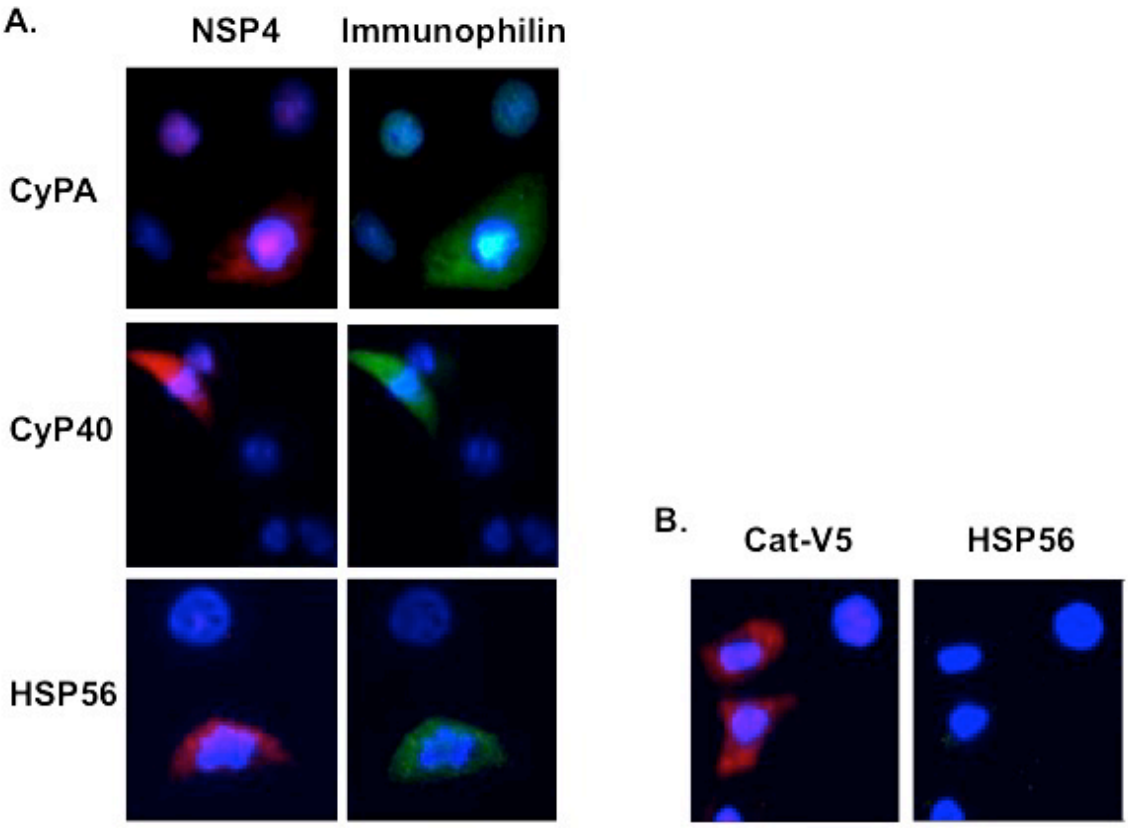

Figure 2.4 Expression of immunophilins was up-regulated in MA104 cells transfected with NSP4. CyPA, CyP40, and HSP56 expression is increased in cells transfected with NSP4 in the absence of virus. Transfected NSP4 is labeled with anti-$NSP4_{150-175}$ followed by a Cy2-$F(ab)_2$ fragment (A; red), and the immunophilins are labeled with their respective antibodies followed by a Cy3-$F(ab)_2$ fragment (A; green). A chloramphenicol acetyltransferase-V5 control does not increase expression of HSP56 (B). Reprinted with permission (Gibbons, 2007).

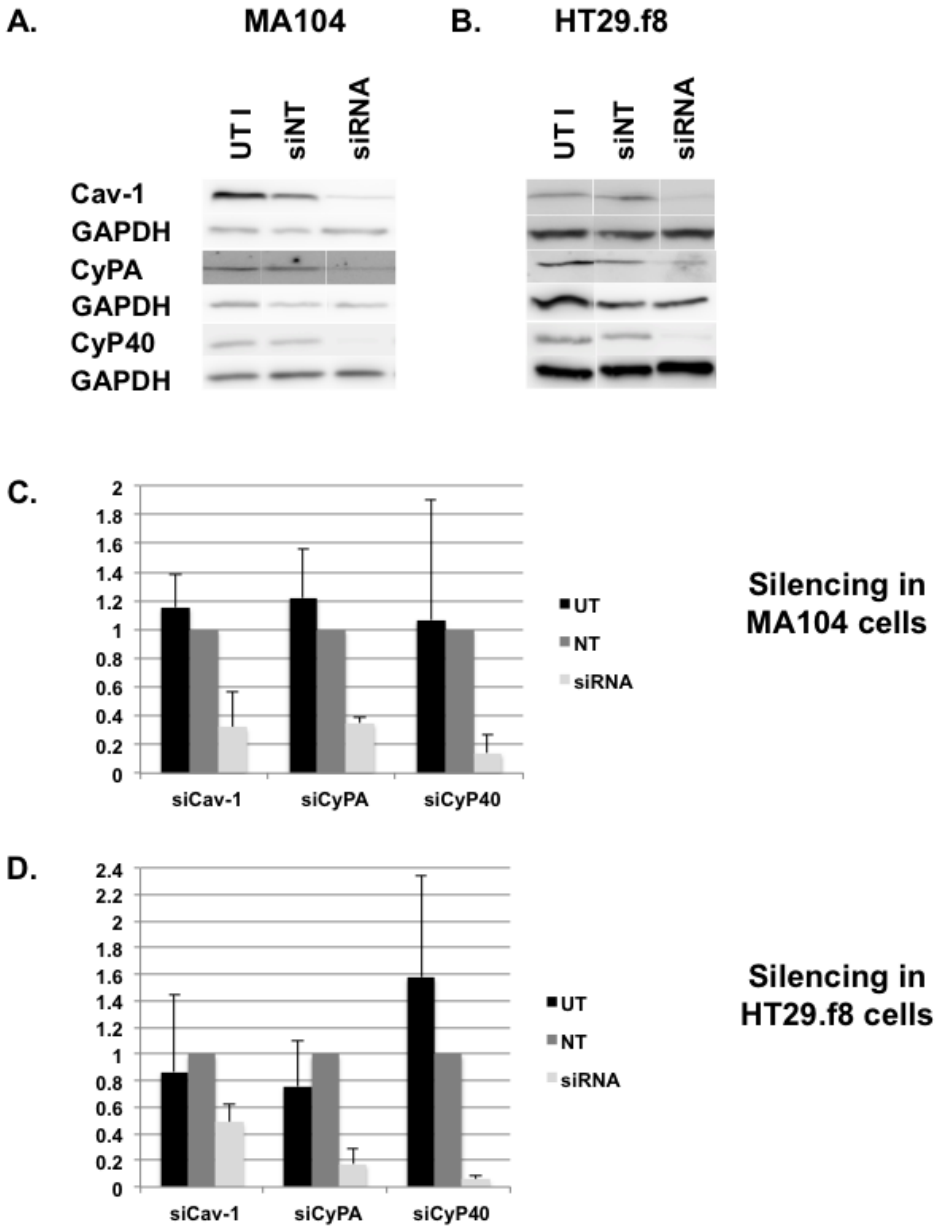

Fig. 2.5. Silencing in MA104 and HT29.f8 cells. Silencing RNA that targets Cav-1, CyPA, or CyP40 transfected into MA104 and HT29.f8 cells were effective at knocking down the proteins to near 60% of the original levels at 60 h post transfection. Samples were analyzed via Western blot with GAPDH serving as the internal control. A and B depict the reduction in protein expression upon silencing, which is graphed in C and D, respectively, with standard error indicated by bars (n=3). All densitometry was normalized to the non-targeting (NT) siRNA control.

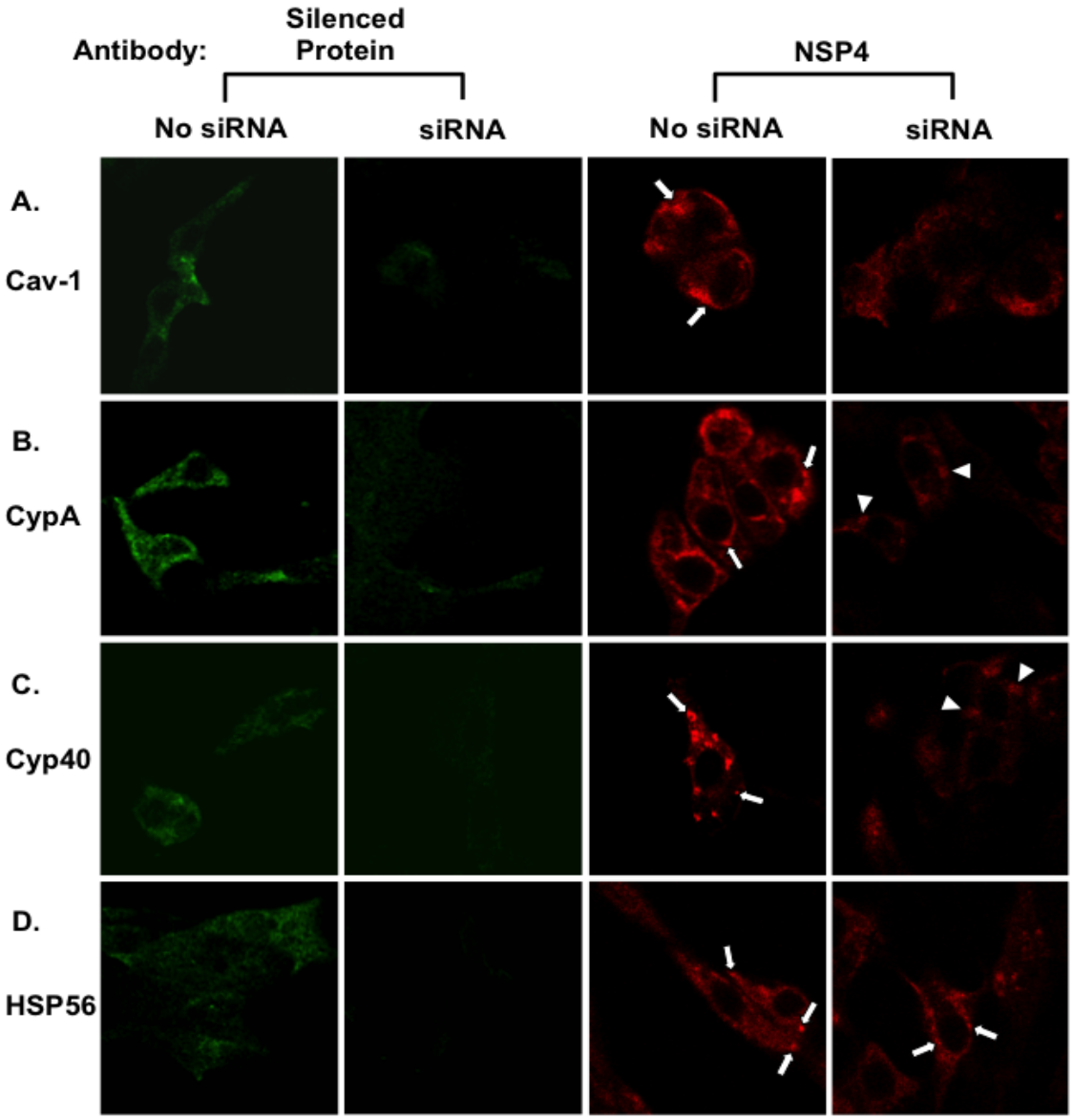

Fig. 2.6 Silencing of Cav-1, CyPA, and CyP40 caused intracellular redistribution of NSP4. Cells were treated with one of four silencing RNA mixtures targeting Cav-1, CyPA, CyP40, or HSP56 for 60 h, infected with RV SA11.4f for 6 h and fixed and permeabilized. Cells were stained with one of the four proteins in the left panels (green) and NSP4 in the right panels (red). Columns 1 and 3 depict cells that were not treated with siRNA, whereas columns 2 and 4 depict cells that were treated with siRNA. In column 4, the abnormal distribution of NSP4 can be seen. NSP4 moves out of its normal, punctate cellular structures (denoted with long arrows) and into a different distribution (denoted by arrowheads), depending on the protein silenced, except in the case of HSP56, which had no effect.

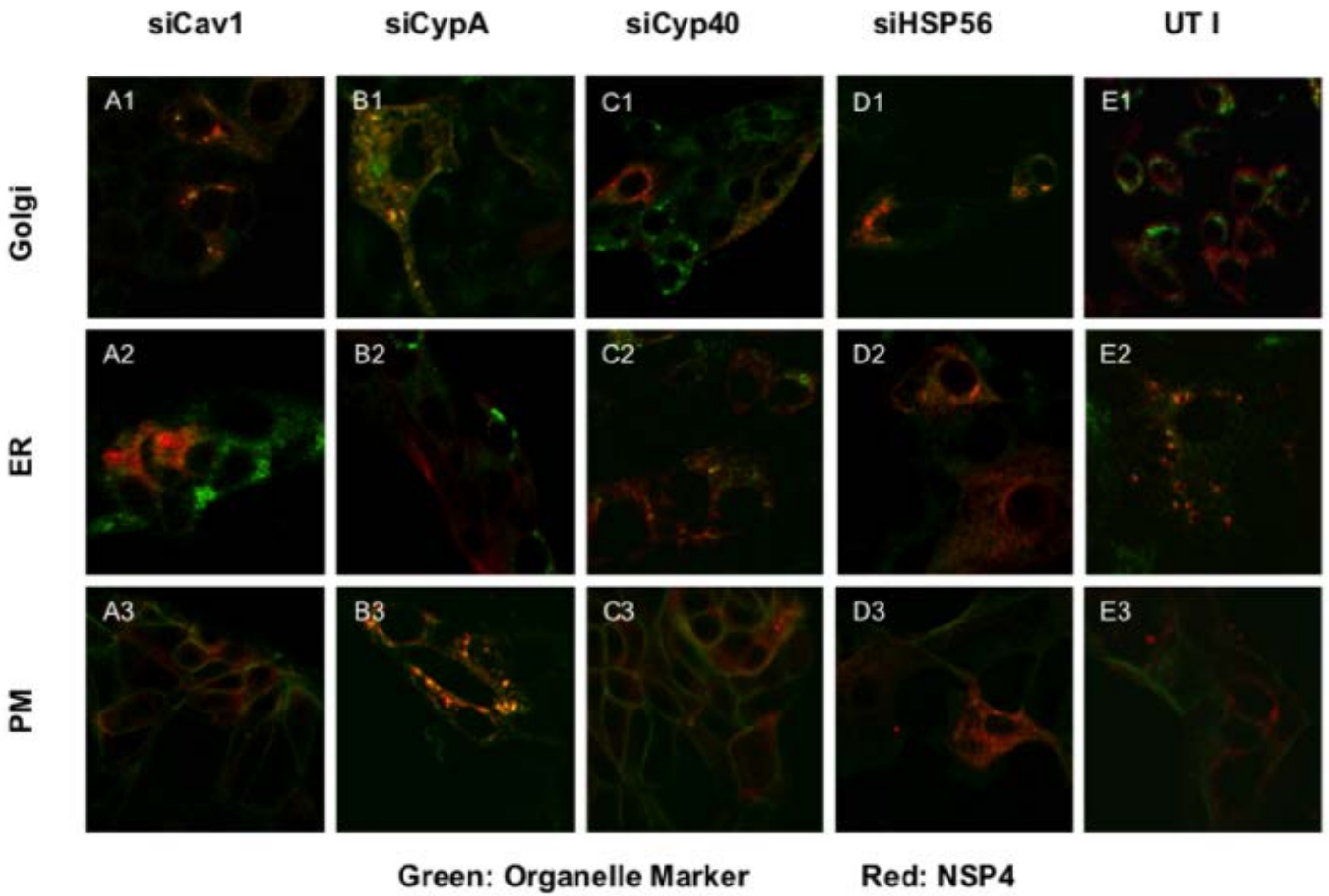

Fig. 2.7 Redistribution of NSP4 and organelle markers in silenced MDCK cells. MDCK cells were silenced for Cav-1 and the immunophilins and infected for 6 h. Cells were fixed and permeabilized at 6 hpi and labeled for Cav-1, CyPA, CyP40, or HSP56 and an organelle marker (PDI for the ER, golgin-97 for the Golgi, and Na^+/K^+-ATPase for the PM). Untransfected, infected (UT I) cells serve as a control. NSP4 was pseudocolored red and the organelles and PM were pseudocolored green. Overlap of the signals from NSP4 and the protein markers can be seen in yellow.

(Storey et al., 2007), and is secreted from infected cells (Bugarcic and Taylor, 2006; Didsbury et al., 2011). NSP4 also is seen in punctate structures similar to that seen in our confocal analysis (**Figure 2.6**, arrows).

When select intracellular components were silenced, NSP4 was distributed in patterns different from those of non-silenced, infected cells (**Figure 2.6**). When Cav-1 was silenced, NSP4 was redistributed from punctate structures (arrows) to a more diffuse cytoplasmic pattern with less intense staining (**Figure 2.6A**). When CyPA was silenced, NSP4 was not distributed as widely throughout the cytoplasm but was localized to distinct, unidentified areas that were less brightly stained (**Figure 2.6B**, arrowheads). When CyP40 was silenced, NSP4 was not distributed as widely throughout the cytoplasm and punctate structures, although present, were not as pronounced as in the non-silenced cells (**Figure 2.6C**, arrowheads). However, when HSP56 was silenced, there was little change in the intracellular distribution of NSP4 (**Figure 2.6D**, arrows). Therefore, silencing of Cav-1, CyPA, and CyP40 altered the intracellular distribution of NSP4, but HSP56 has little effect. In general, silencing of the immunophilins caused a dramatic decrease in fluorescent signal (**Figure 2.6**, columns 1 and 2), agreeing with the Western blot silencing data (**Figure 2.5**).

When NSP4 and organelle markers were compared in silenced cells, the abnormal distribution of NSP4 was more evident (**Figure 2.7**). In cells silenced for Cav-1 and CyPA, there was a limited amount of co-localization of NSP4 with the Golgi marker golgin-97 (**Figure 2.7-A1** and **-B1**) as opposed to untreated, infected cells (UT I), where NSP4 and golgin-97 did not co-localize (**Figure 2.7-E1**). To determine whether this co-

localization was due to redistribution of golgin-97 or to altered NSP4 transport, the infected cell lysates were treated with Endoglycosidase H and subjected to SDS-PAGE. Upon silencing of CyPA, NSP4 was still sensitive to Endo H (**Figure 2.8**), suggesting that silencing of CyPA caused abnormal distribution of the Golgi protein golgin-97 and not transport of NSP4 to the Golgi. Notably, when Cav-1 or CyPA were silenced, there was little co-localization of NSP4 with the ER marker, PDI (**Figure 2.7-A2** and **-B2**), as opposed to untreated cells (**Figure 2.7-E2**), where co-localization of NSP4 and PDI was marked. When CyPA was silenced there was significant co-localization of NSP4 with the PM marker, Na^+/K^+-ATPase, although the co-localization appeared in the cytosol of the cells rather than on the exofacial PM (**Figure 2.7-B3**). It is unclear what is responsible for the redistribution of Na^+/K^+-ATPase.

2.3.6 Silencing Cav-1, CyPA, and CyP40 Failed to Alter Transport of NSP4 to the PM

Since NSP4 is known to traffic to PM caveolae (Storey et al., 2007), we wanted to determine if the interaction of NSP4 with Cav-1, CyPA, and CyP40 contributes to the mechanism utilized by NSP4 to reach the cell surface. Cells were surface biotinylated to detect NSP4 at the PM of silenced and infected cells. Cells were treated with siRNA for 60 h prior to infection with RV SA11.4f at a MOI of 5. At 6 hpi, cells were washed and incubated with a 10 mM solution of a cell-impermeable biotin at 4°C for 30 min for biotinylation of surface proteins. Cells were lysed with RIPA buffer and biotinylated proteins were precipitated with streptavidin agarose at 4°C overnight. Proteins were

dissociated from the streptavidin beads, separated via SDS-PAGE, transferred to nitrocellulose, and blotted with rabbit anti-NSP4$_{112\text{-}140}$. Silencing of Cav-1, CyPA, and

CyP40 failed to alter the transport of NSP4 to the surface of the cell in both MA104 and HT29.f8 cells (**Figure 2.9A**). A non-targeting siRNA (siNT) was used as a control to confirm that the silencing procedure does not interfere with NSP4 transport. The untreated and uninfected cells (UT UI) were evaluated as negative controls and confirmed there was an absence of nonspecific interactions of the antibodies with the surface biotinylation components.

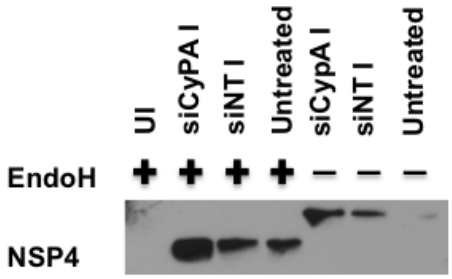

Fig. 2.8 NSP4 was endoglycosidase H sensitive in CyPA silenced cells. Cells were silenced for CyPA, infected with RV SA11.4f and treated with Endoglycosidase H. NSP4 remained sensitive to Endo H digestion when CyPA was silenced.

To further verify that the cyclophilins were not involved in NSP4 transport, cells were treated with cyclosporin A (120 μg/mL; CsA) for 24 h prior to infection with RV. CsA is a small molecule inhibitor of the peptidyl-prolyl isomerase (PPIase) domain of cyclophilin proteins. In the presence of CsA or MeOH only, NSP4 continued to traffic to the exofacial PM, similar to the results seen upon siRNA treatment (**Figure 2.9B**).

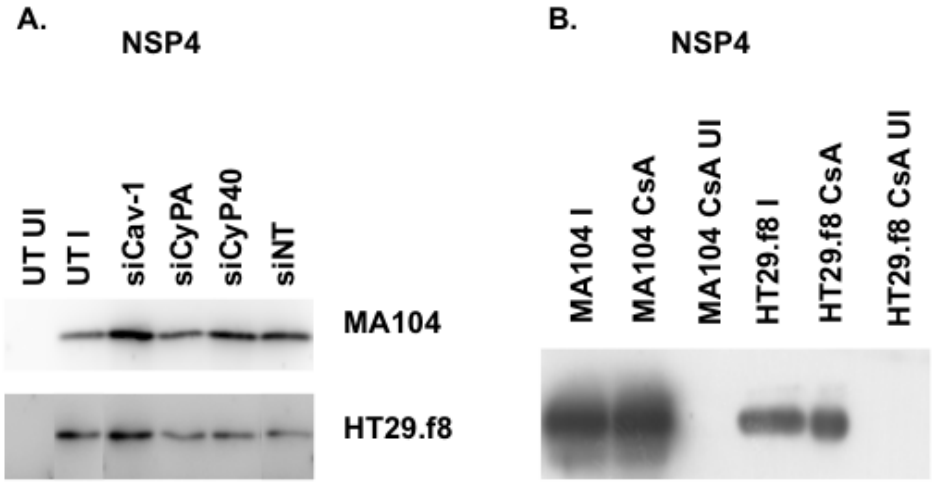

Fig. 2.9 Silencing of Cav-1, CyPA, and CyP40 or treatment with cyclosporin A failed to prevent NSP4 from trafficking the cell surface. **A.** MA104 and HT29.f8 cells that were infected (I) with RV or uninfected (UI), and were untreated (UT) (A; lanes 1 and 2) or treated with siRNA (siCav-1, siCyPA, siCyP40) (A; lanes 3-6) for 60 h. Cells were ^{surface} biotinylated 6 h post infection and biotinylated cells were precipitated with streptavidin agarose. Lysates were separated by SDS-PAGE and subjected to a Western blot with rabbit antibody directed against $NSP4_{112-140}$. **B.** MA104 and HT29.f8 cells were infected (I) or uninfected (UI), and were treated with 1.2 μg/ml cyclosporine A (CsA) for 24 h. Surface biotinylation and further analyses were performed as in **A**.

2.3.7 Lovastatin Treatment Lowers the Amount of NSP4 That Reaches the Cell Surface

We know that NSP4 directly interacts with cholesterol (Schroeder, 2009), so it was reasonable to determine the effect of inhibiting the production of de novo synthesized cholesterol on NSP4 transport to the PM. Cells were treated with Lovastatin (5 μg/ml), an HMG-CoA Reductase inhibitor, for 24 h prior to infection with SA11.4f at an MOI of 5. After a 6 h infection cells were washed, surface biotinylated, scraped into PBS with protease inhibitors (PI), and homogenized. Biotinylated proteins were precipitated with

streptavidin agarose at 4°C overnight, dissociated from the streptavidin, separated via was measured as described in methods.

In **Figure 2.10**, the Western blots depicted that although some NSP4 reached the PM when cholesterol production was decreased (based on densitometry analysis), it was consistently less than that in cholesterol-depleted samples. The role of cholesterol in the transport of NSP4 needs to be investigated further, but it may play an important role in transport of the toxin to the exofacial surface.

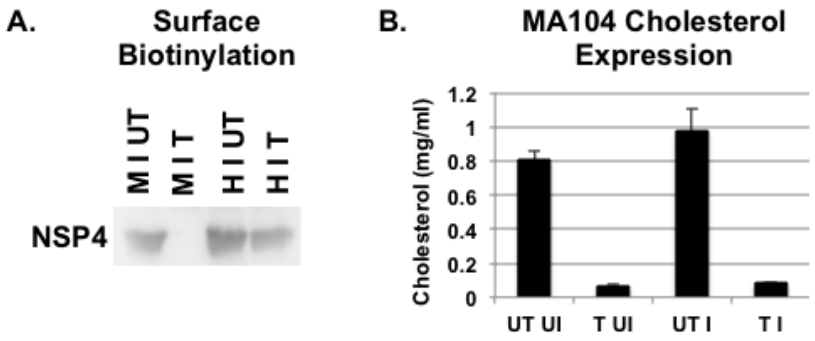

Figure 2.10. NSP4 expression upon intracellular cholesterol depletion. MA104 and HT29.f8 cells were treated with lovastatin to deplete intracellular cholesterol and infected with SA11.4f at an MOI of 5. **A.** Cells were surface biotinylated at 6 h post infection, proteins were precipitated with streptavidin agarose, separated via SDS-PAGE and subjected to Western blot with rabbit anti-$NSP4_{112-140}$. **B.** The concentration of cholesterol (mg/ml) was quantitated with the Wako CholE Kit.

2.4 Discussion

RV NSP4 is a multifunctional glycoprotein with roles in viral replication, pathogenesis, and viral particle assembly (Ball et al., 2005). It serves as a viroporin, eliciting Ca^{2+} efflux from the ER and initiates autophagy, a step required for particle

maturation (Crawford et al., 2012; Hyser et al., 2010). RV NSP4 also is known to interact with caveolin-1 (Parr et al., 2006), to localize to caveolae on the PM (Storey et al., 2007), and to be secreted from cells in different forms (Bugarcic and Taylor, 2006; Gibbons et al., 2011; Zhang et al., 2000). Our lab has shown that NSP4 traverses the PM with the C-terminus exposed to the extracellular environment and the full-length protein is secreted into culture media (Gibbons et al., 2011). Zhang, et al. showed that a cleavage product of NSP4 (residues 112-175) is released into the culture media of MA104 cells when over-expressed (Zhang et al., 2000) and Bugarcić, et al. shows a full-length and partially EndoH-resistant form secreted into the culture media of Caco-2 cells (Bugarcic and Taylor, 2006). Our lab has shown that transport kinetics of NSP4 differ in cultured cells of different tissue origins (Gibbons et al., 2011), suggesting that NSP4 uses multiple pathways with different kinetics to reach the PM, including both a soluble and a vesicular pathway. The precise mechanism by which NSP4 traffics from the ER to the PM and is secreted remains unclear.

In this study we set out to show that NSP4 interacts with CyPA, CyP40 and HSP56, which would influence NSP4 transport. RV NSP4 directly interacted with the cyclophilins by co-localization, co-immunoprecipitation, and FRET analyses and with HSP56 by co-localization and FRET analyses. CyPA, CyP40, and HSP56 are immunophilins that possess PPIase activity and are important for protein folding (Davies and Sanchez, 2005; Fischer et al., 1989). HSP56 and CyP40 are also capable of binding HSP90 and are found as part of steroid heterocomplexes in the nucleus (Davies and Sanchez, 2005). HSP56 is a calmodulin binding protein (Davies and Sanchez, 2005), and

localizes to microtubules (Czar et al., 1994). CyPA, CyP40, and HSP56 all bind dynein, and play a role in retrograde transport of proteins (Czar et al., 1994; Galigniana et al., 2002; Galigniana et al., 2004; Galigniana et al., 2001). Even with evidence that CyP40 and HSP56 are complexed with steroid receptors as well as with a dynein/dynactin complex, it remains unknown whether CyPA is directly involved in the complex. However, it is known that the PPIase subunit of these immunophilins, including CypA, are required for dynein binding (Pratt et al., 2006).

Our findings revealed that these proteins interact with NSP4, but are not solely responsible for the transport pathway of NSP4 to the PM. We demonstrated that silencing the expression of Cav-1, CyPA, and CyP40 with silencing RNA failed to reduce PM-localized NSP4. Blocking the expression of these proteins disturbed the normal intracellular distribution of NSP4, contributing to a more dispersed pattern throughout the cytoplasm. It is likely that the immunophilins are playing a role in protein folding to the non-native RV NSP4. Alternatively, the immunophilins could be necessary for some aspects of the intracellular transport of NSP4, but not for transport of NSP4 to reach the PM. Silencing of the immunophilins and Cav-1 did not affect NSP4 expression intracellularly (detected by Western blot and digital imaging), nor did it affect the amount of virus produced (detected by fluorescent focus assay; data not shown).

Chaperone proteins including this group of immunophilins are known to prevent aggregation of proteins under ER stress. It is well known that rotavirus infection induces ER stress and alters intracellular Ca^{2+} levels (Hyser et al., 2010; Michelangeli et al.,

1991; Zambrano et al., 2008). The up-regulation of the expression of chaperone proteins BiP and endoplasmin (HSP90B1) by both RV infection and NSP4 expression also have been demonstrated (Xu et al., 1998). HSP56 and CyP40 are known binding partners of HSP90 (Ratajczak et al., 2009), which could be involved in the folding of non-native intracellular proteins. These roles in chaperoning activity could account for the intracellular redistribution of NSP4 seen upon silencing of HSP56 and CyP40, but additional studies are needed to determine their exact roles.

In RV-infected cells, NSP4 leaves the ER and is found in punctate structures in the cytoplasm (Crawford et al., 2012), associates with microtubules (Berkova et al., 2007; Xu et al., 2000), and localizes at the PM caveolae (Storey et al., 2007). RV NSP4 travels by an unconventional protein transport pathway, bypassing the Golgi apparatus as it traffics from the ER to the PM (Jourdan et al., 1997; Nickel, 2005). Characteristics of the unconventional transport pathway include: (i) lack of a conventional signal peptide within the protein, (ii) exclusion from the ER and/or Golgi combined with the lack of Golgi-dependent modifications, and (iii) transport not affected by Brefeldin A (Nickel, 2003). NSP4 clearly fits these criteria and can be added to the growing list of proteins that traffic by an unconventional route.

When we silenced Cav-1 and CyPA, there was a redistribution of NSP4 to co-localize with a Golgi marker protein, golgin-97 (**Figure 2.5**). Yet, Endo H digestion of NSP4 from CyPA silenced cells remained sensitive to digestion (**Figure 2.6**). Therefore, silencing of Cav-1 and CyPA are contributing to a redistribution of the Golgi protein and not to NSP4 transport to the Golgi. NSP4 and the ER marker, PDI, in Cav-1- and CyPA-

silenced cells co-localized less than in untreated cells, indicating that silencing Cav-1 and CyPA have some influence on the intracellular distribution of NSP4, although the affect remains unknown.

He, et al. have reported that CyPA is a restrictive factor in RV replication by contributing to the host cell IFN-β production, and that silencing CyPA results in enhanced RV production (He et al., 2013; He et al., 2012). Other reports suggest that CyPA is a positive regulator of coronavirus, hepatitis C virus, and cytomegalovirus maturation and transport (Anderson et al., 2011; Keyes et al., 2012; Tanaka et al., 2013). Our data failed to show a significant effect of silencing CyPA on RV replication, but there was a notable change in the cellular architecture upon silencing of CyPA. In particular, the PM marker that is expressed on the exofacial surface in untreated cells, $Na^{+/}K^{+}$ATPase, also was expressed intracellularly in RV-infected, CyPA-silenced cells (**Figure 7-B3**). While further investigation is necessary to determine the function of CyPA in redistribution of these proteins and organelles, our studies clearly showed that inhibiting CyPA expression does not prevent NSP4 from reaching the cell surface.

A previous study indicated that CyPA is important for intracellular lipid trafficking during HCV infection (Anderson et al., 2011). Reports show that the HCV protein NS5A is displaced upon inhibition of CyPA with a small molecule inhibitor in addition to changes in lipid droplet size (Anderson et al., 2011). Inhibition of cholesterol production by lovastatin in the present study resulted in decreased NSP4 transport to the cell surface. It is possible that CyPA may be involved in the regulation of lipid and cholesterol transport during RV infection as well, but is not sufficient alone for efficient

NSP4 transport. Many questions remain. The answers to these questions may reveal additional roles of NSP4 and disclose a more complete picture of NSP4 transport and activity.

3. INTRACELLULAR CO-LOCALIZATION OF CAVEOLIN-1 AND THE IMMUNOPHILINS, YEAST TWO-HYBRID ANALYSIS OF NSP4 AND HSP56, AND EXPRESSION OF CAVEOLIN-1 AND THE CYCLOPHILINS IN ROTAVIRUS INFECTION

3.1 Introduction

Rotavirus NSP4 interacts with Cav-1, CyPA, CyP40, HSP56, and cholesterol but the roles of these interactions need additional exploration (Gibbons, 2007; Parr et al., 2006; Schroeder, 2009). Silencing of these proteins using siRNA fails to inhibit NSP4 from reaching the exofacial PM in both MA104 and HT29.f8 cells (Yakshe, In Preparation). Upon completion of the studies discussed in **Section 2**, several things were noticed that elicited further questions and experimentation. First, it was noted that the fluorescence intensities of the cyclophilins consistently were higher in cells infected with RV than in uninfected cells while performing LSCM indicating RV up-regulates expression of the cyclophilins. Second, the intracellular distributions of Cav-1 and the immunophilins were very different from each other. Lastly, the difficulty of analyzing HSP56 by Western blot led us to explore another method to evaluate the interaction of NSP4 with this immunophilin, the yeast two-hybrid system. This study further evaluated the roles of these proteins in intracellular trafficking of RV NSP4. We used Western blot analysis, immunofluorescence imaging techniques, and yeast two-hybrid studies to investigate intracellular NSP4 interactions with Cav-1 and the immunophilins.

3.2 Materials and Methods

3.2.1 Cells and Viruses

African green monkey kidney cells MA104 (ATCC, Manassas, VA), a cloned human intestinal cell line HT29.f8 from parental HT29 cells (Mitchell and Ball, 2004), and Madin-Darby canine kidney (MDCK) cells (ATCC) were cultured in Dulbecco's modified Eagle's media (DMEM; CellGro, Manassas, VA) supplemented with 10% fetal bovine serum (FBS; Caisson Labs, North Logan, UT), 0.1 mM non-essential amino acids (NEAA; Gibco, Grand Island, NY), 1 mM sodium pyruvate (Gibco), and 2 mM L-glutamine (Lonza, Basel, Switzerland) at 37°C with 5% CO_2 in a humidified environment. Penicillin-streptomycin was not used in the culture mixture to prevent perturbation cell-signaling pathways. RV SA11 clone 4F (SA11.4F; gift from Mary Estes, Baylor College of Medicine, Houston, TX) was expanded in MA104 cells (Yakshe, 2015) and stored at -80°C.

3.2.2 Infection

Cells were serum starved by incubation in serum-free DMEM for 14 hours before infection. Cells were infected with SA11.4f at a multiplicity of infection (MOI) of 2 for imaging. In brief, virus was thawed on ice and sonicated using a cuphorn attachment with ice for 5 min using a Misonix Sonicator 3000 at 45W (Misonix, Inc., Farmingdale, NY). Virus then was activated in serum-free DMEM with 1 μg/ml trypsin (Worthington Biochemical, Lakewood, NJ) at 37°C for 30 min. The activated RV was added to cells diluted in serum-free DMEM supplemented with 1 μg/ml trypsin at the specified MOI and rocked at 37°C with 5% CO_2 in a humidified environment for 1 h. The viral

inoculum was removed, cells were washed with media to remove unbound virus, and serum-free DMEM was added for various times of infection as indicated in the results section.

3.2.3 Time Course of Expression of Cav-1, CyPA, and CyP40 in RV-infected Cells

MA104 and HT29.f8 cells were plated in 24-well plates and grown until ~80% confluent and serum starved overnight by replacing DMEM with 10% FBS with serum-free DMEM. Cells were infected with SA11.4f RV at an MOI of 2.0. One well of cells was lysed immediately following virus adsorption and every 30 minutes thereafter until 7 hpi. Cells were collected at these time points by addition of 300 µl ice-cold SDS-free RIPA lysis buffer (150 mM NaCl, 50 mM Tris-base, 10% NP-40, 0.5% DOC, pH=8.0) containing protease inhibitors (1.2mM AEBSF, 0.46µM Aprotinin, 12.3µM E-64, 14µM Bestatin, 112µM Leupeptin and 1.16µM Pepstatin) and 0.2 mM phenylmethylsulfonyl fluoride (PMSF). Cell lysates were transferred to 1.2 ml microcentrifuge tubes and stored at -20°C for analysis. The protein concentrations were measured using the Pierce Micro BCA Protein Assay Kit according to the manufacturer's instructions and equal concentrations of protein were loaded and separated on a 12% SDS-PAGE gel, transferred to a 0.45 µm nitrocellulose membrane, and subjected to Western blotting.

3.2.4 Protein Separation by SDS-PAGE and Western Blotting

Western blotting was used to determine the expression of Cav-1, CyPA, and CyP40 at different time points following RV infection. Briefly, equal protein concentrations were dissolved and dissociated in sample reducing buffer, loaded and resolved on a 12% or 15% SDS-polyacrylamide gel (NEXT GEL; Amresco). The proteins were

electroblotted to a 0.45 μM-pore size nitrocellulose membrane (Bio-Rad, Hercules, CA) as per the manufacturer's instructions (Mini-Protean II and Trans-Blot, Bio-rad) at 4°C in Tris-Glycine buffer containing 20% methanol. The nitrocellulose membranes were blocked in 10% (wt/vol) NFDM in PBS for 1 h at room temperature. The membranes then were incubated with primary antibodies diluted in 2.5% NFDM in PBS for 3 h at room temperature with rocking. The membranes were washed once with PBS, twice with PBS-Tween-20 (0.5%), and again with PBS. Secondary antibodies conjugated to HRP were diluted in 2.5% NFDM in PBS, added to the membranes, and incubated for 1 h at room temperature with rocking. The membranes were washed as above and reacted with Immobilon Western Chemiluminescent HRP Substrate (Millipore, Billerica, MA) as per the manufacturer's instructions. The protein-specific bands were visualized using the ImageQuant LAS 4000 gel imager (GE Healthcare Life Sciences, Pittsburgh, PA), and densitometric analyses were performed using ImageJ (NIH).

3.2.5 Densitometry

Gel images were analyzed via ImageJ using the gel analysis function. Briefly, the intensity of each protein band was given a value for the protein being evaluated and for the glyceraldehyde-3-phosphate dehydrogenase (GAPDH) control in the same lane. Each band was background subtracted and measured within the linear range. The intensity value of the protein band was divided by the intensity value of the GAPDH control band to obtain a ratio of the protein amount to protein loading control (GAPDH band intensity).

The experiments were performed in triplicate and the standard error was calculated using:

$$SE = \sqrt{\frac{\sum(X - M)^2}{n - 1}}$$

where *X* is the sample value, *M* is the mean, and *n* is the number of experimental replicates.

3.2.6 Laser Scanning Confocal Fluorescent Microscopy (LSCM)

MDCK cells were plated on #2 German borosilicate Labtek well coverslips (Nalge Nunc International, Naperville, IL). At specific time points, the medium was removed, cells were washed with ice-cold PBS and fixed and permeabilized with ice-cold methanol:acetone (1:1, vol/vol) for 20 min at -20°C. The fixed and permeabilized cells were prepared for immunofluorescence using a modification of a previously described method (Storey et al., 2007). Briefly, fixed cells were blocked with 3% NFDM in PBS and incubated with primary antibodies (**Table 3.1**) diluted in 0.5% NFDM in PBS for 3 h at room temperature. After the cells were washed three times with PBS the secondary antibodies conjugated to a fluorescent dye (**Table 3.2**) were diluted in 0.5% NFDM, and incubated for 1 h at room temperature in the dark. Primary and secondary antibody controls were included to exclude non-specific reactivity of the antibodies. Cells were washed as above in the dark and the fluorescent images were captured with a MRC-124MP BioRad LSCM system (BioRad) using a Zeiss inverted Axiovert microscope (Carl Zeiss, Inc., Thornwood, NY), a 63X Zeiss oil apochromat objective, and the 488-, 568- or 647-nm excitation lines of an argon/krypton ion laser source or the 405 nm line of a Ti:Sapphire diode laser. Fluorescence emission from the labeled cells cultured on

coverslips was detected using 405-nm excitation with a bandpass emission filter for the Pacific Blue™ fluorophore (ex=410 nm, em=455 nm) (blue channel) and 568 nm excitation with a HQ598/40 band-pass emission filter for Cy5 fluorophore (ex=650 nm, em=670 nm) (red channel). LaserSharp 3.0 (BioRad) and Image J (public domain Java image-processing program inspired by NIH Image) were used to capture the pixilated photomultiplier tube (PMT) data, convert the image data to .tiff format, and adjust for contrast curves to construct the final images.

Table 3.1. Primary Antibodies Used in Immunofluorescence

Primary Antibody Target	Host Animal	Antibody Dilution	Comments
Caveolin-1	Rabbit	1:100	caveolae structural protein
Cyclophilin A	Rabbit	1:50	chaperone; cytoplasm localized peptidyl-prolyl isomerase
Cyclophilin 40	Rabbit	1:200	chaperone; mitochondrial localized peptidyl-prolyl isomerase
Heat Shock Protein 56	Rabbit	1:75	chaperone; heat shock protein
Caveolin-1	Mouse	1:50	caveolae structural protein
Cyclophilin A	Mouse	1:50	chaperone; cytoplasm localized peptidyl-prolyl isomerase

Table 3.2. Secondary Antibodies Used in Immunofluorescence

Secondary Antibody Target	Host Animal	Antibody Dilution	Comments
Mouse IgG (H+L)	Goat	1:100	Cy5 conjugated
Rabbit IgG (H+L)	Goat	1:100	Pacific Blue™ conjugated

3.2.7 Co-localization

Cells were infected and treated as above, incubated with antibodies targeting the immunophilins and a secondary antibody labeled with Pacific Blue™ and Cy-5 labeled

rabbit anti-NSP4$_{150\text{-}175}$ together. Images were collected as above. The extent of co-localization of the pixels in the confocal images were calculated with the Image J Coloc 2 plugin using the overlap coefficient (MOC) according to Manders (Manders, 1993),

$$\mathrm{MOC}=\frac{\sum_i (R_i \times G_i)}{\sqrt{\sum_i R_i^2 \times \sum_i G_i^2}}$$

where R_i and G_i represent the intensity values of the red and green channels, respectively, in a given pixel, i (Manders et al., 1992).

3.2.8 Cloning of HSP56 into Gateway® Entry-level Vector, pENTR11

The HSP56 cDNA clone in a pCMV6-XL5 vector was purchased from OriGene Technologies. (Rockville, MD) and amplified using a cloned Pfu DNA polymerase (Stratagene, La Jolla, CA) with primers that produce a blunt end and an XhoI site (Forward-ATGATGCAAATCTGCGACACCTACAA, Reverse with XhoI site-TCTAGATATCTCGAGTCAGTGGCCCCAATTGCCGA). The resulting PCR product was digested with XhoI (Fermentas, Thermo-Fisher) and the pENTR11 vector was digested with XhoI and XmnI (Fermentas, Thermo-Fisher) for 10 min at 37°C. The PCR fragment was isolated with the UltraClean® PCR Clean-Up kit (Mo Bio, Carlsbad, CA) according to the manufacturer's instructions. The linear fragment of pENTR11 was separated on an 1% agarose gel and purified with the UltraClean® GelSpin® DNA Extraction Kit (Mo Bio) according to the manufacturer's instructions. DNA concentrations of the purified PCR fragment and linearized vector were determined by measuring the absorbance on a Nano Drop 1000 spectrophotometer.

3.2.9 Ligation of HSP56 PCR Fragment into pENTR11 Vector and Amplification of pENTR11-HSP56

The HSP56 PCR fragment and pENTR11 vector were ligated in a 3:1 ratio using 1 µl T4 ligase (NEB) in a 20 µl reaction. The ligation mixture was incubated at room temperature for 10 min. The T4 ligase was inactivated at 65°C for 10 min. Five µl of the inactivated ligation mixture was transformed into chemically competent DH5α *E. coli*. Briefly, the *Escherichia coli* (*E. coli*) were incubated with the ligation mixture for 15 min on ice, heat shocked at 42°C for 60 sec and added to 1 ml pre-warmed to 37°C Luria-Burtani media (LB; 10 g/L tryptone, 5 g/L yeast extract, and 5 g/L NaCl). The mixture was shaken at 250 rpm for 1 h at 37°C. The *E. col*i was pelleted by centrifugation at 2500 rpm for 5 min and resuspended in 50 µl LB media. The *E. coli* were plated on LB agar plates containing 50 µg/ml kanamycin and grown at 37°C overnight.

Individual colonies were picked and expanded in 5 ml LB media with 50 µg/ml kanamycin with shaking at 250 rpm and 37°C until the optical density at 600 nm (OD_{600}) reached 0.4. The *E. coli* was pelleted at 2500 rpm for 10 min and the media decanted and discarded. The pENTR11-HSP56 plasmid was isolated from the *E. coli* using the GeneJET Plasmid MiniPrep Kit (Fermentas, Thermo Scientific) as per the manufacturer's protocol. The concentration of the resulting plasmid was measured by absorbance on a NanoDrop 1000 spectrophotometer and was stored at -20°C. Restriction

enzyme digestion of the plasmid and sequencing of the insert were used to verify correct plasmid construction.

3.2.10 Recombination of pENTR11 Vectors with Y2H Plasmids

pENTR11 contains attL sites while the bait and prey plasmids, pDEST™32 and pDEST22™, respectively, contain attR sites. The entry vector (pENTR11) and destination vector (bait or prey) were mixed 1:1 (150 ng/µl) with 2 µl of LR Clonase II enzyme and incubated for 1 h at room temperature. LR Clonase II is a proprietary mixture that catalyzes a recombination reaction between attL and attR sites. The enzyme was inactivated with 1 µl of Proteinase K and incubated at 37°C for 10 min. The resulting recombinant plasmids were transformed into DH5α *E. coli* for amplification. Briefly, the *E. coli* was incubated with the ligation mixture for 15 min on ice, heat shocked at 42°C for 45 sec and added to 1 ml 37°C LB media. The mixture was shaken at 250 rpm for 1 h at 37°C. The *E. coli* was pelleted by centrifugation at 2500 rpm for 5 min and resuspended in 50 µl LB media. The *E. coli* transformed with the pDEST22™ recombinants were plated on LB agar plates containing 100 µg/ml ampicillin and the pDEST32™ recombinants were plated on LB agar plates containing 10 µg/ml gentamycin and grown at 37°C overnight. Both pDEST22™ and pDEST32™ contain the ccdB gene within the attR recombination sites, so vectors that have not undergone recombination will not grow on LB media. Vector sequences were verified using the manufacturer's suggested sequencing primers for the PDEST22™ and pDEST32™ vectors.

3.2.11 Yeast Two-hybrid Analysis of NSP4 Interaction with HSP56

The ProQuest™ Two-Hybrid System was used for yeast two-hybrid analysis as described previously (Parr et al., 2006). NSP4 was used as the prey while HSP56 was used as the bait. The prey vector, pDEST22™, contains a transcription factor activation domain, while the bait vector, pDEST32™, contains a transcription factor DNA-binding domain specific to the *GAL4* gene in the MAV-203 *S. cerevisiae* strain, which has been engineered to control the reporter gene *lacZ*, and auxotrophic markers, *HIS3* and *URA3*. Genes inserted into the pDEST22™ and pDEST32™ vectors will be produced as fusion proteins with the *GAL4* activation domain and DNA-binding domains, respectively. When the proteins interact with each other, the activation and DNA-binding domains come within interacting distance of each other and cause activation of transcription of the *GAL4* gene. The transcription of *GAL4* can be verified by analysis of *lacZ, HIS3*, and *URA3* activation. When *lacZ* has been transcribed, an X-gal (5-bromo-4-chloro-3-indolyl-β-D-galactopyranoside) assay is performed and yeast will turn blue. When *HIS3* has been transcribed, cells will grow in the presence of 3-Amino-1,2,4-triazole (3AT) and absence of histidine. When *URA3* has been transcribed, cells will grow in the absence of uracil and not grow in the presence of 5-fluorouracil (5FOA).

To perform the yeast two-hybrid analyses, yeast are grown on complete synthetic media (CSM) lacking leucine (leu) and tryptophan (trp) for 24 h at 30°C. Yeast are then replica plated using sterile velvet squares and grown for 24 h at 30°C on CSM containing 12.5 μg/ml 3AT, 50 μg/ml 3AT, or 100 μg/ml 3AT and lacking histidine (his), leu, and trp (CSM-leu-trp-his+3AT), CSM containing 0.2% 5FOA and lacking leu

and trp (CSM-leu-trp+5FOA), CSM lacking leu, trp, and uracil (ura) (CSM-leu-trp-ura), and YPAD yeast medium (1% bacto yeast extract, 2% bacto peptone, 2% glucose, and 2% bacto agar) overlayed with a 125-mm Whatman 541 filter paper for X-gal analysis (GE Life Sciences, Pittsburgh, PA) **Table 3.3**. The plates are replica cleaned after 24 h of growth and allowed to grow for 48 h at 30°C until analysis. Replica cleaning is performed using sterile velvet squares and pressing the plates with moderate pressure to remove as many yeast as possible. All yeast growth was recorded after 48 h of growth following replica cleaning.

Table 3.3. **Media Used for Plating and Selecting Yeast Transformed with Plasmids Expressing pDEST22™-NSP4 and pDEST32™-HSP56**

Media Base	Additives	Media Deficiency	Purpose
CSM	-	-leucine	Transformation Controls
CSM	-	-leucine, -tryptophan	All controls and interaction test
CSM	+12.5mM 3AT, +50mM 3AT, +100mM 3AT	-leucine, -tryptophan, -histidine	Evaluate growth while *HIS3* is inhibited by 3AT
CSM	+0.2% 5FOA	-leucine, -tryptophan	Evaluate growth while uracil production is inhibited by 5FOA
CSM	-	-leucine, -tryptophan, -uracil	Evaluate growth without uracil
YPAD	-	-	X-Gal Assay

Controls included MAV-203 transformed with the plasmids listed in **Table 3.4**. A negative control consists of MAV-203 with no plasmids, two self-activation controls, pDEST22™ with pDEST32™-HSP56 and pDEST32™ with pDEST22™-NSP4, and 5 controls provided with the ProQuest Y2H system, which ranks protein interactions from

no interaction to very strong interaction (**Table 3.5**).

Table 3.4. **Yeast Two-hybrid Plasmid Combinations for Each Interaction Test**

Plate	Binding Domain	Activation Domain	Media	Purpose
1	None	None	CSM-Leu CSM-Leu-Trp	Transformation Control
2	pDBLeu	None	CSM-Leu	Transformation Control
3	pDEST32™-HSP56	pEXP-AD502	CSM-Leu-Trp	Self-activation Control
4	pDBLeu	pEXP-AD502	CSM-Leu-Trp	Self-activation Control
5	pDBLeu	pDEST22™-NSP4	CSM-Leu-Trp	Self-activation Control
6	pDEST32™-HSP56	pDEST22™-NSP4	CSM-Leu-Trp	Interaction Test

*Two controls in this table test for self-interactions of HSP56 and NSP4 with the *GAL4* activation and binding domains in the bait and prey plasmids. Negative controls include the MAV-203 yeast strain with no plasmids, the *GAL4* activation domain alone, the *GAL4* binding domain alone, and the *GAL4* binding and activation domains together.

Table 3.5. Control Yeast Strains Provided with the ProQuest™ Two-Hybrid System

Control Strain*	Plasmids	Insert	Interaction
A	pPC97 pPC86	None None	None
B	pPC97-RB pPC86-E2F1	Human RB aa 302-928 Human E2F1 aa 342-437	Very Weak
C	pPC97-*CYH2*^{S}-dDP pPC86-dE2F	*Drosophila* DP aa 1-377 *Drosophila* E2F aa 225-433	Weak
D	pPC97-Fos pPC86-Jun	Rat cFos aa 132-211 Mouse cJun aa 250-325	Strong
E	pCL1 pPC86	GAL4 aa 1-881 None	Very Strong

*A is the weakest interaction and E is the strongest interaction (Chevray and Nathans, 1992; Du et al., 1996; Fields and Song, 1989; Vidal, 1997; Vidal et al., 1996). This table is adapted from the manufacturer's manual.

3.3 Results

3.3.1 CyPA and CyP40 Expression, but Not Cav-1 Expression Were Up-regulated During RV Infection

It was previously determined that the RNA levels for CyPA and CyP40 remain constant during RV infection (Gibbons, 2007). However, during immunofluorescence assays, an increase in signal of CyP40 was consistently noted (data not shown). To determine if the intracellular protein expression of Cav-1, CyPA, and CyP40 were increased, time course experiments were performed in SA11.4f-infected cells. MA104 and HT29.f8 cells were infected with RV at an MOI of 2.0. Cells were collected and lysed before infection, after virus adsorption, and every 30 min to 1 h after infection until 7 hpi. Cell lysates were separated by SDS-PAGE, transferred to a nitrocellulose membrane, and blotted with either rabbit anti-CyPA, rabbit anti-Cyp40, or rabbit anti-Cav-1 followed by goat anti-rabbit-HRP. Western blots revealed that both CyPA and CyP40 expression were up-regulated after infection in both cell lines. CyP40 remained at undetectable levels until 4 hpi, while CyPA was slightly enhanced starting at 4 hpi, where it remained at a constant level (data not shown). Cav-1 expression remained constant up to 7 h post-infection, indicating that RV infection had no effect on Cav-1 expression (**Figure 3.1**).

3.3.2 Cav-1, CyPA, CyP40, and HSP56 Interacted at Differing Levels Intracellularly

Immunofluorescence was performed to determine the co-localization of Cav-1 and each of the immunophilins with each other. Only certain pairings were analyzed due to limited antibody selection. HSP56 co-localization with CyP40 was not determined

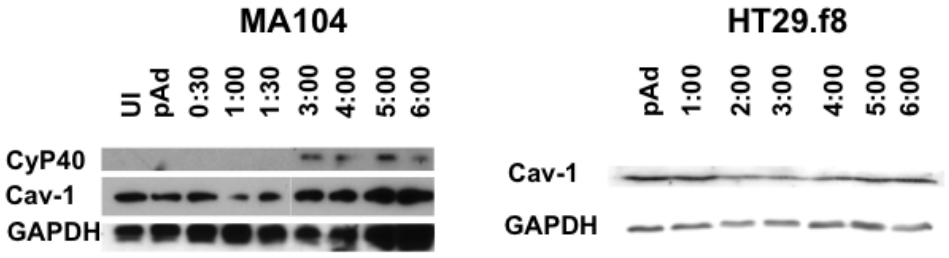

Figure 3.1. Expression of Cav-1 and CyP40 in MA104 and Cav-1 in HT29.f8 cells. Cells were uninfected or infected with RV SA11.4f at an MOI of 2.0 and collected at various timepoints post-infection (post adsorption to 6 h). Equal concentrations of cell lysates were separated on an SDS-PAGE, transferred to nitrocellulose and blotted with indicated antibodies.

because the antibodies were synthesized in the same host species. In each pairing, a rabbit host antibody and a mouse host antibody were used, and goat anti-mouse-Cy5 and goat anti-rabbit-PB secondary antibodies were used. Examples of images showing co-localization are displayed in **Figure 3.2** with the mean MOCs displayed to the right of the images. In all cases, the Costes value was above 0.95, indicating that the co-localization was not due to random signal correlation. The Costes value is obtained from a statistical significance test whereby the pixels from the analyzed images are scrambled and the signal correlations between the scrambled image and analyzed image are

measured. A Costes value of 0 indicates that the MOCs occur by random chance and a

Costes value

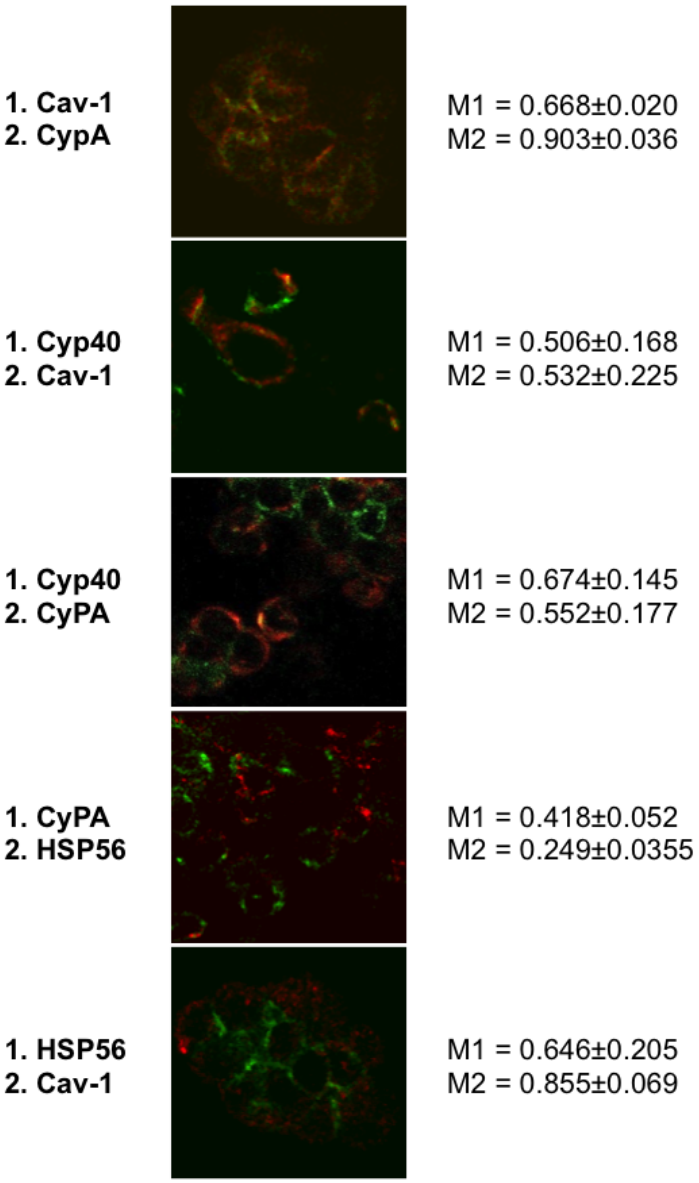

Figure 3.2 Co-localization of Cav-1, CyPA, CyP40, and HSP56 with each other. MDCK cells were fixed and permeabilized and incubated with antibodies directed against 2 of the proteins in pairs. Rabbit anti-PB and mouse anti-Cy5 were used to visualize the proteins. The first protein listed is seen in red and the second is seen in green. Mander's overlap coefficients are listed next to each protein pair (n=3).

Table 3.6. Results of Yeast Two-hybrid Assay

Yeast	CSM -leu-trp	CSM -leu-trp -his+3AT*	CSM -leu -trp+5FOA	CSM -leu-trp -ura	YPAD/ X-gal
Control A	+	-/-/-	-	-	-
Control B	+	+/-/-	+	-	-
Control C	+	+/-/-	-	-	+
Control D	+	+/+/+	-	+	++
Control E	+	+/+/+	-	++	++
Self-Activation Bait	+	-/-/-	+	-	-
Self-Activation Prey	+	-/-/-	+	-	-
NSP4/HSP56 Interaction Test	+	-/-/-	+	-	-

*CSM-leu-trp-his+3AT are plated at 3 concentrations 12.5 mM/ 50 mM/ 100 mM of 3AT

of 1 indicates that no randomized image has better co-localization than the analyzed image (Costes et al., 2004).

The results indicated that Cav-1 co-localized somewhat with CyPA (MOC=0.668) and CyP40 (MOC=0.532), and co-localized more with HSP56 (MOC=0.855). CyPA co-localized significantly with Cav-1 (MOC=0.903), and slightly with CyP40 (MOC=0.553), and HSP56 (MOC=0.418). CyP40 co-localized marginally with Cav-1 (MOC=0.506) and slightly more with CyPA (MOC=0.674), and we were not able to evaluate the co-localization with HSP56 due to antibody limitations. HSP56 co-localized more than anticipated with Cav-1 (MOC=0.646), and very little with CyPA (MOC=0.249). These results indicate that while some of the proteins co-localize with each other intracellularly, they do not associate with each other exclusively. These data support that a complex consisting of Cav-1 and these immunophilins likely does not exist in MA104 cells.

3.3.3 Yeast Two-hybrid Analysis of the HSP56 Interaction with NSP4

Yeast two-hybrid screening was performed with vectors containing full-length HSP56 and full-length NSP4. Protein expression of HSP56 from this vector was not confirmed because of limited antibody reaction using the Western blot technique. However, sequencing of the vector showed that HSP56 was correctly inserted into pDEST32™ for yeast two-hybrid analysis. In this system, there are four phenotypes analyzed to determine whether there is a protein-protein interaction: 1) yeast growth in the presence of (3AT), a *HIS3* inhibitor, 2) yeast color in the presence of X-gal, 3) yeast growth in the presence of uracil, and 4) absence of yeast grown in the presence 5-fluorouracil (5FOA). After plating on CSM-leu-trp, and replica plating onto the selective media (**Table 3.3**), the self-activation controls and transformation controls all grew as expected (**Table 3.6**). The control yeast strains (A-E) showed expected growth on selection media (**Table 3.6**). The interaction pair, pDEST22™-NSP4 and pDEST32™-HSP56, grew in a similarly to yeast control strain A (**Table 3.6**), indicating that HSP56 and NSP4 do not interact directly using yeast two-hybrid system analysis. However, these results cannot be proved without verifying yeast expression of HSP56.

3.4 Discussion

Rotavirus infection is known to up-regulate the unfolded protein response (UPR), as well as the expression of several proteins related to ER stress and Ca^{2+} homeostasis (Cuadras et al., 2002; Zambrano et al., 2011). Up-regulated proteins include immunophilin cyclophilin B, several chaperone proteins including endoplasmin and BiP, and caveolins (Cuadras et al., 2002; Xu et al., 1998). We know that NSP4 directly or

indirectly interacts with Cav-1 (Parr et al., 2006) and immunophilins, CyPA, CyP40, and HSP56 (**Section 2**), but the roles of these proteins in RV infection have not been fully determined.

This study further evaluated the amount of protein expression of Cav-1, CyPA, and CyP40 over time via Western blot analysis. The amount of CyP40 noticeably increased starting at around 4 hpi, the amount of CyPA increased, although less than CyP40, and the Cav-1 expression pattern didn't change throughout infection (**Figure 3.1**). This increase in protein expression simply could be the result of the host cell's need for chaperone proteins to fold the excess proteins in the ER. However, the reason for up-regulation of CyPA and CyP40 expression remains unknown.

We also evaluated the co-localization of Cav-1 and the immunophilins to determine whether they are interacting with each other under normal cellular conditions. It had become evident during previous microscopy studies that the intracellular distribution patterns of these four proteins varied significantly from each other. It is known that CyP40 and HSP56 compete for binding in a complex containing endoplasmin (Davies and Sanchez, 2005), and that CyPA, CyP40, and HSP56 all bind dynein and are involved in retrograde transport (Czar et al., 1994; Galigniana et al., 2004). Therefore, we wanted to determine if these proteins were co-localizing intracellularly with each other, since they were once reported to interact in a complex with each other. Co-localization analysis revealed that while the proteins do co-localize with each other, most of the co-localization was nominal **Figure 3.2**. Thus, while the proteins do co-localize somewhat,

they clearly are playing individual roles intracellularly rather than functioning as a complex.

Finally, we had a great difficulty detecting HSP56 on a conventional Western blot or by other techniques, such as a non-denaturing gel and dot-blot to determine if HSP56 was interacting directly with NSP4. We tried several different antibodies from several companies without success. We previously reported that HSP56 and NSP4 do resolve within 10 nm of each other via intracellular FRET, but this does not conclusively prove a direct interaction. In this study, we tested a direct interaction using the ProQuest™ Yeast Two-Hybrid System. We found that NSP4 and HSP56 likely do not interact directly using this method, confirming some of our co-localization data, which revealed little co-localization of NSP4 with HSP56 (**Section 2**). However, we know that NSP4 and HSP56 localize very close to each other intracellularly by FRET, so they may be both binding a common protein intermediate.

The roles of the Cav-1, CyPA, CyP40, and HSP56 proteins in the transport of NSP4 need to be further evaluated. Whether they interact simply to assist in protein folding or to aid in intracellular protein transport, it remains our interest to determine their function.

4. CONSTRUCTION OF A RECOMBINANT LENTIVIRUS EXPRESSING SHORT-HAIRPIN RNA TARGETING CAVEOLIN-1, CYCLOPHILIN A, CYCLOPHILIN 40, AND HEAT SHOCK PROTEIN 56

4.1 Introduction

In our studies, we have determined that NSP4 transport to the PM is not affected by silencing of Cav-1, CyPA, or CyP40 using surface biotinylation. The method of silencing (siRNA) is costly and therefore is limited to examination of a small number of cells. This led us to investigate a more cost-effective way to scale up our reactions so that we could quantify the amount of NSP4 that traffics to the exofacial PM. We chose to use a lentivirus-vector system that expresses a short hairpin RNA (shRNA), blocking the synthesis of a specific protein, similarly to siRNA.

A shRNA is processed in a similar fashion to a siRNA, but lentivirus delivery allows for continuous expression of the shRNA, instead of a transient transfection. A lentivirus-vector based delivery system allows for incorporation of the shRNA into the cellular genome for creation of a stable expressing cell line. After transduction of the lentivirus, the shRNA is incorporated into the cellular genome. Upon expression of the primary shRNA transcript, it associates with Drosha and DGCR8 in the nucleus for processing into a pre-shRNA. The pre-shRNA is transported into the cytoplasm, where it is further processed by Dicer and loaded onto the RISC complex (Rao et al., 2009).

We were unsure of how well cells would grow without Cav-1 or the immunophilins for an extended time, so we chose a system that would allow for inducible expression of

the shRNA. The TripZ system is a Tet-inducible shRNA expression system that allows for reversible protein knockdown. We obtained the proper packaging vectors, pCMVΔR8.91 containing the necessary lentivirus proteins driven by a CMV promoter, and pMD.G, which contains VSV-G.

In this study, we report construction of the vectors expressing shRNA directed against Cav-1, CyPA, CyP40 and HSP56. Stable HEK-293T cell lines expressing shRNA against Cav-1 and the immunophilins, and MA104 cell lines expressing shRNA against CyP40 and HSP56 were created. We also report the knockdown of these CyP40 and HSP56 and the transport of NSP4 to the cell surface in the presence of shRNA in MA104 cells.

An overview of the steps to create a shRNA-expressing lentivirus are outlined as follows:

- Design shRNA using siRNA design tools from Invitrogen, Dharmacon, and guidelines from Reynolds, et al. (Reynolds et al., 2004)
- Use the RNAi Central website to obtain a shRNA including the siRNA molecule with miR30 ends (Lab)
- Add restriction enzyme site to the shRNA inserts
- Ligate the shRNA sequence into the pTripZ vector
- Sequence vector
- Transfect HEK-293T cells with the pTripZ shRNA vector
- Select for cells containing the incorporated vector with puromycin
- Transfect cells with lentivirus packaging vectors, pCMVΔ8.91 and pMD.G

- Collect budded lentiviruses from media
- Titer lentiviruses by fluorescence forming units using VSV-G antibody
- Infect MA104 and HT29.f8 cells with lentiviruses
- Generate stable transgene-expressing MA104 and HT29.f8 cell lines
- Induce transgene expression and analyze for knockdown of specific proteins by WB

4.2 Materials and Methods

4.2.1 Vectors and *E. coli* Cells

Dr. Charles Long kindly provided us with all vectors needed for establishment of the lentivirus vector system. In addition, Dr. Long provided us with the HEK-293T cell line for stable expression of the shRNA insert and Stbl3 *E. coli* cells (Invitrogen) for growth of the large pTripZ vector containing the LTRs (Dharmacon). The lentivirus system consisted of pTripZ, pCMVΔR8.91, and pMD.G (**Appendix A**).

4.2.2 Expansion of Chemically Competent Stbl3 *E. coli* Stocks

Stbl3 *E. coli* were isolated from a single colony and grown in super optimal broth (SOB) media (20 g/L tryptone, 5 g/L yeast extract 5 g/L NaCl, and 2.5 mM KCl) overnight with shaking at 200 rpm at 37°C. Five ml of the started colony was placed in a 250 ml Erlenmeyer flask and shaken overnight at 200 rpm at room temperature until cultures reached an $OD_{600}$of 0.4. Cells were pelleted by centrifugation at 2500 rpm for 10 min at 4°C. All media was removed and cells were gently resuspended in 80 ml Inoue solution (55 mM $MnCl_2$, 15mM $CaCl_2$, and 250 mM KCl) at 4°C. Cells were pelleted at 2500 rpm for 10 min at 4°C, Inoue solution was removed and cells were gently

resuspended in 20 ml fresh Inoue solution with 15% sterile glycerol at 4°C. Cells were aliquoted into 50 µl aliquots and stored at -80°C. Transformation efficiency was checked with the pUC19 vector (Invitrogen).

4.2.3 shRNA Design

The shRNA were designed based on the rational outlined by Reynolds, et al (Reynolds et al., 2004). Three siRNA sequences were designed for each protein to be silenced to ensure the most efficient silencing results. The siRNA sequences were incorporated into primers that have miR30 sequences flanking each end using the website: http://cancan.cshl.edu/RNAi_central/RNAi.cgi?type=shRNA. The shRNA inserts were ordered as long oligonucleotides from Life Technologies (**Table 4.1**). An XhoI and EcoRI site was added to the 5' and 3' ends of the shRNA inserts, respectively, using the forward primer 5'-CAGAAGGCTCGAGAAGGTATATTGCTGTTGACAGTGAGCG-3' and reverse primer 5'-CTAAAGTAGCCCCTTGAATTCCGAGGCAGTAGGCA-3'. Briefly, the shRNA inserts were amplified with the primers containing the restriction endonuclease cleavage sites using Phusion® High-Fidelity DNA polymerase. The inserts were purified using the UltraClean® PCR Clean-Up Kit (Mo Bio) according the manufacturer's instructions.

4.2.4 Amplification and Isolation of pTripZ, pCMVΔR8.91, and pMD.G Vectors

The pTripZ vector was amplified in Stbl3 *E. coli*, while pCMVΔR8.91 and pMD.G were amplified in DH5α *E. coli*. Briefly, *E. coli* was placed on ice, mixed with 1 µl of

the vector, and incubated for 15 min. *E. coli* then were heat shocked at 42°C for 45 seconds and immediately placed on ice for 5 min. One ml of SOC media was added to

Table 4.1 shRNA Inserts Ordered from Life Technologies.

Protein	shRNA sequence*
Cav-1	TGCTGTTGACAGTGAGCG**AGCAGACGAGCTGAGCGAGAAGTA**GTGAAGCCAC AGATGTA**CTTCTCGCTCAGCTCGTCTGCC**TGCCTACTGCCTCGGA
	TGCTGTTGACAGTGAGCG**AACCTTCACTGTGACGAAATACTA**GTGAAGCCACA GATGTA**GTATTTCGTCACAGTGAAGGTG**TGCCTACTGCCTCGGA
	TGCTGTTGACAGTGAGCG**CAGTTCCAAGTTGCTAATACAGTA**GTGAAGCCACA GATGTA**CTGTATTAGCAACTTGGAACTT**TGCCTACTGCCTCGGA
CyPA	TGCTGTTGACAGTGAGCG**ACTAGCTGGATTGCAGAGTTAATA**GTGAAGCCACA GATGTA**TTAACTCTGCAATCCAGCTAGG**TGCCTACTGCCTCGGA
	TGCTGTTGACAGTGAGCG**CGTGGTGTTTGGCAAAGTGAAATA**GTGAAGCCACA GATGTA**TTTCACTTTGCCAAACACCACA**TGCCTACTGCCTCGGA
	TGCTGTTGACAGTGAGCG**ATGGCATCTTGTCCATGGCAAATA**GTGAAGCCACA GATGTA**TTTGCCATGGACAAGATGCCAG**TGCCTACTGCCTCGGA
CyP40	TGCTGTTGACAGTGAGCG**CGCTGCAACCTATAGCTTTAAGTA**GTGAAGCCACA GATGTA**CTTAAAGCTATAGGTTGCAGCT**TGCCTACTGCCTCGGA
	TGCTGTTGACAGTGAGCG**AGGAGCAATTGACAGTTGTTTATA**GTGAAGCCACA GATGTA**TAAACAACTGTCAATTGCTCCC**TGCCTACTGCCTCGGA
	TGCTGTTGACAGTGAGCG**CGGACAGTTCAAAGGCTGTTATTA**GTGAAGCCACA GATGTAA**TAACAGCCTTTGAACTGTCCA**TGCCTACTGCCTCGGA
HSP56	TGCTGTTGACAGTGAGCG**AGCAAGGACAAATTCTCCTTTGTA**GTGAAGCCACA GATGTA**CAAAGGAGAATTTGTCCTTGCG**TGCCTACTGCCTCGGA
	TGCTGTTGACAGTGAGCG**CGGTGGAGTTGTTTGAGTTTAATA**GTGAAGCCACA GATGTA**TTAAACTCAAACAACTCCACCT**TGCCTACTGCCTCGGA
	TGCTGTTGACAGTGAGCG**CGGGAGAAGATCTGACGGAAGATA**GTGAAGCCAC AGATGTA**TCTTCCGTCAGATCTTCTCCCT**TGCCTACTGCCTCGGA

* The siRNA sequences are seen in bold letters.

each tube and the tubes were shaken at 250 rpm for 1 h. The transformed *E. coli* were pelleted at 2500 rpm for 5 min, resuspended in fresh SOC, plated on LB agar with appropriate antibiotics, and grown overnight at 37°C. pTripZ was selected for with ampicillin (100 μg/ml) and zeocin (25 μg/ml), and pCMVΔR8.91 and pMD.G were selected for with ampicillin (100 μg/ml). Individual colonies were picked and expanded in 5 ml LB with shaking at 250 rpm overnight at 30°C for Stbl3 *E. coli* and 37°C for

DH5α *E. coli*. Each 5 ml culture was pelleted at 2500 rpm for 10 min and the media removed. The plasmids were isolated from the *E. coli* using the GeneJET Plasmid MiniPrep Kit (Thermo Fisher Scientific) according to the manufacturer's instructions. DNA concentrations were determined by measuring the absorbance on a NanoDrop 1000. Vectors were verified using restriction enzyme digestion.

4.2.5 Construction of shRNA-expressing Vectors

The pTripZ vector and amplified primers were subjected to endonuclease restriction with EcoRI and XhoI, gel purified, and ligated together using the T4 Ligase enzyme. Briefly, TripZ or shRNA oligonucleotides containing restriction enzyme sites were added to 2 µl of 10X FastDigest buffer, 1 µl each of EcoRI and XhoI (Fermentas FastDigest), and enough water to bring the reaction to a final volume of 20 µl. The reaction was incubated in a 37°C water bath for 1 h. pTripZ and the shRNA oligonucleotides were gel-purified through a 1% agarose gel and the correct band was isolated with the UltraClean® GelSpin® DNA Extraction Kit (Mo Bio) according to the manufacturer's directions.

The linearized pTripZ vector and the restricted shRNA oligonucleotides were ligated together with T4 DNA Ligase (NEB). Molar ratios were calculated for the vector and insert and added to the reaction in a 1:3 molar ratio. Two µl 10X T4 ligase buffer (NEB), 1 µl T4 DNA Ligase, and nuclease-free water were added for a final volume of 20 µl. The reaction was incubated at room temperature for 10 min, or in some cases, 16°C overnight. The reaction then was heated to 60°C for 10 min to inactivate the ligase and the resulting TripZ vector was transformed into Stbl3 *E. coli* as described above. The *E.*

coli was grown at 30°C because the 14 kb vector was very large and could not be maintained if the bacteria were grown at higher temperatures. The vector was isolated from *E. coli* as above and the concentration read by absorbance on a NanoDrop 1000.

4.2.6 Puromycin Kill Curve for HEK-293T, MA104, and HT29.f8 Cells

HEK-293T, MA104 and HT29.f8 cells were plated in 48-well plates and grown until ~85% confluent. Puromycin dissolved in DMSO was added to the media at 0-15 μg/ml in triplicate. Media and puromycin were refreshed every 2 days and cells were assessed by light microscopy every day from the third day of treatment until the sixth day of treatment. DMSO was added to cells at the same volumes as a control.

4.2.7 Transfection of pTripZ-shRNA Vectors into HEK-293T Cells

HEK-293T cells were grown until ~85% confluent and transfected with pTripZ using Lipofectamine 2000. Briefly, 1 μl of Lipofectamine was added to 100 μl of serum-free DMEM, and 500-1000 ng pTripZ vector was added to 100 μl of serum-free DMEM. The solutions were mixed, incubated for 5 min at room temperature, and added to the cells without removing the growth media. The cells were treated with 1 μg/ml doxycycline and incubated for 48 h at 37°C. Induced cells were analyzed for transgene expression using an Olympus IX-70 epi-fluorescence microscope equipped with a mercury arc lamp and a Texas Red™ filter cube (Olympus).

4.2.8 Selection of HEK-293T Cells for Stable Expression of pTripZ-shRNA

Transfected HEK-293T cells were grown in 48-well plates in DMEM supplemented with 5 μg/ml puromycin. Media was replaced every two days. At 10 days post-transfection the cells were treated with 1 μg/ml doxycycline and incubated for 48 h at

37°C. Induced cells were analyzed for transgene expression using an Olympus IX-70 epi-fluorescence microscope. Most cells were expressing the transgene at 14 days post-transfection. Cells were expanded into 6-well plates and then into 25-cm^2 tissue-culture flasks. Stocks of cells were frozen down in 10% DMSO and 50% FBS.

4.2.9 Transfection of Packaging Vectors, pCMVΔR8.91 and pMD.G into HEK-293T Cells and Purification of Lentivirus Particles

HEK-293T cells expressing the transgenes and under selection of puromycin were grown until ~85% confluent in 6-well plates. Transfection of pCMVΔR8.91 and pMD.G was performed with Lipofectamine as above, scaled up appropriately in a ratio of 1 μg pCMVΔR8.91 to 1.7 μg pMD.G. The transfected cells were incubated overnight and the media was removed and replaced with DMEM containing 5% FBS. Cells were incubated for and additional 48 h for lentivirus production.

Supernatants were collected from transfected cells and centrifuged at 1000 rpm for 10 min to remove cellular debris. The supernatant containing the budded lentivirus was collected, mixed well and aliquoted into 250 μl fractions. The lentivirus stocks were frozen for further use at -80°C.

4.2.10 Titer of Lentivirus Particles Containing shRNA Inserts

HEK-293T cells were plated in 24-well plates and grown until ~85% confluent. Lentivirus was serial diluted in triplicate and added to the HEK-293T cells. After incubation for 48 h post-transduction, the cells were fixed with 1:1 methanol:acetone for 15 min at -20°C. The cells were blocked with 5% non-fat dry milk (NFDM) and RV particles were labeled with rabbit anti-inactivated SA11.4f and goat anti-rabbit-Cy5.

Fluorescent colonies were counted using an Olympus IX70 inverted epi-fluorescence microscope and titers were determined.

4.2.11 Transduction of Lentivirus Particles into MA104 and HT29.f8 Cells and Construction of Stable Transgene-expressing Cell Lines

MA104 and HT29.f8 cells were grown until ~85% confluent. Recombinant lentivirus was added to the cells at an MOI of 1.0 in serum-free DMEM. DMEM with 10% FBS and 7.5 μg/ml puromycin was added to the cells without removing the lentivirus inoculum 6 hours post transduction. The cells were maintained in DMEM with 10% FBS and 7.5 μg/ml puromycin for 10 days with media changes every 2 days. The HT29.f8 cells did not survive and were discarded. The MA104 cell lines were expanded and stocks were frozen at -80°C.

4.2.12 Doxycycline Induction of shRNA Expression and Quantification of Knockdown in Transduced MA104 Cells

Transduced MA104 cells under puromycin selection were grown in 24-well plates until ~85% confluent. Doxycycline (1 μg/ml) was added to the cells and cells were incubated for 48 h. Cells were visualized via epi-fluorescence to verify transgene expression. Cells were lysed with SDS-free RIPA lysis buffer (150 mM NaCl, 50 mM Tris-base, 10% NP-40, 0.5% DOC, pH=8.0) containing protease inhibitors (1.2mM AEBSF, 0.46μM Aprotinin, 12.3μM E-64, 14μM Bestatin, 112μM Leupeptin and 1.16μM Pepstatin; Amresco, Solon, OH) and 0.2 mM phenylmethylsulfonyl fluoride (PMSF; Sigma, St. Louis, MO). Cell lysates were separated on a 12% SDS-PAGE gel, transferred to a nitrocellulose membrane, and subjected to Western blot.

4.2.13 RV Infection and Surface Biotinylation of Transduced MA104 Cells

Cells were infected with SA11.4f at a MOI of 5. Briefly, virus was thawed on ice and sonicated using a cuphorn attachment with ice for 5 min using a Misonix Sonicator 3000 at 45W (Misonix, Inc., Farmingdale, NY). RV was then was activated in serum-free DMEM with 1 μg/ml trypsin (Worthington Biochemical, Lakewood, NJ) at 37°C for 30 min. The activated virus was added to cells diluted in serum-free DMEM supplemented with 1μg/ml trypsin at the specified MOI and rocked at 37°C with 5% CO_2 in a humidified environment for 1 h. The viral inoculum was removed, cells were washed with media to remove unbound virus, and serum-free DMEM was added for the remainder of the infection.

Infected cells expressing shRNA were plated in 24-well flat bottom tissue culture plates and were surface biotinylated as described previously (Gibbons et al., 2011). Briefly, at 6 hpi, cells were washed with ice-cold PBS-CM (1X PBS supplemented with 0.1 mM $CaCl_2$ and 1 mM $MgCl_2$) three times to remove unbound extracellular material. A solution of 6 mg/ml membrane-impermeable EZ Link® Sulfo-NHS-SS-Biotin (Pierce-Thermo) in ice-cold PBS-CM was added to the cells at a 10 mM concentration, and was incubated with rocking for 30 min at 4°C. Excess biotin was quenched by adding cold DMEM supplemented with 10% FBS for 10 min at 4°C. Cell were lysed with SDS-free RIPA lysis buffer containing protease inhibitors and immediately added to the cells for 20 min at 4°C. The cell lysates were transferred to sterile microcentrifuge tubes, to which 30 μL of streptavidin-agarose slurry (Pierce-Thermo, Rockford, IL) was added per 1 ml of lysate. The mixture was incubated with rotation at 4°C for 16 hours.

The biotinylated proteins were collected by pelleting the bound streptavidin-agarose at 2500 x g for 5 min. The supernatant was collected and saved for analysis of the protein silencing experiments, and the pellet was washed three times in ice-cold SDS-free RIPA lysis buffer with protease inhibitors. The biotinylated proteins were removed from the streptavidin-agarose beads by suspending them in sample reducing buffer (Laemmli, 1970) (62.5 mM Tris pH=6.8, 10% glycerol, 2% SDS, 5% 2-mercaptoethanol, and 0.001% bromophenol blue) and boiling for 10 min. The beads were centrifuged for 5 min at 2500 x g, and the sample reducing buffer supernatant containing the biotinylated exofacial plasma membrane proteins was collected for electrophoretic analysis. To ensure that there was a lack of non-specific binding to the streptavidin-agarose beads, un-infected and mock-biotinylated samples were analyzed as controls.

4.2.14 Western Blotting

Western blotting was used to confirm the extent of silencing of each of the silenced proteins and to determine the presence of NSP4 at the plasma membrane. Briefly, the samples were dissolved and dissociated in sample reducing buffer, loaded and resolved on a 12% or 15% SDS-polyacrylamide gel (NEXT GEL; Amresco). The proteins were electroblotted to a 0.45 μM-pore size nitrocellulose membranes (Bio-Rad, Hercules, CA) as per the manufacturer's instructions (Mini-Protean II and Trans-Blot, Bio-rad). The nitrocellulose membranes were blocked in 10% (wt/vol) NFDM in PBS for 1 h at room temperature. The membranes then were incubated with primary antibodies (rabbit anti-CyP40, rabbit anti-HSP56 and mouse anti-GAPDH) diluted in 2.5% NFDM in PBS for 3

h at 27°C with rocking. The membranes were washed once with PBS, twice with PBS-Tween-20 (0.5%), and again with PBS. Secondary antibodies (goat anti-rabbit-HRP or goat anti-mouse-HRP) were diluted in 2.5% NFDM in PBS, added to the membranes, and incubated with rocking for 1 h at 27°C. The membranes were washed as above and reacted with Immobilon Western Chemiluminescent HRP Substrate (Millipore, Billerica, MA) per the manufacturer's instructions. The protein-specific bands were visualized using the ImageQuant LAS 4000 gel imager (GE Healthcare Life Sciences, Pittsburgh, PA), and densitometric analyses were performed using ImageJ.

4.2.15 Densitometry

Gel images were analyzed via ImageJ using the gel analysis function. Briefly, the intensity of each protein band was given a value for the silenced protein and for the glyceraldehyde-3-phosphate dehydrogenase (GAPDH) control in the same lane. Each band was background subtracted and measured within the linear range. The intensity value of the protein band was divided by the intensity value of the GAPDH control band to obtain a ratio of the protein amount to protein loading control (GAPDH band intensity).

4.3 Results

4.3.1 Construction, Growth, and Isolation of the pTripZ Vectors Were Successful

The pTripZ vectors are very large vectors that do not grow as well as smaller vectors. We attempted to grow the vectors in DH5α *E. coli* cells before we discovered the Stbl3 *E. coli* cell line. This cell line is designed for unstable vectors that are large and contain direct repeat sequences such as the long terminal repeats in pTripZ. The

competency of our Stbl3 cells was greater than 1 x 10^7 cfu/ml. Although it was difficult to grow the TripZ vector, we were finally successful in growing the Stbl3 cells at 30°C instead of 37°C and shaking at 175 rpm rather than 250 rpm (**Figure 4.1**). The vectors containing shRNA were digested with SalI to verify the correct construction (**Figure 4.2**). The restricted DNA sizes should be 7104 bp, 4028 bp, and 2188 bp, so the correct vectors were produced.

To further verify that the inserts were correctly inserted into the vector, we attempted to sequence the shRNA insert. Unfortunately, we tried several methods to sequence the vectors and were able only to sequence up to the shRNA insert, but not through the actual hairpin sequence. We are still attempting to sequence the shRNA to verify the correct sequences. However, we continued the planned experiments with the pTripZ-shRNA vectors.

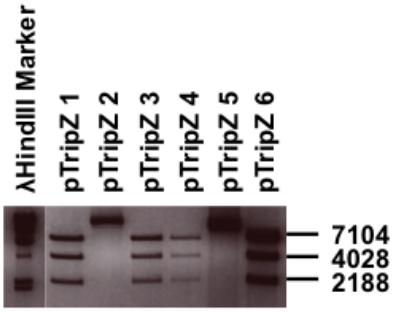

Figure 4.1 TripZ vectors isolated from Stbl3 cells. Six individual colonies were expanded in LB media and pTripZ vectors were isolated. The vectors were digested with SalI and run on a 2% agarose gel, which should yield three bands at 2188 bp, 4028 bp, and 7104 bp. Four of the six vectors were good.

4.3.2 Construction of Stable-expressing HEK-293T Cell Lines

Before transfection of the pTripZ-shRNA constructs, a puromycin kill curve was performed in HEK-293T cells. HEK-293T cells were sensitive to puromycin at 5 μg/ml and the DMSO control had no effect. All 12 of the pTripZ-shRNA vectors were transfected into HEK-293T cells with Lipofectamine 2000. The transfected cells were selected for with puromycin and maintained for 14 days in selective media. At 10 days post-transfection, cells were treated with 1 μg/ml doxycycline and checked every 2 days to determine that the majority of them were expressing the transgene.

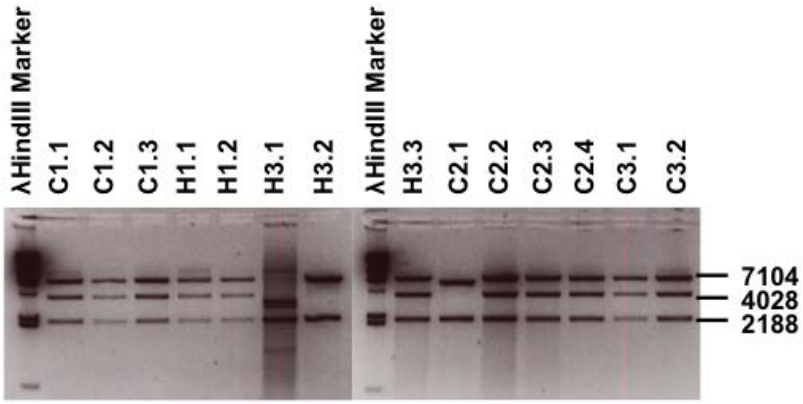

Figure 4.2 TripZ vectors containing shRNA sequences for CyP40 and HSP56. Three or four colonies were picked and expanded for each shRNA insert. The vectors were isolated, and digested with SalI. The vector isolated from each colony is named C1, C2, and C3 for CyP40 and H1 or H3 for HSP56. No colonies grew for the second HSP56 shRNA insert. Only the vectors that were digested correctly were used in subsequent experiments.

4.3.3 Production of Lentivirus Containing the shRNA Insert

To produce recombinant lentivirus, both the pCMVΔR8.91 and pMD.G vectors were transfected into the HEK-293T cell line using Lipofectamine 2000 at a ratio of 1:1.7. Virus was collected, cell debris was pelleted and discarded, and the recombinant lentivirus was titered in HEK-293T cells. The titers for the lentivirus containing the shRNA inserts for CyP40 were between 1.0 x 10^6-2.4 x 10^6 transduction units (TU)/ml. The titers for the lentivirus containing the shRNA inserts for HSP56 were between 1.0 x 10^6-8.0 x 10^6 TU/ml. The titers for lentivirus expressing shRNA inserts targeting Cav-1 and CyPA have not been calculated.

4.3.4 Construction of Stable Transgene-expressing MA104 and HT29.f8 Cell Lines

Before transduction, a puromycin kill curve was performed on MA104 and HT29.f8 cells. MA104 cells were sensitive to puromycin at a concentration of 7.5 μg/ml, while HT29.f8 cells were sensitive at 10 μg/ml. For consistency, all experiments with the TripZ-shRNA vectors were carried out using 7.5 μg/ml puromycin. MA104 and HT29.f8 cells were plated in 24-well plates and grown until ~85% confluent. Cells were transduced at an MOI of 1.0. Six hours after transduction, puromycin and FBS were added to the media. DMEM with puromycin was changed every 2-3 days and the cells were monitored for growth. HT29.f8 cells did not survive puromycin treatment following the transduction of lentiviruses. MA104 cells grew well and were expanded under puromycin selection 10 days following transduction. Eventually, stocks of MA104 cells were frozen down for future use.

Transduction was repeated in HT29.f8 cells and the virus inoculum was removed before puromycin treatment to reduce toxicity. The HT29.f8 cells survived for 4 days under puromycin selection and once again died. The puromycin concentration was lowered to 5 μg/ml and the cells still died. Thus, generation of HT29.f8 cell lines that are stable transgene-expressing lines was unsuccessful.

4.3.5 TripZ-shRNA Vectors Containing an Insert That Targets CyP40 Efficiently Knocked Down CyP40 in Uninfected MA104 Cells

MA104 cells expressing the shRNA targeting CyP40-1 or CyP40-2 were induced with 1 μg/ml doxycycline. Cells were incubated for 48 h and checked via epi-fluorescence microscopy to verify transgene expression. Cells were lysed every 24 h for 4 days to determine the time for the most effective silencing. The cell lysates were separated by SDS-PAGE, proteins were transferred to a nitrocellulose membrane, and the membranes were blotted with rabbit anti-CyP40 and mouse anti-GAPDH (**Figure 4.3**). CyP40 was silenced effectively at 4 days following transgene induction. We attempted to measure the HSP56 concentration by Western blot, but due to antibody limitations we were unable to detect HSP56.

4.3.6 NSP4 Continued to Traffic to the Exofacial PM in Cells Expressing shRNA Targeting CyP40 and HSP56

Transduced and doxycycline-treated MA104 cells under puromycin selection and expressing shRNA targeting CyP40 and HSP56 were infected with RV at an MOI of 5 for 6 h. Cells were surface biotinylated, pulled down with streptavidin-agarose, and released from the agarose by boiling. Recovered proteins were separated by SDS-PAGE,

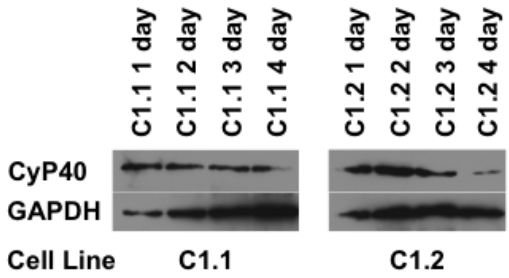

Figure 4.3 CyP40 expression in MA104 cells expressing shRNA targeting CyP40. MA104 cells expressing shRNA targeting CyP40 were induced with doxycycline and lysed every 24 h for 98 h. Cell lysates were separated by SDS-PAGE, transferred to a nitrocellulose membrane and subjected to Western blot. CyP40 expression is shown with GAPDH expression serving as an internal control.

transferred to a nitrocellulose membrane, and blotted with rabbit anti-$NSP4_{112-140}$. NSP4 continued to traffic to the exofacial PM when shRNA targeting CyP40 and HSP56 were expressed in MA104 cells (**Figure 4.4**), corroborating our silencing data. Therefore, NSP4 transport is not dependent upon CyP40 or HSP56 expression for transport to the PM.

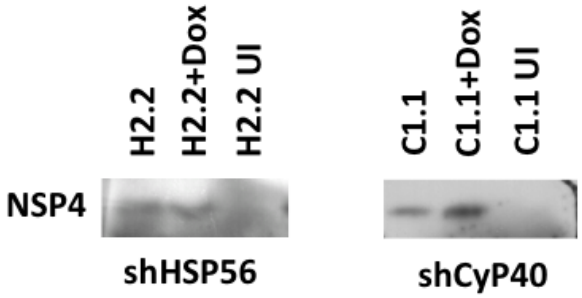

Figure 4.4 NSP4 reached the PM in cells expressing shRNA targeting CyP40 or HSP56. Stable MA104 cells expressing the shRNA targeting CyP40 or HSP56 were induced with doxycycline, or not, and infected with RV, or not. Cells were surface biotinylated, proteins were separated via SDS-PAGE, transferred to nitrocellulose, and blotted with peptide antibodies targeting NSP4.

4.4 Discussion

Recombinant lentiviruses expressing shRNA have become very useful tools for studying cellular processes. There are now many available systems for construction of lentiviral vectors to express shRNA, such as the TripZ™ system. The TripZ™ system allowed for inducible expression of shRNA targeting Cav-1, CyPA, CyP40, and HSP56, so that cells would grow properly and expression could be silenced when ready for analysis.

The construction of this particular system proved to be very difficult due to several factors. First, the growth of large vectors that contain long terminal repeats are very difficult in many commonly used *E. coli* strains. There are now strains available, such as the Stbl *E. coli* cell lines through Life Technologies. These cell lines often have their drawbacks, but make the production of vectors with LTRs much easier. Second, sequencing through a hairpin structure is often difficult. Whether this is due to the secondary structure or the sequence depends on the particular hairpin. However, there are special methods that can be used to make sequencing easier, such as transferring the shRNA segment to a smaller vector that can be sequenced easily. Third, creation of a stable cell-line is dependent on the cell line chosen. Some cell lines, such as the cloned HT29.f8 cell line tend to be very susceptible to toxicity due to the vectors. We attempted to lower toxicity by lowering the puromycin concentration used for selection, but it appeared that the recombinant lentivirus itself was toxic to the cells. There are ways to reduce the toxicity due to lentivirus transduction, but we found that these methods did not work for HT29.f8 cells.

We attempted many different methods to obtain a sequence from the TripZ vectors. Initially, we used the sequencing primer recommended by the manufacturer. When that did not work, we designed our own primers to sequence the shRNA insert. We attempted to melt the shRNA structure before addition of the DNA polymerase. We tried designing primers that would partially bind to the shRNA structure, thereby keeping it open and making it easier to sequence. While we were able to sequence the DNA segment before and after the shRNA, we were not able to sequence through the shRNA segment. We will continue to attempt sequencing by transferring the shRNA insert from the pTripZ vector to a smaller vector, pCR8/GW/TOPO, which should make the inserts much easier to sequence.

Viral vectors expressing shRNA have many advantages over the use of siRNA. The major advantage is that viral vectors expressing shRNA can be made in large amounts. siRNA must be purchased from a company that specializes in small RNA segment production and can be very costly. Viral vectors expressing shRNA can be made inducible or not. There are advantages to both systems. A knockout cell line can be produced when a non-inducible system is used. If the knockout is toxic to the cell long term, the system can be made inducible, so that expression can be turned on and off using an antibiotic, such as doxycycline. Silencing RNAs are always transient, and can be ineffective if performing long-term studies. A major disadvantage of shRNA-expressing systems is that they can often be leaky. In inducible systems, shRNA can be expressed in the absence of induction, which can affect the outcome of the control cells and cause additional toxicity to the stable transgene-expressing cell lines.

In this lab, we planned to use the available shRNA-expressing cell lines to continue study of the interactions of NSP4 with Cav-1, CyPA, CyP40, and HSP56. However, after determining that these proteins may not play an important role in NSP4 transport to the PM, the stable shRNA-expressing cell lines may not be necessary for future studies.

5. ROTAVIRUSES: EXTRACTION AND ISOLATION OF RNA, REASSORTANT STRAINS, AND NSP4 PROTEIN

5.1 Introduction

Group A rotaviruses (RVs) are readily and efficiently replicated in mammalian tissue culture as described in Basic Protocol 1 Unit 15C.3. To further investigate these viruses, utilization of a variety of additional techniques is necessary. RV easily recombines upon co-infection of two or more strains, which becomes more prevalent as multiple strains are introduced in close proximity. Recombinant forms of RV function differently than the parental strain depending on which of the segments are swapped. To evaluate the recombinants and to sequence multiple viral strains, the isolation of viral RNA is critical. Viral RNAs reside within the inner-layer of the triple-layered virus particle, making it easier to isolate viral RNA in the absence of cellular mRNA. Once the viral RNA is isolated, electrophoretic typing will elucidate the electrophoretic pattern of the RNA genome, hence the virus strain.

The RV enterotoxin, NSP4, is a nonstructural, multi-function viral glycoprotein that contributes to RV replication, morphogenesis and pathogenesis. NSP4 elicits diarrhea in the absence of virus in a murine model and is thought to be responsible for the early stages of diarrhea following infection with RV in mammals. Recent data reveal NSP4 associates with autophagosomes before transport to the plasma membrane (PM) for

*Reprinted with permission from "Rotaviruses: Extraction and isolation of RNA, reassortant strains, and NSP4 protein" by Yakshe, K.A., Franklin, Z.D., and Ball, J.M., 2015. *Curr. Protoc. Microbiol*, 37, 15C.6.1-15C.6.44., Copyright 2015 by Wiley.

secretion from the cell. NSP4 has been the focus of investigation for many years despite its many unique properties that frequently complicate these studies. The isolated protein has a strong tendency to oligomerize, forming dimers, trimers and up to octamers. Isolation for detailed studies of NSP4 is essential to dissect the many parameters of NSP4's multiple activities. Several manuscripts note that there appears to be distinct pools of NSP4 within the cell with diverse functions. It is not surprising that multiple NSP4 isolation techniques have been reported.

This unit covers techniques that are helpful for the study of rotavirus and NSP4. Generation of reassortant viruses (Basic Protocol 1) is important for studying the viral lifecycle and viral pathogenesis. Extraction (Basic Protocol 2, Alternate Protocol 1, Alternate Protocol 3) and analysis of viral RNAs via polyacrylamide gel electrophoresis (Basic Protocol 2) are essential for electrophoretic typing of the parental and reassortant virus strains. The expression and purification of NSP4 from the media of infected mammalian (Basic Protocol 3) and the lysates of recombinant baculovirus-infected Sf9 insect cells (Alternate Protocol 3, Supporting Protocol 1, Basic Protocol 4) are described.

5.2 Basic Protocol 1: Generation of Reassortant Rotavirus Strains from Parental Rotavirus Strains

The segmented genome of rotavirus facilitates the generation of recombinant strains post infection. These newly formed reassortants may impact the virulence and host specificity of the infecting parental virus. To investigate the effect(s) on progeny RV and to determine the frequency of recombination, reassortants are generated in culture. Data collected on these viral recombinants are useful for detailed analyses of changes in

virulence, pathogenicity, and host specificity. In addition, reassortants can be used to model vaccines that are safe and efficacious. To generate the reassortants, the parental strains must be plaque purified and expanded for the co-infections. Two or more virus strains are mixed at a pre-determined multiplicity of infection (MOI) and then allowed to replicate in cell culture before additional plaque purification.

5.2.1 Solutions and Specific Equipment

Plaque-purified parental RV strains with known concentration based on plaque forming units (PFU)

Minimum Essential Medium (MEM), 1X or 2X, supplemented with L-glutamine, non-essential amino acids (NEAA), Sodium Pyruvate, Pen-Strep or equivalent (see recipe)

MA104 cells (ATCC #CRL-2378™)

Worthington trypsin (1 mg/ml)

Low-melt agarose (It is recommended that you use SeaPlaque™ (Lonza) or GenePure (ISC BioExpress))

Sterile Serological Pipettes

Sterile flint glass Pasteur pipettes

Suction bulb

6-well tissue culture plates with lids

Autoclaved dH_20

Pancreatin

Neutral Red Solution (see recipe)

15 ml polypropylene conical tubes

Platform rocker

-70°C Freezer

Inverted light microscope

37°C water bath

Additional reagents and equipment for this procedure are included in Basic Protocol 3 Unit 15C.3.

5.2.2 Steps and Annotations

This protocol should be used in conjunction with Basic Protocol 1 and Basic Protocol 3 in Unit 15C.3. However the protocol below requires the use of two or more viruses, instead of one, and 6-well plates for co-infections, instead of flasks.

1. Plate MA104 cells in a 6-well plate at 3.0×10^5 cells per well with supplemented MEM containing 10% FBS.
2. Incubate for 3 to 5 days or until 100% confluent.
3. Calculate the amount of RV needed to infect at a MOI of 5 for each virus using the formula: No. cells × MOI = PFU needed.

   A six well plate generally supports $1.2x\ 10^6$ cells in each well so 6.0×10^6 (MOI 5) viral particles of each virus usually is sufficient (total virus particles per well is $1.2x10^7$).
4. Thaw the RV strains on ice.

5. Individually activate the viruses by adding 10 µl of a 1 mg/ml solution of Worthington trypsin per 1 ml of virus (final concentration of 10 µg/ml) and incubating for 1 h in a 37.5°C water bath to for allow for cleavage of the outer spike protein, VP4.

   Basic Protocol 1 UNIT 15C.3 uses porcine pancreatic type IX trypsin, but we find the Worthington trypsin more reliable. The amount of virus activated will depend on the amount needed to formulate a MOI of 5 for each viral strain (MOI 10 total for 2 viruses).

6. Prepare the activated, plaque purified RV strains of choice in media without fetal bovine sera (FBS) by mixing the strains to yield a MOI of 5 each in a 15 ml conical tube. You will need at least 1 ml of media with virus to cover the cells in one well of a 6-well plate. Vortex well.

   Each individual strain can be activated in a separate tube and combined before addition to the cells.

7. Wash the confluent MA104 cells in the 6-well plate twice with 2 ml/well of phosphate buffered saline (PBS) or serum free medium.

   In order to remove residual FBS, which can inhibit the activation of RV, the wells are rinsed. One change of serum free medium can also be incubated for several hours to ensure the removal of FBS.

8. Carefully remove the serum-free MEM or PBS from the cell monolayer. Add at least 1 ml of the diluted virus solution to each well of the MA104 cells. Incubate with gentle rocking at 37°C for 1 h for virus adsorption.

9. Remove the virus inoculum and wash the cells once with 2 ml of pre-warmed PBS or serum-free MEM.
10. Add 2 ml of pre-warmed serum-free MEM and allow the viruses to replicate for 72 hours post infection or until 90% CPE.
11. Freeze-thaw plates containing infected cells 3 times at -70 °C.
12. Transfer the virus-containing media to 15 ml conical tubes.
13. Sonicate in a cuphorn sonicator in an ice bath at 45 W for 5 min.

    The cell culture supernatant is sonicated on ice to break up membranes and release the virus particles. RV is known to be cell-associated.
14. Clarify the supernatant containing RV to remove cellular debris by low-speed centrifugation at 300 x g for 10 min. Transfer the virus-enriched cell supernatant to another tube.
15. Perform the plaque assay using the protocol described in Basic Protocol 3 Unit 15C.3

    The individual reassortant viruses are isolated by 3 sequential plaque purifications. Each reassortant generally has distinct plaque morphology. RNA electrophoretic analyses of the plaques will ensure individual plaques contain discrete recombinants.
16. Isolate the plaques using a Pasteur pipette with a bulb attached. The Pasteur pipet tip is gently pushed through the agarose overlay and the plaque is aspirated into a test tube as described in Basic Protocol 3 Unit 15C.3.
17. Repeat the plaque purification 3 times (see Basic Protocol 3 Unit 15C.3).

18. Expand the plaque-purified RV strains in roller bottles or flasks (see Basic protocol 3 and Alternate Protocol 1 Unit 15C.3), aliquot and store at -80°C.
19. To verify the purity of the reassortant virus, the RNA is extracted and analyzed via sequencing and/or by PAGE with Silver Staining (under electrophoretic typing protocol, Basic Protocol 2).

    Note: It is important to run the parental strains and MW markers alongside the potential reassortants to allow for comparison.

5.3 Basic Protocol 2: Phenol-Chloroform Extraction of RNA for Electrophoretic Typing of Rotavirus dsRNA Segments

Electrophoretic typing is used as a diagnostic tool for the detection of RNA segments of the parental and recombinant strains. Viral RNA is extracted from RV grown in cell culture or collected from stool samples and classified into either group A, B, or C depending on its electrophoretic profile.

Group A mammalian rotaviruses are composed of a (L) long or short electrophoretic profile depending on the length of gene segment 11. Gene segment 11 encodes for two proteins, non-structural protein-5 (NSP5) and non-structural protein-6 (NSP6). The short pattern is due to a larger gene segment 11 encoding a larger NSP5, resulting in slower migration. The large gene segment runs between segments 9 and 10 rather than after segments 9 and 10. There also are reports of super short profiles.

When the 11 segments are separated on a polyacrylamide gel, there is a tendency for the RV RNA segments to group together dependent on their origin (Group A, Group B, or Group C rotavirus). The electrophoretic separation pattern of the RV dsRNA

segments will assign the virus into the proper group based on the RNA migration pattern. The dsRNA of Group A mammalian rotaviruses have four size classes: 4 large segments (more than 2000 base pairs), 2 medium-sized segments (above 1000 base pairs), 3 small segments (900-1000 base pairs), and 2 smallest segments (less than 900 base pairs) for a 4-2-3-2 pattern (**Table 5.1**).

Table 5.1. Rotavirus Group RNA Segment Patterns

Rotavirus strain	RNA segments	RNA pattern designation
Mammalian Group A	4 large, 2 medium, 3 small, 2 smallest	4-2-3-2
Avian Group A	5 large, 1 medium, 3 small, 2 smallest	5-1-3-2
Rotavirus Group B	4 large, 2 medium, 1 small, 1 smallest	4-2-1-1
Rotavirus Group C	4 large, 3 medium, 2 small, 2 smallest	4-3-2-2
Avian Group D	5 large, 2 medium, 2 small, 2 smallest	5-2-2-2

Viral RNA Extraction is best performed using purified virus, so that there is no contaminating cellular RNA. The two methods described herein are (1) phenol-chloroform extraction for isolation of viral RNA from fecal samples in Basic Protocol 2 and (2) TRIzol® extraction for isolation of viral RNA from cell-culture supernatants, as described in Alternate Protocol 1.

5.3.1 Solutions and Specific Equipment

Fecal samples

0.1% sodium acetate buffer (pH 5) (see recipe)

1% (w/v) sodium dodecyl sulfate (SDS)

Phenol mixture (see recipe)

Chloroform

1.5 ml microcentrifuge tubes

Benchtop microcentrifuge

5.3.2 Steps and Annotations

1. Dilute the fecal sample 1:4 by weight with 0.1 M sodium acetate buffer (pH 5) containing 1% (wt/vol) SDS.

   0.25 g of feces will extract enough RNA for 10 separate electrophoretic analyses.

2. Add an equal volume of a 3:2 (v/v) phenol:chloroform mixture and vortex for 1 min.
3. Centrifuge at 1,200 x g for 10 min.
4. Remove the upper aqueous layer containing the viral RNA.

   If the aqueous layer is absent, centrifuge again for 3 min at 16,000 x g in a microcentrifuge or add 0.5 ml of 0.1 M sodium acetate buffer, mix and centrifuge for 12,000 x g for 10 min.

5. Aliquot the aqueous layer into 0.6 ml microcentrifuge tubes and store at -70 °C until ready for further analysis.

5.4 Alternate Protocol 1: Extraction of Rotavirus RNA from Cultured Cells Using TRIzol®

TRIzol® can be used to isolate rotavirus RNA from cultured cells by modifying the protocol reported in the World Health Organization (WHO) manual (Organization, 2009). Instead of using a stool suspension, RV-infected cell-culture supernatant is utilized.

5.4.1 Solutions and Specific Equipment

TRIzol® (Life Technologies)

Chloroform

Isopropyl alcohol

Molecular-biology-grade water

Pipettors

Screw-cap microcentrifuge tubes

Filtered pipette tips

Vortexer

Benchtop microcentrifuge

Sonicator with a cuphorn attachment, ice bath sonicator, (Misonix sonicator 300; Misonix Inc. Farmingdale, NY) or equivalent

5.4.2 Steps and Annotations

1. Incubate the RV-infected MA104 cells grown in T-75 or T-25 flasks until the monolayer is at least 90% disrupted due to CPE.
2. Freeze and thaw the flask(s) containing the RV-rich cell lysates 3 times at -70°C and room temperature, respectively.
3. Transfer the thawed supernatant to a sterile 50 ml conical tube and sonicate at 45 W for 5 minutes using a cuphorn attachment, ice bath sonicator.
4. Remove the cellular debris by high-speed centrifugation at 8,000 x g for 30 min.

5. Transfer 250 µl of the clarified cell culture supernatant to a sterile 1.5-ml microcentrifuge tube, and add 750 µl of *TRIzol*®. Vortex the tube for 30 sec to thoroughly mix, and incubate at room temperature for 5 min.
6. Add 200 µl of chloroform to the sample and vortex for 30 sec. Incubate the sample at room temperature for 3 min.
7. Centrifuge the samples at 9,300 x g for 5 min at 4°C or room temperature to separate the phases.
8. Carefully transfer the upper aqueous phase into a sterile microcentrifuge tube.

   It is important to avoid the white interface and pink/clear organic phase.
9. Add 2 volumes (approximately 700 µl) of ice cold isopropyl alcohol. Mix gently by inverting the tube 4-6 times and incubate at -20°C for 20 min.
10. Centrifuge at 9,300 x g at 4°C for 15 min to pellet the dsRNA. Discard the supernatant immediately. Carefully air dry the pellets for 10-15 min at room temperature.
11. Resuspend the dried pellet in 20 µL of sterile deionized water. The volume of water can be reduced to 15 µL.
12. Store the sample at -20°C until ready for analysis.

5.5 Alternate Protocol 2: Extraction of Rotavirus RNA from Cell Culture Supernatant Using QIAamp Viral RNA Mini Kit

RNA can be isolated directly from cell culture supernatants using the QIAamp Viral RNA Mini kit. Although the kit is more costly than other RNA extraction methods, it is

fast, easy, and provides high quality and pure viral RNA. The manufacturer's protocol should be followed for RV RNA extraction. The protocol briefly is described below.

5.5.1 Solutions and Specific Equipment

QIAamp Viral RNA Mini kit (Qiagen, cat # 52904)

Ethanol (96-100%)

1.5 ml microcentrifuge tubes

Sterile, RNase-free pipet tips (aerosol barriers to prevent cross contamination are recommended)

Benchtop Microcentrifuge capable of cooling to 4 °C.

Alternatively, the centrifuge may be placed in a refrigerated space.

5.5.2 Steps and Annotations

1. Infect the cells with RV and harvest as described in Alternate Protocol 1, steps 1-4

2. Follow the manufacturer's protocol for the remainder of the RNA extraction.

   If the virus titer is low, you can double the amount of the cleared supernatant (280 µl instead of 140 µl) for a higher concentration of recovered RNA.

5.6 Basic Protocol 3: Polyacrylamide Gel Electrophoresis (PAGE) for Electrotyping Rotavirus Strains

RNA is best visualized using PAGE and silver staining. This section explains the setup and separation of the RNA samples on a polyacrylamide gel and subsequent staining of the gel for identification of the RNA segments. This protocol also explains how to prepare a 7.5% acrylamide gel for the best separation of RNA fragments. A higher percentage of acrylamide can be used but will show different migration patterns.

5.6.1 Solutions and Specific Equipment

30% acrylamide stock (see recipe)

Resolving gel buffer (see recipe)

Stacking gel buffer (see recipe)

10% ammonium persulfate (APS)

Tris-glycine running buffer (see recipe)

Mini-PROTEAN gel setup (BioRad) or equivalent

PAGE sample loading buffer (see recipe)

Silver Stain Kit (Thermo Scientific Pierce) (Cat #24612)

95% Ethanol

Acetic Acid

Small glass dish to fit the gel

Larger glass dish to fit the cellophane for gel drying

Cellophane

Gel drying frames

Binder clips

5.6.2 Steps and Annotations

1. Degas all solutions for at least 15 min.
2. Thoroughly clean the 0.75 mm mini-gel glass plates so they are free of dust, residue or fingerprints and assemble them in the casting apparatus.

The gel will leak if the glass plates are uneven or if the bottom is not sealed properly. A piece of Parafilm M® at the bottom of the plates can be helpful if the gel leaks.

3. Add the comb. Make a mark on the plate 1 cm below the teeth of the comb and then remove the comb.
4. To prepare two mini gels, add the following reagents to a 25 ml Erlenmeyer flask: 3.75 ml of 30% acrylamide/bis-acrylamide (29:1) mixture, 3.75 ml of resolving gel buffer, 7.43 ml of dH_20, and 75 µl of freshly made 10% APS. Mix well with a serological pipette before adding 14 µl of TEMED.

   Caution must be taken when working with acrylamide. Gloves must be worn and if working with the powder form, a face mask is required. Acrylamide is a known neurotoxin.

   Some scientists recommend that additional degassing of the acrylamide solutions improve the clarity of the gel.
5. Quickly mix the resolving gel solution and dispense between the glass plates up to the mark made in Step 3 (approximately 3.30 ml).
6. Fill the remainder of the plates with sterile dH_2O and allow the gel to solidify for 45-60 min.
7. Pour off the dH_20 and dry the inside of the glass plates by blotting with a thin piece of absorbent filter paper to remove all water. Be careful not to touch the resolving gel with the filter paper.

8. In a 25 ml Erlenmeyer flask add 0.99 ml of 30% acrylamide/bis-acrylamide, 1.89 ml stacking buffer, 4.58 ml of dH_20, 75 µl of freshly made 10% APS. Mix the solution well pipetting up and down gently so that there are no bubbles formed.

   See caution above concerning acrylamide (step 4).

9. Add 3.75 µl of TEMED and mix well with a pipette. Fill the glass plates to the top with the acrylamide solution.
10. Add the comb to the newly added stacking gel solution and allow the gel to solidify for 45-60 min.

    The combs can vary in the number of teeth depending on the number and volume of the samples.

11. Remove the comb and rinse the individual wells with running buffer.

    This can be accomplished using a syringe and 21-gauge needle or Hamilton syringe.

12. Assemble the gel running apparatus per manufacturer's instructions.
13. Add the tris-glycine running buffer to the fill line of the gel tank and remove any air bubbles from the wells.
14. Load the gel with the samples:
    a. Add the sample-loading buffer 1 to 1 (v/v) with the sample.
    b. For the marker lane, load 3-5 µl of marker, which is sufficient for most commercial, pre-stained markers. If the marker is not pre-stained, QS to10 µl with dH_2O and add sample-loading buffer 1:1 (i.e., add 3 µl marker and 7 µl dH_20 for a total of 10 µl and mix with 10 µl of sample loading buffer).

All RNA samples should be thawed on ice and should remain in the -70°C freezer until needed. The amount of sample will depend on the size of the comb. A 20 µl volume will fit into a 10 well comb for a 0.75 mm mini gel.

15. Run mini gels at 150 V for 2 h.

    Note: Large and mid-sized gels should be run at 100 V for 16-20 h.

    Some equine RV strains have a different migration pattern for VP4 if run on an alternate % of acrylamide gel.

16. When the gel stops running, add 1 cm of dH_2O to a small dish.
17. Take the plates out of the gel running apparatus and slowly wedge a plate separator between the glass plates at the top corner. Once the plates start to separate add a continuous amount of light force until the suction is released.

    Forcing the plate separator between the glass plates quickly and hard will cause the glass to break.

18. Remove the stacking gel and add a small notch to one of the top corners of the gel to mark gel orientation.

    The gel is thin, delicate, and tears very easy. Take care not to pull too quickly when removing it from the glass plate.

19. Release the sides of the gel by slowly running the plate separator down the left and right sides of the plate.
20. Lift one corner of the gel and turn it upside down above the small plate with dH_2O. Slowly peel the gel off and allow it to fall gently into the dish.
21. Follow the manufacturer's protocol for the silver staining process.

22. After the gel has been stained, developed, and stopped using the silver staining kit, rinse the gel in dH_2O for 5 min, 2 times, with rocking.

    Note: At this step, the gel can be imaged using a gel imaging system, or by taking a digital photograph before drying.

23. For drying, cut two pieces of cellophane to fit the gel-drying frames.
24. Place 1 inch of dH_2O in a large dish (large enough to fit the cellophane pieces)
25. Wet the first piece of cellophane with dH_2O and place it onto the back of the drying frame. Be sure to remove all air bubbles. This can be done by pressing one corner of the cellophane to the frame and working from one side to the other.

    If a bubble appears, pull the cellophane back from one corner to release the bubble. Gently rolling a test tube on the cellophane also may remove the bubbles.

26. Add the gel to center of the frame removing any air bubbles.
27. Wet the second piece of cellophane with dH_2O and add the cellophane over the top of the gel to create a cellophane sandwich with the gel in the middle. Remove any air bubbles to prevent cracking while drying. If necessary, remove top cellophane layer and add more water to remove all air bubbles.
28. Place the top layer of the frame over the top cellophane layer.

    Be sure that the frame is touching only the cellophane and not smashing the gel.

29. Clamp all four sides of the frame and set it at an angle to dry for at least 24 h.

    The gel can be viewed while drying.

    Note: Alternatively, a gel dryer (BioRad) can be used to facilitate faster gel drying (2-3 h).

30. Take the dried gel out of the drying frame and place it under pressure with a heavy object such as a textbook.
31. Use a ruler to visualize the migration pattern and compare the parental strains to the reassortant strains. See Figure 1.

5.7 Basic Protocol 4: Purification of Rotavirus NSP4 from the Media of Cultured Mammalian Cells

RV expresses a unique nonstructural glycoprotein, NSP4, which functions as an enterotoxin, eliciting a secretory diarrhea from enterocytes, even in the absence of virus (Ball et al., 1996). When NSP4 is extracellularly added to cultured cells or mouse pup unstripped intestinal mucosa, it initiates the influx of Ca^{2+} into the cytoplasm of the cells by a phospholipase C-dependent mechanism ((Tian, 1995). Recently NSP4 has been shown to function as a viroporin when expressed intracellularly. The viroporin stimulates the release of Ca^{2+} from the endoplasmic reticulum by activating calcium/calmodulin-dependent kinase kinase-β (CaMKK-β) and initiates autophagy (Crawford et al., 2012; Hyser et al., 2010). Purified NSP4 is a vital reagent for many studies as NSP4 plays an integral part of the viral life cycle and initiates fluid loss or diarrhea. This protocol describes the isolation of NSP4 from the media of RV-infected mammalian cells (Didsbury et al., 2011) employing ConA affinity chromatography, followed by separation on a Mono S 5/50 GL FPLC column, and NSP4 IgG affinity chromatography.

An abundance of NSP4 is expressed in the media of Caco-2 cells, whereas MA104 cells express less NSP4 in the media. The amount of NSP4 produced in the media is also

RV strain dependent. Thus the combination of cells and viral strain should carefully be considered.

5.7.1 Solutions and Specific Equipment

Caco-2 cells (ATCC® #HTB-37™) or MA104 cells (ATCC® #CRL-2378.1™)

Rotavirus strain of choice

Tissue Culture Flasks

Minimum Essential Media, supplemented, with 10% fetal bovine serum (see recipe)

Minimum Essential Media, supplemented, without 10% fetal bovine serum (see recipe)

Phosphate Buffered Saline (PBS; see recipe)

1 mg/ml Trypsin (Worthington #TRL3; see recipe)

Ultra-Centrifugal Filter with 10kD cut off (Amicon #UFC901008 or equivalent)

Glass Econo-Column® (Bio-Rad) or equivalent

Econo-Column® flow adaptor (Bio-Rad) or equivalent

Concanavalin A Sepharose™ 4B (GE Healthcare #71-7077-00 AG)

Con A Binding Buffer (see recipe)

Con A Elution Buffer (see recipe)

HPLC or FPLC

Mono S 5/50 GL column for FPLC (GE Healthcare Life Sciences #17-5168-01)

Mono S Start Buffer (see recipe)

Mono S Elution Buffer (see recipe)

5.7.2 Steps and Annotations

5.7.2a Expression of NSP4 in Media of RV-infected Mammalian Cells

1. In a T-160 flask, grow a monolayer of Caco-2 or MA104 cells until ~95% confluent in supplemented MEM with 10% FBS.
2. Infect the cell monolayer (Basic Protocol 1, Unit 15C.3) using a high MOI of RV (10 pfu/cell).
3. At approximately 36 hours post infection (or other optimized time, dependent on the virus strain) collect the media from the cell monolayer.
4. Clarify the media of cellular contaminants by high-speed centrifugation at 8,000 x g for 30 min.
5. Ultracentrifuge the clarified media at 100,000 x g for 1 h to remove virus particles and other cellular debris from the media. Collect and save the supernatant without disturbing the pellet.
6. Add the supernatant to an Amicon Ultra Centrifugal Filter with a 10 kD cutoff and centrifuge according to the manufacturer's instructions.
    a. Pre-rinse the filter with 0.1 N NaOH followed by Milli-Q water to remove any interfering contaminants.
    b. Add up to 15 ml of sample if using a swinging bucket rotor or 12 ml of sample if using a fixed angle rotor.
    c. Centrifuge at 4,000 x g for 60 min in a swinging bucket rotor or 5,000 x g for 60 min in a fixed angle rotor to concentrate the sample.
    d. Desalt if desired by adding solvent and repeating step c.

e. Collect the concentrated sample from the inside of the filter unit using a small-tipped pipette and store at -80°C.

5.7.2b ConA Affinity Chromatography

7. Prepare the Concanavalin A Sepharose 4B (GE Healthcare) column and equilibrate according to the manufacturer's instructions:

Con A is known to bind α-D-mannopyranosyl, α-D-glucopyranosyl and sterically related residues and is frequently utilized in separation of glycoproteins. Note that columns can be purchased pre-packed.

a. Bring the sepharose to room temperature and degas the slurry.

Con A sepharose 4B is provided as a slurry in 0.1 M acetate buffer, pH 6, with essential sodium and magnesium salts, and 20% ethanol as a preservative.

b. Remove the preservative by washing with about 10 bed volumes of binding buffer.

The ligand density is 10 – 16 mg/ml of drained slurry, which can be utilized to determine the amount of slurry to use.

c. Prepare the slurry at a ratio of 25% buffer to 75% settled sepharose.

d. Allow the sample, buffers and slurry to equilibrate to room temperature and degas.

e. Flush the end pieces and column with binding buffer to remove any trapped air

f. Pour the sepharose slurry into the column in one movement being careful not to introduce air bubbles, and then fill the column to the top with ConA Binding Buffer.

g. Add the column top piece

h. Connect a reservoir of ConA Binding Buffer to a peristaltic pump and fit to the column top piece

i. Pack the slurry until a constant bed height is obtained. Open the outlet, pump the buffer at maximum flow rate, and leave 1 cm of buffer above the packed bed. (You will only use 75% speed during chromatography).

   To determine the flow rate the following formula is utilized: linear flow rate = volumetric flow rate (cm^3/h) / column cross-sectional area (cm^2).

j. Maintain the maximum flow rate for 3 column volumes after the constant bed height is reached.

k. Adjust adapter so that the O-ring sits against the column wall, but does not compress the beads.

l. Purge the flow adaptor with equilibration buffer to remove all air bubbles before attaching to the column.

m. Latch the flow adaptor onto the column and insert the flow adaptor into the column until it touches the buffer.

n. Push the cam latch all the way down to the column bed and turn it slightly counterclockwise to lock it in place.

o. Run 3 column volumes of ConA Binding Buffer through the column after packing

p. Mix the sample with ConA Binding Buffer and overlay onto column.

q. Allow the sample to run through the column at a reduced flow rate and save all of the eluent.

r. Elute with a gradient (linear or step) of elution buffer (see recipe). Use a fraction collector to collect each fraction.

Many glycoproteins elute at 0.1 – 0.2 M α-D-methylmannoside or α-D-methyl-l glucoside, however higher concentrations may be necessary. A lower pH also may contribute to elution of the glycoprotein, but do not go below pH 4

An alternative elution buffer is 0.1 M borate buffer, pH 6.5, which forms complexes with the cis-diols of the sugar residues and consequently functions as a competing eluate.

s. Repeat steps j through l for 3-5 times. Check final flow through for antigen using dot blot.

t. Regenerate the column for re-use as recommended by the manufacturer and store at 4°C in 0.1 M acetate buffer, pH 6, with 1 mM sodium, calcium, manganese and magnesium salts. Add 20% ethanol as a preservative.

5.7.2c Mono S 5/50 GL Anion Exchange Chromatography

8. After elution of NSP4 from the ConA affinity column, continue the purification on a commercially acquired Mono S 5/50 GL cation exchange column for FPLC:

a. Exchange the buffer of the sample from step 7s to 20 mM MES, pH 6 (Mono S start buffer).

    i. Amicon Ultra Centrifugal Filter with a 10 kD cutoff and centrifuge according to the manufacturer's instructions.

    ii. Pre-rinse the filter with 0.1 N NaOH followed by Milli-Q water to remove any interfering contaminants.

    iii. Add up to 15 ml of sample if using a swinging bucket rotor or 12 ml of sample if using a fixed angle rotor.

    iv. Centrifuge at 4,000 x g for 60 min in a swinging bucket rotor or 5,000 x g for 60 min in a fixed angle rotor to concentrate the sample.

    v. Add the MES solvent and repeat step iv.

    vi. Collect the concentrated sample from the inside of the filter unit using a small-tipped pipette and store at -80°C.

    vii. For use, dilute the sample in 20 mM MES, pH 6 (Mono S start buffer).

b. Equilibrate the Mono S 5/50 GL column according to **Table 5.2**:

Table 5.2. Mono S 5/50 GL Column Flow Rate

Volume (ml)	Flow Rate (ml/min)	Buffers (see recipe)
5	1	Milli-Q dH2O
5	2	Start Buffer
5	2	Elution Buffer
5	2	Start Buffer

c. Once the column is equilibrated, set the flow rate to 1 ml/min and load the sample onto the column in Mono S start buffer.

d. Wash the column with 5 – 10 column volumes of Mono S start buffer to remove unbound material.

e. To elute, use a gradient of NaCl up to 0.5 M. Collect 1.0 ml fractions using a fraction collector while monitoring the UV absorbance to visualize the protein peaks.

f. Once the sample is eluted, wash the column with 2 – 5 column volumes of 1 M NaCl.

g. Flush the column with Milli-Q water and store in Milli-Q water with 0.2% sodium azide at 4°C.

Sodium azide is a known mutagen, and can be explosive and toxic when in contact with certain metals and acids. Take precaution when working with sodium azide by wearing the proper personal protective equipment.

9. Verify the purity of the protein corresponding to the UV peaks by running a small fraction of the eluate on a 15% SDS polyacrylamide gel (see Appendix 3M) and visualize by silver staining (see Basic Protocol 3, Step 21) or Coomassie Blue staining (see Appendix 3M). Pool the NSP4-rich samples and verify that the protein is RV NSP4 by SDS-PAGE and immunoblotting (see Unit 14E.1, Basic Protocol 6).

NSP4 can be difficult to transfer for immunoblotting. From the lab's experience, it has been shown that the best way to transfer NSP4 is to use a

0.45 um nitrocellulose membrane with tris-glycine transfer buffer containing 20% methanol at 200 mA for 2 h at 4°C.

10. Store the enriched NSP4 by preparing small aliquots of the sample and freeze at -80°C. It is critical to avoid freeze-thaw of the protein sample. Alternatively the sample can be dialyzed and lyophilized (see Support Protocol 1, steps 21 and 22).

5.8 Alternate Protocol 3: Production of NSP4 in SF9 Cells Using a Recombinant Baculovirus

NSP4 can be expressed by generating a recombinant baculovirus expressing NSP4 and subsequently infecting Sf9 cells. The protein is collected from the infected Sf9 cell lysates. The use of insect cells for glycoprotein production is preferred over the use of bacterial cells because of the glycosylation of NSP4 at residues 8 and 18 and the potential endotoxin contaminants associated with bacterial cultures (Adapted from Dong, et al. 1997).

Sf9 cells are incubated at 27°C and require no CO_2. To produce large quantities of NSP4, it is beneficial to use spinner cultures with increased volumes and aeration, rather than attached cultures.

5.8.1 Solutions and Specific Equipment

Spodoptera frugiperda 9 (Sf9) cells (ATCC® #CRL-1711™)

6-well tissue culture plates

Baculovirus pAC461-G10 plasmid expressing gene 10 of RV (Tian et al., 1996) or equivalent

Hink's Medium, unsupplemented

Hink's Medium, supplemented, with 10% fetal bovine serum (see recipe)

Fetal Bovine Serum (FBS)

100X Penicillin-Streptomycin-Amphotericin B (Lonza, #17745)

Cellfectin II reagent (Life Technologies #10362-100)

Sterile Milli-Q water

Beckman Ultracentrifuge with SW-28 rotor or equivalent

Beckman Ultracentrifuge 25x89mm Ultra-Clear open top tubes that can hold up to 38ml, or equivalent

Sucrose solutions (see recipes)

SeaPlaque™ Agarose (Lonza #50101)

FPLC (Waters or equivalent) that generates a binary gradient.

Neutral Red Solution (see recipe)

Spinner flasks

Trypan Blue in PBS

Hemocytometer

Sterile 50 ml conical tubes

Low-Speed Centrifuge

27°C incubator; no CO_2 required

5.8.2 Steps and Annotations

5.8.2a Bacmid Transfection and Baculovirus Production

1. Obtain or construct a bacmid plasmid as described by Tian, et al., 1995 or by inserting the NSP4 gene (RV gene 10) with the help of a system such as the Bac to Bac or BaculoDirect™ systems (Invitrogen).
2. Seed the Sf9 cells in a 35-mm plate at a density of 8 x 10^5 cells/well in Hink's media, supplemented and allow the cells to attach at 27°C for a minimum of 1 h.

   NOTE: The media should be free of antibiotics, as antibiotics negatively impact the transfection efficiency.

3. Transfect the bacmid into plated Sf9 cells using Cellfectin II reagent according to the manufacturer's protocol:
   a. Mix 8 of µl Cellfectin reagent with 100 µl Hink's medium (no FBS) and vortex.
   b. Dilute 2 µg bacmid DNA in 100 µl Hink's medium
   c. Gently mix the diluted Cellfectin II with the bacmid DNA, and incubate for 15-30 min at room temperature.
   d. Carefully add the mixture dropwise to the plated Sf9 cells and incubate for 3-5 h at 27°C.
   e. Remove the transfection mixture and replace with supplemented Hink's medium with 10% FBS.
4. Incubate the transfected Sf9 cells at 27°C for 36 h and collect the media containing the recombinant baculovirus (Tian, 1995).

This time can be optimized for maximal protein production depending on the bacmid you are using.

5. Sediment the virus through a 3.0 ml, 20% sucrose cushion in a 25 x 89 mm Beckman Ultra-clear tube at 35,000 x g for 30 min. Resuspend the viral pellet in sterile Milli-Q water.
6. Prepare a discontinuous sucrose gradient (20-60% w/v) by adding 5 mls of each of the of the following sucrose solutions: 20%, 30%, 35%, 40%, 50%, and 60%. Add each solution to a 25 x 89 mm Beckman Ultra-clear tube using sterile Pasteur pipettes from the most dense at the bottom of the tube to the least dense at the top of the tube.

   Add the sucrose solutions very slowly and be careful not to disturb the sucrose layers. There are several ways to make the gradient. You can use a gradient maker with the 60% sucrose solution in one chamber and the 20% sucrose solution in the other chamber. Add a small amount of the 60% sucrose to the bottom of the tube then allow the 20% sucrose to slowly mix with the 60% solution, increasing the 20% sucrose solution portion as the gradient is made (continuous gradient). An alternative is to overlay the sucrose layers one by one from 60% at the bottom of the tube to 20% at the top of the tube making sure the solutions don't mix (step gradient). Or prepare the gradient by underlaying with increasing glucose solutions. Place a Pasteur pipette in the tube, slowly add 5 ml of 20% sucrose to the pipette and allow the solution to run into the bottom of the tube. Then add 30%

sucrose to the pipette and let it underlay the 20% sucrose. Continue to underlay the higher percentage of sucrose (step gradient). If a continuous gradient is preferred, simply incubate the step gradient at 4°C overnight and allow the concentrations to diffuse.

7. Overlay the sucrose gradient with the sedimented virus. Weigh the tubes to ensure they are within 0.1 g of each other. Add dH_2O to balance. Centrifuge at 82,000 x g at 4°C for 1 h
8. Collect the bands by puncturing the tube with a needle connected to a syringe immediately below the band and aspirate the solution including the band into the syringe. Always start from the bottom of the tube so if there is any leakage from the puncture, it will not mix with the bands above it.

   Alternatively, the bands are collected by removing the sucrose from the top of the tube using a sterile Pasteur or serological pipette until a band is reached.

9. Sediment the virus at 35,000 x g for 30 min. Resuspend in 1-3 ml of media, dependent on the pellet size. Store at 4°C.

5.8.2b Expand Purified Baculovirus in Spinner Cultures

10. Add 1 x 10^6 Sf9 cells/ml of supplemented Hink's media to a spinner flask.

    A small spinner culture can be started from an adherent culture and further subcultured into larger spinners with increasing volumes.

    The spinner flask must be filled at least 30% full of media so that the spinner paddle is submerged (i.e. A 100 ml flask needs to contain at least 30 ml of media).

11. If the Sf9 cells reach a density higher than 2.5 x 10^6 cells/ml, split the cells back to 1 x 10^6 cells/ml.

    Cells normally reach the higher density in 24-72 h.

12. Examine cell viability by removing 1 ml of Sf9 culture and mixing with 1 ml of 0.4% Trypan Blue vital stain in PBS. Allow mixture to stand for 5 min but not more than 15 min.
13. Clean and dry the counting chamber and cover slip of the hemocytometer. Using a Pasteur pipette, add the cell mixture to the counting chamber and view under the microscope (100 X)
14. Count the cells in the 4 large corner squares noting the number of blue and clear cells.

    A hand tally counter is useful for this step. Note that each of the large corner squares are divided into 16 smaller squares. Cells that are dead will absorb the trypan blue and appear blue, while live cells will remain unstained.

15. Cell viability must be around 95% before infection with the baculovirus. To calculate the numbers of viable cells/ml use the following formula: (total number of cells / number of squares counted) x counting chamber conversion factor x dilution = number of cells per ml. To determine the % viable cells use: (number of unstained viable cells / total number of cells) x 100

    No of squares counted = 4; counting chamber conversion factor = 10,000; dilution = 2

When ready to infect the Sf9 cells, count them as in Step 15 and determine the MOI of infection based on the PFU/ml as determined below (steps 20-31).

Suspend baculovirus from step 8 in Hink's media with no serum. This is your virus inoculum.

An MOI of 1 is typically used for production of a high baculovirus titer, but the MOI can be optimized.

16. Pellet the cells by transferring the spinner flask culture to sterile 50 ml conical tubes and centrifuging at 2000 x g for 10 min. Resuspend the cells with the proper amount of virus inoculum at a cell density of 1 x 10^7 cells/ml. Incubate at 27°C for 1 h without agitation
17. Remove the inoculum by pelleting the cells as above in Step 17 and resuspend the pellet in fresh Hink's medium. Transfer the infected cells back to the spinner flask with an appropriate amount of media.
18. Incubate the baculovirus-infected Sf9 cells for 72 h for optimal recombinant baculovirus production (Tian, 1995).

5.8.2c Plaque Assay Using Sf9 Cells and Neutral Red Stain to Determine Baculovirus Titer

19. Seed Sf9 cells in a 6-well plate at 8 x 10^5 cells/well
20. Allow the cells to attach to the well at 27°C for 30 min.
21. Prepare dilutions of virus from step 8 in supplemented Hink's medium with 10% FBS in 1.5 ml microcentrifuge tubes. Make sure viral dilutions at 10^{-3}, 10^{-4}, 10^{-5},

10^{-6}, and 10^{-7} are included. Dilutions lower or higher than these are usually not necessary.

22. Add 0.7 ml of diluted virus to each well of a 6-well plate (can be done in duplicate).
23. Rock for 1 h at 27°C for adsorption.
24. Prepare overlay by microwaving 1.5 g of SeaPlaque™ agarose in 50 ml sterile MilliQ water until completely dissolved and allowing it to cool in a 37°C water bath. Pre-warm Hink's media to 37°C.

    Warm the Hink's media sufficiently or the agarose will solidify on contact with the cooler media.
25. Mix the agarose and pre-warmed 2X Hink's medium 1:1 and allow to cool, but not until it is solidified.
26. Remove the virus and carefully overlay with the Hink's/Agarose mixture. Allow Hink's/Agarose mixture to cool slightly until solidified (about 10 min).
27. Incubate for 4-5 days at 27°C in a humidity chamber.

    To make your own humidity chamber, place the 6-well plates in a sterile container within a bag filled with wet paper towels.
28. Overlay the wells with a secondary overlay containing 0.6% SeaPlaque™ agarose, 1X Hink's medium, 10% FBS, and 0.03% neutral red.
29. Incubate at 27°C until cells they absorb the neutral red (4 – 5 h).
30. To determine the titer, count the number of plaques as described in *Basic Protocol 3* Unit 15C.3.

5.8.2d Recombinant Baculovirus Infection and Expression of NSP4 in Sf9 Spinner Cultures

31. Prepare Sf9 spinner cultures as in steps 10-11, and infect with an MOI of 3 PFU/cell.
32. Incubate the cells and virus for 36 h while spinning for optimal NSP4 expression (Tian, 1995).
33. Pellet the cells at 2000 x g for 10 min and remove the supernatant. Wash the cells by resuspending in PBS and pelleting again. Resuspend in Hink's media, supplemented and store at 4°C, or lyse the cells by resuspending in DOC lysis buffer as described in step 2 of Support Protocol 1.

5.9 Support Protocol 1: Quaternary Methylamine (QMA) Anion Exchange Chromatography for Semi-Purification of NSP4 from Sf9 Cell Lysates

NSP4 expressed from recombinant baculovirus in Sf9 cells in media or lysis buffer must first be semi purified by anion exchange chromatography before further purification (affinity chromatography) described in Support Protocol 2 .

5.9.1 Solutions and Specific Equipment

AccellPlus Quaternary Methylamine Anion (QMA) packing (Waters #WAT010742)

Advanced Purification 2 (AP-2) Column (20 x 300 mm) (Waters #WAT027503)

HPLC grade methanol, filtered through 0.45 μm filter

HPLC Milli-Q water, filtered through 0.45 μm filter

0.2% Sodium Azide (see recipe)

Waters FPLC or equivalent *Capable of accurately generating specific gradients and a 4.5 ml/min flow rate*

Fraction Collector

Test Tubes for Collection

QMA Solution A: 0.1 M Tris-HCl, sterile filtered (see recipe)

QMA Solution B: 0.1 M Tris-Base, sterile filtered (see recipe)

QMA Solution C: 2.0 M NaCl, sterile filtered (see recipe)

QMA Solution D: Milli-Q H_2O, sterile filtered

Deoxycholate (DOC) lysis buffer (See recipe)

5.9.2 Steps and Annotations

If cells were stored in media, re-pellet the cells at 2000 x g for 10 min and remove the supernatant. Add DOC lysis buffer to the Sf9 cell pellet as described in step 2 of Support Protocol 1.

5.9.2a Preparation of QMA Column

1. Weigh 44 grams of QMA beads for 88 mls of bed volume.

   Note: Each gram of beads will yield 2 ml of bed volume and can be adjusted to the size of the column.

2. Swell the beads in HPLC grade methanol by adding 3-5 times the volume of the beads.
3. Allow the beads to settle and remove the methanol.
4. Wash the beads with 150 ml filtered, MilliQ water and degas.
5. Attach an AP-2 column or equivalent to a support stand using utility clamps.
6. Remove the inlet connector assembly from the column and place the packing funnel into the inlet cap.

7. Pour the water and bead slurry into the funnel and plug the outlet cap when finished.
8. Let the beads settle and remove excess water from the top of the column.

    The column bed may be too high. If this is the case, remove some of the slurry so that the bed fits into the column.
9. Attach the inlet connector and adjust the inlet connector assembly until the plunger contacts the column bed.
10. Store the column in 0.2% sodium azide at 4°C with the column inlet and outlet plugged.

    Sodium azide is a known mutagen, and can be explosive and toxic when in contact with certain metals and acids. Take precaution when working with sodium azide by wearing the proper personal protective equipment.

5.9.2b Quaternary Methylamine Anion Chromatography

11. Prepare QMA Solutions A, B, C, and D.
12. Attach the prepared column to the FPLC.
13. Equilibrate the QMA column as follows:
    a. Run QMA Solution D (MilliQ sterile water) at a rate of 4.5 ml/min for 30 min.
    b. Run 80% QMA Solution C + 20% QMA Solution D at 4.5 ml/min for 30 min.
    c. Repeat steps a and b at least 3-5 times or until the baseline UV (280 nm) signal is stable.
    d. Run QMA Solution D at a rate of 4.5 ml/min for 60 min.
    e. Run 10% QMA Solution A + 10% QMA Solution B + 80% QMA Solution D at 4.5 ml/min until the pH of the eluate is consistently 8.1.

14. Sonicate the infected Sf9 cells in lysis buffer at 45 W for 3 min.
15. Dilute the lysate to 50 ml with 10% QMA Solution A + 10% QMA Solution B + 80% QMA Solution D.
16. Filter the diluted lysate through a 0.22 um filter.
17. Load the filtered lysate in the inlet port of an FPLC with the equilibrated QMA column attached and run the sample through the column at a speed of 2 ml/min.
18. Wash the column with 10% Solution A + 10% Solution B + 80% Solution D with a flow speed of 4.5 ml/min for 360 min until the Abs 280 nm drops to the background levels.

    NOTE: You may run this overnight at a flow rate of 1.5 ml/min for a total volume of 1500 ml.

19. Elute NSP4 from the column using the following parameters:

Minute	Flow	A%	B%	C%	D%	Curve
0	0.5	10	10	--	80	--
2	4.5	10	10	8	72	6 (linear)
20	4.5	10	10	8	72	6
120	4.5	10	10	80	--	6
121	0.0	--	--	--	--	--

20. Collect all fractions for each min (4.5 ml per fraction after the first 2 min).
21. Fractions corresponding to the presence of NSP4 (based on dot blot data) are pooled, dialyzed and lyophilized
    a. Dialyze in a large (2 L beaker) with a large volume of 50 mM NH_4HCO_3 and mixing slowly with a stir bar. A minimum of 3 buffer changes should be made to ensure the fractions are now in the ammonium bicarbonate solution.

b. Remove the sample from the dialysis bag or cassette and shell freeze by placing in a 1:1 solution of dry ice and ethanol and swirling the solution should go up onto the sides of the tube and freeze. Store sample at -70°C until ready for lyophilization.

To remove the samples from the dialysis bag, it is best to initially use a syringe and needle. When most of the solution is recovered then you can wring out the dialysis tubing into the lyophilization tube. The sample can be recovered from the cassettes using a 16G needle as described by the manufacturer.

c. Precool the lyophilizer and turn the vacuum on. Follow the instructions provided with the lyophilizer to add your sample.

Generally when a sample initially is added to a lyophilizer, the vacuum will drop temporarily. It is important that you wait and watch the vacuum gauge to ensure the vacuum is reestablished. Check you samples for the first couple of hours to make sure they are not melting. If there is evidence of melting (bubbles, dampness), remove the samples from the lyophilizer, repeat the shell freeze and then add to the lyophilizer again.

22. Lyophilize until dry and store in a desiccator at -20°C. To achieve greater purification, continue to Support Protocol 2 for affinity purification.

5.10 Support Protocol 2: Generate and Enrich NSP4-Specific IgG for Use as Ligand in the NSP4 Affinity Column

There are many types of affinity columns, chemistries and ligands that can be used, but the author is more experienced with the cyanogen bromide-activated column. Alternately, you may use the Affi-Gel Hz column (Bio-Rad) according to the manufacturer's instructions. In this unit, the generation and purification of NSP4 peptide or protein-specific IgG is described for the preparation of the NSP4 antibody affinity column.

Given the difficulties in acquiring a significant quantity of purified NSP4 this protocol will focus on NSP4-specific peptides. We have been successful using NSP4$_{114-135, 120-147, or 90-140}$ peptide alone or in combination.

5.10.1 Solutions and Specific Equipment

HCl, 1 mM

Coupling buffer (see recipe)

Blocking buffer (see recipe)

Washing buffers of alternate pH (see recipe)

Binding buffer (sterile filtered PBS, pH 7.5, see recipe)

Elution buffers (pH 4.5 and 3.0, see recipe)

NaOH, 0.5 M

Ammonium bicarbonate, 0.05 mM in dH_2O

CnBr-activated Sepharose 4B (GE Healthcare) (catalog # 17-0430-01), 4% agarose, average bead size of 90 μm, coupling capacity of 25-60 mg of α-chymotrypsinogen, stable pH 3-11

Sintered glass filter, porosity of G3, or Büchner funnel #6

Stoppered flask

Pipettes

Collection tubes

Glass column with or without adaptor

NSP4-specific, purified antibody or other ligand (5-10 mg of protein per ml of column gel)

NSP4-specific immune-dominant synthetic peptides

Dialysis tubing, 12 kD MWCO, or dialysis cassette (Slide-A-Lyzer Dialysis Cassette, 10 kD MWCO, Thermo Scientific #66810)

Balance

Lyophilizer

Rotator

Peristaltic pump (Cole Palmer or equivalent)

UV detector (Isco UA6 or equivalent)

Chart recorder

Fraction collector

Spectrophotometer

Peristaltic Pump

Saturated ammonium sulfate

Keyhole limpet hemocyanin

Glutaraldehyde (EM grade)

Dialysis tubing or dialysis cassette (3000 MWCO)

Glycine, 1 M, pH 7.5

Freund's Complete and Incomplete adjuvant

Emulsifying needle

New Zealand white rabbits

Protein A sepharose 4G

Ammonium bicarbonate, 50 mM

Glycine-HCl, 0.1 M, pH 3.5

MicroBCA kit (Thermo Pierce, catalog # 23235)

5.10.2 Steps and Annotations

If availability of pure NSP4 is problematic, synthetic peptides are a good alternative. Previous studies have shown peptides to be highly immunogenic and reactive to the native protein if carefully selected. However, the peptides must be cross-linked to a carrier protein such as keyhole limpet hemocyanin (KLH) prior to immunization of the laboratory animals.

5.10.2a Preparation of Antigen

1. NSP4 protein (70-75% pure) can be directly emulsified in a suitable adjuvant for immunization, whereas synthetic peptides (90-95% pure) must be cross-linked to a

carrier protein. An alternative is to employ the protein separated by SDS-PAGE by removing the gel band. Another alternative is the solubilization of nitrocellulose filters in which the protein has been absorbed. Proteins isolated from a gel band have the advantages of being highly immunogenic due to the polyacrylamide and can be used when only small quantities of protein are available.

The gel band is frozen, pulverized, and lyophilized. The gel pieces then can be removed from the tube, weighed, dissolved in PBS, pH 7.5, and emulsified.

When using synthetic peptides, the peptides must be carefully selected. Check the literature to determine if immune-dominant epitopes are published. If not, there are several programs that predict antigenic sites on the web. Use of multiple peptides may be best if the immune reactivity is not known.

2. To glutaraldehyde-link the peptides to KLH, mix the KLH and peptide solutions at a ratio of 1 nmol KLH to 100 nmol peptide (or 1:100). This can be scaled up or down as long as the ratio remains the same.

The KLH and peptide solutions are prepared in water or PBS. The volume is independent since you are working in nmol. Mix the 2 solutions in a small beaker or vial with a stir bar.

3. Add glutaraldehyde to a final concentration of 0.4%.

4. Stir for 1 h at room temperature.

The solution may become cloudy. Continue with the protocol as the efficiency of cross-linking is not altered.

5. Quench the reaction by adding 1 M glycine to a final concentration of 200 mM and stir for another 30-45 min.
6. Transfer the solution to a dialysis bag (Spectra/Por CE) or cassette (Thermo Scientific), 3000 MWCO.
7. Dialyze against PBS, pH 7.5, or 50 mM ammonium bicarbonate depending on the desired final volume of cross-linked peptide. The dialysis solutions should be sterile and endotoxin free. Change the dialysis buffer a minimum of 3 times over a minimum of 24 h using large volumes.
8. If dialyzed against PBS, remove the cross-linked peptide solution from dialysis and emulsify with an equal volume of adjuvant. If dialyzed against ammonium bicarbonate, shell freeze and lyophilize, which enables you to hydrate the lyophilized powder in the desired volume. Emulsify in adjuvant using an emulsifying needle.

There are a number of adjuvants available. Animal care personnel should be consulted about the adjuvants shown to enhance the immune response and allowed in the animal facility. When using synthetic peptides as the immunogen, we find Freund's adjuvant to be the best despite the well-documented problems with Freund's Complete, which only is used for the first injection. We generally write a justification for its use and clearly state that Freund's Complete only will be administered intramuscularly (IM). Subsequent

boosts are given in Incomplete Freund's IM, subcutaneously (SC) across the neck, and intraperitoneally (IP) in the abdomen.

9. Follow established protocols for antibody generation in terms of number of injections and bleeds. Final bleeds should be completed only after serum from a test bleed is shown to be reactive to the native protein at a reasonable titer (ELISA and/or Western blot). Test bleeds should be acquired after the second and all subsequent boosts.

When working with peptides, at least 3 boosting doses generally are required.

All animals must be humanely treated and the investigator must follow Animal Use guidelines. Any discomfort or stress to the animals must be limited to that which is absolutely necessary. Anesthetics, analgesics and tranquilizing drugs will be used when appropriate to minimize discomfort to the animals.

The species of the laboratory animals used for antibody production varies. However we obtain higher titers with New Zealand white rabbits; and rabbit IgG readily binds Protein A. If rabbits are employed, the following guidelines should be followed: for the first immunization, a maximum of 0.1 ml can be injected into each hip containing a maximum of 150 nmol of peptide or 3 nmol of protein. Subsequent boosting inoculations are a maximum of 0.05 ml when administered subcutaneously (SC) and the total volume should not exceed 0.5 ml. About the same amount of peptide/protein will be given in each boost.

10. Once the immune sera from the final bleed has been collected, and shown to be reactive with the cognate protein by ELISA and/or Western blot, the IgG is isolated from the serum. The goal here is the removal of non-protein components and non-IgG proteins such that the IgG is enriched with minimal contaminants.

    There are many recommended IgG isolation protocols and several commercial kits are available. We typically utilize ammonium sulfate precipitation, desalting, and reactivity with Protein A on magnetic beads. Various HPLC columns are available as well as a variety of ion exchange methods.

5.10.2b Ammonium Sulfate Precipitation

11. For $(NH_4)_2SO_4$ precipitation, clarify the serum by centrifugation at 10,000 rpm for 10 min. Remove supernatant and chill in an ice bucket.
12. While the serum is stirring at 4°C, slowly add the saturated ammonium sulfate solution to a final concentration of 40% (volume of saturated ammonium sulfate is 0.66 x the volume of serum) and let the solution slowly stir at 4°C for 4 h.
13. Pellet the precipitate by centrifugation at 10,000 rpm for 20 min at 4°C. Remove the supernatant.
14. Dissolve the pellet in half the initial volume of the serum with either sterile dH_2O or PBS, pH 7.5. The precipitation reaction can be repeated to ensure all of the IgG is precipitated.

The total protein concentration of the serum usually is 60-70 mg/ml with immunoglobulins representing 20-24% of the total protein with IgG as the primary antibody component.

15. Dialyze against sterile PBS, pH 7.5, following the protocol above (see step 6) using dialysis tubing with a 100 kD MWCO.

It is helpful to determine the protein concentration of the IgG prior to starting the next step. Any commercial kit can be used. We recommend the Micro BCA Kit (Pierce Thermo).

5.10.2c Protein A Affinity Column

16. Protein A binds 2 immunoglobulin molecules with a strong affinity for the Fc region. Protein A-Sepharose is commercially available from a number of sources. A column can be prepared with the Protein A-Sepharose or a batch method can be used.
17. For the batch method, which is quick and easy, add PBS to the hydrated sepharose beads and equilibrate for 1 h at 4°C. Centrifuge the beads at 2000 x g for 5 min and discard the supernatant. Add the dialyzed IgG, which is now in PBS to the equilibrated Protein A beads and mix on a platform rotator in the cold (4°C) for 4 – 12 h.

Similarly, the beads can be poured into a column and attached to a peristaltic pump for equilibration (see above steps 1-3). Slowly Add the IgG solution to the top of the column and collect the flow-through for protein concentration analysis.

18. Again pellet the beads as in step 17, and this time, keep the supernatant for determining protein concentration (should be significantly lower). If the concentration of the supernatant fails to significantly drop, repeat step 17.
19. For elution of the IgG from the beads, the company from which the beads were purchased will provide recommendations and should be followed. A commonly recommended elution buffer is 50 mM glycine, pH 3.0. To elute, pellet the beads, keep the supernatant for protein concentration assay, and add the elution buffer.

    Note: The elution buffer should not be incubated for an extended length of time. After the antibody is eluted, immediately neutralize the slurry with 1M Tris, pH 8.0.

20. Pellet the beads again and transfer the supernatant to dialysis tubing (12,000 MWCO) or dialysis cassettes (Pierce Thermo). The molecular weight of IgG is around 150,000.
    a. Dialyze in a large (2 L beaker) with a large volume of 50 mM NH_4HCO_3 and mixing slowly with a stir bar. A minimum of 3 buffer changes should be made to ensure the fractions are now in the ammonium bicarbonate solution.
    b. Remove the sample from the dialysis bag or cassette and shell freeze by placing in a 1:1 solution of dry ice and ethanol and swirling to cause the solution to go up onto the sides of the tube and freeze. Store sample at -70°C until ready for lyophilization.

       To remove the IgG sample from the dialysis bag, it is best to initially use a syringe and needle. When most of the solution is recovered then

you can wring out the dialysis tubing into the lyophilization tube. The sample can be recovered from the cassettes using a 16G needle as described by the manufacturer.

c. Precool the lyophilizer and turn the vacuum on. Follow the instructions provided with the lyophilizer to add your sample.

Generally when a sample is added to a lyophilizer, the vacuum will drop temporarily. It is important that you wait and watch the vacuum gauge to ensure the vacuum is reestablished. Check the samples for the first couple of hours to make sure they are not melting. If there is evidence of melting (bubbles, dampness), remove the samples from the lyophilizer, repeat the shell freeze and then add to the lyophilizer again.

d. Lyophilize until dry and store in a desiccator at -20°C.

5.10.2d Isolation of NSP4-specific IgG Employing a NSP4-peptide or Protein Affinity Column

Since the purpose of the affinity column is to isolate NSP4 expressed in the media of mammalian cells or insect cell lysates (Alternate Protocol 3) the use of NSP4-specific peptides is recommended as the ligand if immune-dominant peptides are available.

21. To isolate NSP4-specific antibody, the IgG must be bound with either NSP4 or NSP4-specific peptides. Since we generally employ synthetic peptides for this step, the focus of the protocol will be on the NSP4-specific peptides as ligand. Because of the size of KLH, many of the antibodies will be directed against the carrier protein.

Thus separation of the IgG specific to NSP4 from anti-KLH and other rabbit IgG is important. Immuno-affinity purification is the most frequently utilized method to purify antigen-specific antibodies from polyclonal antibodies.

An alternative to isolating the NSP4-specific IgG by NSP4 peptide affinity is to prepare a KLH affinity column to remove the abundant KLH antibodies from the IgG pool (see below). In this case, the ligand is KLH and the supernatant is collected, dialyzed and lyophilized. The KLH IgG can be eluted from the column, the column restored and subsequently stored at 4°C for future use.

If using a KLH affinity column, the NSP4-specific IgG is enriched but other rabbit immunoglobulins to other antigens are still present.

22. To prepare the NSP4-peptide or protein affinity column CnBr-activated beads are employed.

    a. Activate the CnBr-activated Sepharose 4B beads by suspending the appropriate amount of the Sepharose product in 1 mM HCl (pH 3 is recommended) and allow to swell for 1 to 2 min.

       1 g of lyophilized CnBr-activated Sepharose 4B swells to about 3.5 ml of column volume. The amount of resin to swell depends on the column size and the amount of NSP4 to be purified.

    b. Remove additives from the activated sepharose by washing for 15 min with the 1 mM HCl on a sintered glass filter with a porosity of G3 or

Büchner funnel #6. 200 ml of 1 mM HCl per gram of dried CnBr-activated sepharose is sufficient and should be added in aliquots.

c. Dissolve the ligand (for our purposes, enriched NSP4 protein or NSP4-specific peptide will be the ligand) in coupling buffer at a ratio of 5 ml coupling buffer to 1 g of ligand. The ligand should be in a powdered or freeze-dried form. It is recommended to employ 5-10 mg of ligand per ml of gel slurry.

Take an Absorbance$_{280}$ reading of the ligand solution prior to adding to sepharose beads as an indication of NSP4 peptide or protein (ligand) concentration.

d. Add the coupling buffer with the dissolved ligand to the prepared sepharose suspension in a stoppered flask. Gently rotate the mixture end-over-end for 1 h at room temperature or overnight at 4°C.

Other methods of mixing can be employed, however a magnetic stirrer should be avoided as it damages the sepharose beads.

23. Pellet the beads at 350 x g for 1 min. Take an Absorbance$_{280}$ reading of the supernatant

The Absorbance$_{280}$ should be at least 10-fold lower than that in step c insuring the ligand has been bound. If there is no drop in the absorbance reading, this indicates that there is a problem with the activation of the sepharose 4B and the ligand failed to bind the sepharose beads. You should start over with the activation step (step a).

24. Remove unbound ligand by washing with 5 column volumes of the coupling buffer.
25. Block the active groups by mixing the beads with the blocking buffer and incubating for 2 h at room temperature or 16 h at 4°C.
26. Treat the sepharose slurry with alternate pH washing buffers. Wash for a minimum of 3 cycles, preferably 4 cycles, of the alternating pH with 5 ml of volume in each wash.
27. Pack the column with the NSP4 or peptide-bound CnBr-activated Sepharose 4B (for purification of the specific IgG).
    a. Prepare the slurry with PBS, pH 7.5 (binding buffer) in a ratio of 75% settled beads to 25% binding buffer.

       It is important that the buffers lack amines as these will couple to the gel. NSP4 should also be prepared in the PBS binding buffer.
    b. De-gas the gel slurry to reduce bubbles and flush the end pieces of the column with binding buffer to eliminate trapped air. Close the column outlet with a few cm of buffer remaining.
    c. Equilibrate all material to be used to the same temperature.
    d. Pour the slurry into the column in one smooth movement being careful not to form bubbles (see Basic Protocol 4, step 7a-7d).

       To further reduce bubbles, pour the slurry down a glass rod that is held against the wall of the column.
    e. Fill the remainder of the column with binding buffer. Mount the top piece onto the column and attach to a peristaltic pump (Cole Parmer)

f. As with the preparation of the ConA affinity column (Basic Protocol 4) the maximum flow rate for the Sepharose 4B beads is 75 cm/h at room temperature, which is limited to packing of the column. 75% of the maximum flow should be use for the remainder of the chromatographic procedure.

g. Pump a minimum of 3 column volumes of binding buffer through the column. Ensure a constant bed height is reached.

28. Attach the adaptor to the column (same as in Basic Protocol 4, step 7e-7h)

a. Adjust adapter so that the O-ring sits against the column wall, but does not compress the beads.

b. Purge the flow adaptor with equilibration buffer to remove all air bubbles.

c. Latch the flow adaptor onto the column and insert the flow adaptor into the column until it touches the buffer.

d. Push the cam latch all the way down to the column bed and turn it slightly counterclockwise to lock it in place.

29. Binding and elution of NSP4-specific IgG.

a. The IgG lyophilized sample should be diluted in the same PBS, pH 7.5, in which the column was equilibrated.

b. Carefully add the IgG solution to the top of the column and allow the solution to enter the column bed. Immediately add additional binding buffer.

c. Establish an air-free connection between the column and the UV detector. Also set up the fraction collector (the flow should go from the column-peristaltic pump to the UV detector to the chart recorder and fraction collector)

d. Continue to pump binding buffer until the baseline is stable (wash with about 5 columns of binding buffer while watching the UV monitor).

e. Elution of NSP4 IgG can be accomplished by changing the pH or ionic strength of the buffer. In this system altering the pH works well. Add about 5 column volumes of elution buffer A (pH 4.3) while watching the UV monitor. Be sure the absorption at 280 nm has returned to baseline before the next step.

   It is useful to add 0.05 ml or more depending on the fraction size of 0.5 M NaOH to each collection tube to neutralize the acid as it exits the column.

f. Elute with about 5 column volumes of elution buffer B (pH 2.3) while watching the UV monitor. Be sure the absorption at 280 nm has returned to baseline before equilibrating the column with binding buffer containing 0.02% sodium azide. Store at 4°C.

g. Collect the tubes from the fraction collector that corresponds to the UV 280 nm peaks. Pool fractions as appropriate.

h. Immediately transfer the fractions to dialysis tubing or dialysis cassettes for dialysis and lyophilization (step 20d – 20g above).

5.11 Support Protocol 3: Affinity Chromatography of Semi-Purified NSP4 Using Purified NSP4 IgG as Ligand

5.11.1 Solutions and Specific Equipment

HCl, 1 mM

Coupling solution (see recipe)

Blocking buffer (see recipe)

Washing buffers of alternate pH (see recipe)

Binding buffer (sterile filtered PBS, pH 7.5, see recipe)

Elution buffers (pH 4.5 and 3.0, see recipe)

NaOH, 0.5 M

Ammonium bicarbonate, 0.05 mM in dH_2O

CnBr-activated Sepharose 4B (GE Healthcare) (catalog # 17-0430-01), 4% agarose, average bead size of 90 μm, coupling capacity of 25-60 mg of α-chymotrypsinogen, stable pH 3-11

Sintered glass filter, porosity of G3, or Büchner funnel #6

Stoppered flask

Pipettes

Collection tubes

Glass column with or without adaptor

NSP4-specific, purified antibody or other ligand (5-10 mg of protein per ml of column gel)

Dialysis tubing, 12,000 MWCO, or dialysis cassette (Slide-A-Lyzer Dialysis Cassette, 10,000 MWCO, Thermo Scientific #66810)

Balance

Lyophilizer

Rotator

Peristaltic pump (Cole Parmer or equivalent)

UV detector (Isco or equivalent)

Chart recorder

Fraction collector

Spectrophotometer

Saturated ammonium sulfate

Keyhole limpet hemocyanin

Glutaraldehyde (EM grade)

Dialysis tubing or dialysis cassette (3000 MWCO)

Glycine, 1 M, pH 7.5

Freund's Complete and Incomplete adjuvant

New Zealand white rabbits

Protein A or G agarose beads

Ammonium bicarbonate, 50 mM

Glycine-HCl, 0.1 M, pH 3.5

MicroBCA kit (Thermo Pierce, catalog # 23235)

5.11.2 Steps and Annotations

Protocols below are adapted from The Protein Protocols Handbook and Cell Biology: A Laboratory Manual (Walker, 1996).

Most of the steps are identical to Support Protocol 2 except that the NSP4 IgG is used as the ligand to purify the expressed NSP4 from the baculovirus recombinant-infected Sf9 lysates prepared in Alternate Protocol 2.

1. Immobilization of purified NSP4-specific IgG (see Support Protocol 2).

a. Activate the CnBr-activated Sepharose 4B beads by suspending the appropriate amount of the Sepharose product in 1 mM HCl (pH 3 is recommended) and allow to swell for 1 - 2 min.

   1 g of lyophilized CnBr-activated Sepharose 4B swells to about 3.5 ml of volume. Weigh out an adequate amount of activated sepharose to prepare the column to be used.

b. Remove the additives from the activated sepharose by washing for 15 min with 1 mM HCl on a sintered glass filter with a porosity of G3 or Büchner funnel #6. 200 ml of 1 mM HCl per gram of dried CnBr-activated sepharose is sufficient and should be added in aliquots.

c. Dissolve the lyophilized NSP4-specific purified IgG in coupling buffer at a ratio of 5 ml coupling buffer to 1 g of ligand. It is recommended to use 5-10 mg per ml of gel slurry.

   Take an Absorbance$_{280}$ reading of the antibody solution prior to adding to the sepharose beads as an indication of antibody concentration.

d. Add the coupling buffer with the dissolved NSP4-specific IgG to the prepared sepharose suspension in a stoppered flask. Gently rotate the mixture end-over-end for 1 h at room temperature or overnight at 4°C.

   Avoid a magnetic stirrer for mixing as it damages the sepharose beads.

e. Spin down the beads at 350 x g for 1 min. Take an Absorbance$_{280}$ reading of the supernatant.

The Absorbance$_{280}$ should be at least 10-fold lower than that in step b insuring the IgG has been bound. If there is no drop in the absorbance reading, this indicates that there is a problem with activation of the sepharose 4B and the antibody (ligand) failed to be bound by the sepharose beads. You should start over with the activation step (step a).

f. Remove unbound ligand by washing with 5 column volumes of coupling buffer.

g. Block active groups by mixing the beads with the blocking buffer and incubating for 2 h at room temperature or 16 h at 4°C.

h. Treat the sepharose slurry with alternate pH washing buffers. Wash for 4 cycles of the alternating pH with 5 ml of volume in each wash.

2. Pack the column with the purified IgG-bound CnBr-activated Sepharose 4B (for purification of the NSP4-specific IgG, see Support Protocol 2 above).

a. Prepare the slurry with PBS, pH 7.5 (binding buffer) in a ratio of 75% settled beads to 25% binding buffer.

It is important that the buffers lack amines as these will couple to the gel. The Sf9 lysates containing NSP4 should also be prepared in the PBS binding buffer.

b. De-gas the gel slurry to reduce bubbles and flush the end pieces of the column with binding buffer to eliminate any trapped air. Close the column outlet with a few cm of buffer remaining.

c. Equilibrate all solutions to the same temperature.

d. Pour the sepharose slurry into the column in one smooth movement.

To further reduce bubbles, pour the slurry down a glass rod that is held against the wall of the column.

e. Fill the remainder of the column with binding buffer. Mount the top piece onto the column and attach to a peristaltic pump (Cole Parmer).

f. The maximum flow rate for the Sepharose 4B beads is 75 cm^3/h at room temperature, which should only be used when packing the column. 75% of the maximum flow should be use for the remainder of the chromatographic procedure.

g. Pump a minimum of 3 column volumes of binding buffer through the column. Ensure a constant bed height is reached.

3. If using an adaptor, the adaptor should be fitted at this point. Note that the protocol can be achieved in the absence of an adaptor.

a. Close the column outlet and remove the top piece from the column. Carefully fill the remainder of the column with binding buffer.

b. Insert the adaptor onto the top of the column at an angle, making sure that no air is trapped. Ensure that the tubing that connects the adaptor to the peristaltic pump is bubble-free.

c. Insert the plunger by slowly sliding it down the column. The capillary tubing should be displaced with eluent.

d. Lock the adaptor in place when it reaches the bed surface and open the column outlet. Pass eluent through the column to ensure the column bed is stable. The detector should be at baseline.

4. Binding and Elution of NSP4.

a. Dilute the NSP4 from the QMA column in the same PBS, pH 7.5, in which the affinity column was equilibrated.

b. Carefully add the lysates to the top of the column and allow entry into the column bed. Immediately add additional binding buffer.

c. Establish an air-free connection between the column and the UV detector. Also set up the fraction collector.

d. Continue to pump binding buffer until the baseline is stable (wash with about 5 columns of binding buffer while watching the UV monitor).

e. Elution of NSP4 can be accomplished by changing the pH or ionic strength of the buffer. For NSP4, altering the pH works well. Add about 5 column volumes of elution buffer A (pH 4.3) while watching the UV monitor. Be sure the $Absorbance_{280}$ has returned to baseline before the next step.

It is useful to add 0.05 ml or more depending on the fraction size of 0.5 M NaOH to each collection tube to neutralize the acid.

f. Elute NSP4 with about 5 column volumes of elution buffer B (pH 2.3) while watching the UV monitor. Be sure the absorption at 280 nm has returned to baseline.

g. Collect the tubes from the fraction collector that corresponds to the UV 280 nm peaks. Pool fractions as appropriate.

h. The column is equilibrated with binding buffer containing 0.02% sodium azide. Store at 4°C.

i. Immediately transfer the fractions to dialysis tubing or dialysis cassettes.

5. Dialyze in a large (2 L beaker) with a large volume of 50 mM NH_4HCO_3 and mix slowly with a stir bar. A minimum of 3 buffer changes should be made to ensure the fractions are now in the ammonium bicarbonate solution.

6. Remove the samples from the dialysis bag or cassette. Shell freeze sample by placing in a 1:1 solution of dry ice and ethanol and swirling the solution up onto the sides of the tube. Store sample at -70°C until ready for lyophilization.

   To remove the fractions from the dialysis bags, it is best to initially use a syringe and needle. When most of the solution is recovered then you can wring out the dialysis tubing into the lyophilization tube. The sample can be recovered from the cassettes using a 16G needle as described by the manufacturer.

7. Precool the lyophilizer and turn the vacuum on. Follow the instructions provided with the lyophilizer to add your samples.

Generally when a sample is added to a lyophilizer, the vacuum will drop temporarily. It is important that you wait and watch the vacuum gauge to ensure the vacuum is reestablished. Check you samples for the first couple of hours to make sure they are not melting. If there is evidence of melting (bubbles, dampness), remove the samples from the lyophilizer, repeat the shell freeze and then add to the lyophilizer again.

8. Store the semi-purified NSP4 in a desiccator at -20°C.

5.12 Reagents and Solutions

5.12.1 Tissue Culture Reagents

5.12.1a Minimum Essential Media, Supplemented with 10% FBS

To 860 mL of a 1X solution of MEM, add 10 mL of 200 mM L-Glutamine, 10 mL of 10 mM Sodium Pyruvate, 10 mL of 100X Non-Essential Amino Acids, 10 mL of 10,000 U/ml -10 µg/ml Pen-Strep Antibiotics, and 100 mL Fetal Bovine Serum. Mix well and sterile filter through a 0.22 µm filter. For a 2X solution, repeat the above using a 2X solution of MEM and two times the amount of supplements. Store supplemented media for up to 2 months at 4°C.

5.12.1b Minimum Essential Media, Supplemented with 10% FBS

To 960 mL of a 1X solution of MEM, add 10 mL of 200 mM L-Glutamine, 10 mL of 10 mM Sodium Pyruvate, 10 mL of 100X Non-Essential Amino Acids, and 10 mL of 10,000 U/ml -10 µg/ml Pen-Strep Antibiotics. Mix well and sterile filter through a 0.22 µm filter. Store supplemented media for up to 2 months at 4°C.

5.12.1c Hink's Medium, Supplemented, with 10% FBS

To 445 ml of Hink's medium, add 5 ml of Penicillin-Streptomycin-Amphotericin B, and 50 ml FBS. Filter sterilize and store at 4°C.

5.12.1d Worthington Trypsin

Dissolve 1 mg of Worthington in 1 mL of autoclaved dH_2O. Filter sterilize with a syringe filter (0.22 μm). Aliquot 100 μL in microcentrifuge tubes and store at -20°C.

5.12.1e Sf9 Lysis Buffer (10 mM Tris, 0.1 mM EDTA, 2% Sodium Deoxycholate)

To 900 mL, add 1.21 g Tris-HCl, 50 mL of 2 M EDTA, pH 8, and 2 g DOC. Filter sterilize and store at 4°C for up to 3 months.

5.12.1f Sucrose Solutions

Add solutions to ~20 mls H_2O, dissolve, and transfer to a graduate cylinder and fill to 30 mls. Filter sterilize all solutions. It may be necessary to warm the solutions to 42°C to dissolve the sucrose completely.

20%: 6 g in 30 mls H_2O

30%: 9 g in 30 mls H_2O

35%: 10.5 g in 30 mls H_2O

40%: 12 g in 30 mls H_2O

50%: 15 g in 30 mls H_2O

60%: 18 g in 30 mls H_2O

65%: 19.5 g in 30 mls H_2O

5.12.2 RNA Purification Reagents

5.12.2a 0.1 M Sodium Acetate Buffer (pH 5)

To 950 mL of dH_2O, add 2.06 ml of acetic acid and 5.25 g of sodium acetate. Q.S. to 1 L, autoclave, and store at room temperature for up to 6 months.

5.12.2b Phenol Mixture

Add 500 g of phenol and 70 g of m-cresol, to 200 ml of water containing 0.5 g of 8-hydroxquinoline. Keep protected from light and store at 4°C.

5.12.2c 30% Acrylamide Stock

Dissolve 30 g of acrylamide and 0.8 g of N,N'methylenebisacrylamide in 60 ml of distilled water. Q.S. to 100 mL and filter through 0.45 μm. Store in a dark or foil-covered bottle, and store at 4°C for up to 1 month.

5.12.2d Resolving Gel Buffer

Dissolve 18.15 g of Tris base in 40 ml of dH_2O. Adjust the pH to 8.8 with 1N HCl. Q.S. to 100 ml with dH_2O. Store at 4°C for up to 1 month.

5.12.2e Stacking Gel Buffer

Dissolve 5.98 g of Tris base in 50 ml of distilled water. Adjust the pH to 6.8 with 1N HCl. Q.S. to 100 ml with distilled water. Store at 4°C for up to 1 month.

5.12.2f 10% Ammonium Persulfate

Dissolve 0.1 g of APS in 1 ml of autoclaved dH_2O before use and store for a maximum of 3 days at 4°C. It is best if 10% APS is made fresh immediately before use.

5.12.2g 5X Tris-glycine Running Buffer

Dissolve 15.1 g of Tris-base and 94 g of glycine in 800 mL dH_2O. Q.S. to 1,000 ml with dH_2O. Store at 4°C for up to 3 months.

5.12.2h 1X Tris-glycine Running Buffer

Dilute 200 ml 5X Tris-glycine buffer with 800 ml of dH_2O. Store at 4°C for up to 3 months.

5.12.2i PAGE Sample Loading Buffer

Dissolve 10 mg of bromophenol blue and 1 ml of glycerol in 5 ml of stacking gel buffer. Q.S. to 10 mL with dH_2O. Store at room temperature for up to 1 month.

5.12.3 Protein Purification Reagents

5.12.3a Con A Binding Buffer (20 mM Tris-HCl, pH 7.4 with 0.5 M NaCl)

Dissolve 1.21 g Tris-HCl and 14.61 g NaCl in 350 mL dH_2O. Adjust the pH to 7.4 with 10 N KOH. Adjust the volume to 500 ml with Milli-Q® H_2O and sterile filter. Store at room temperature for up to 3 months.

5.12.3b Con A Elution Buffer (0.5 M α-D-methyl-mannopyranoside in ConA Binding Buffer)

Dissolve 24.27 g of α–methyl-mannopyranoside in ConA Binding Buffer. Q.S. to 250 mL with ConA Binding Buffer. Sterile filter and store at 4°C for up to 1 month.

5.12.3c Mono S Start Buffer (20 mM 2-[N-morpholino] Ethanesulphonic Acid (MES), pH 6.0)

To 350 mL dH_2O, add 2.13 g of MES free acid monohydrate. Adjust the pH to 6.0 with 10N NaOH. Q.S. to 500 mL with dH_2O. Filter sterilize and store at 4°C for 1 month.

5.12.3d Mono S Elution Buffer (20 mM MES, 1.0 M NaCl, pH 6.0)

Dissolve 14.61 NaCl in 200 mL 20 mM MES. Q.S. to 250 mL with 20 mM MES. Filter sterilize and store at 4°C for 1 month.

5.12.3e 0.2% Sodium Azide

Dissolve 2 g sodium azide in 1000 ml Milli-Q H2O. Filter through a 0.45 μm filter and store at 4°C.

5.12.3f QMA Solution A

Dissolve 31.52 g of Tris-HCl in 2 L of dH_2O. Filter solution through a 0.45 μm filter. Store at room temperature for 3 months.

5.12.3g QMA Solution B

Dissolve 24.23 g of Tris-Base in 2 L of dH_2O. Filter solution through a 0.45 μm filter. Store at room temperature for 3 months.

5.12.3h QMA Solution C

Dissolve 233.76 g NaCl in 2 L of dH_2O. Filter sterilize and store at room temperature for 3 months.

5.12.3i Saturated Ammonium Sulfate

Dissolve 53.1 g of $(NH_4)_2SO_4$ per 100 ml dH_2O; prepare at room temperature and cool to 4°C. Store overnight at 4°C prior to using.

5.12.3j Glycine-HCl, 0.1 M, pH 3.5

Dissolve 1.12 g glycine-HCl in 75 mL dH_2O. Adjust the pH with 2 M HCl and q.s. to 100 ml.

5.12.3k 50 mM NH_4HCO_3 Dialysis Buffer

To 3.5 L of dH_2O, add 15.81 g of NH_4HCO_3. Q.S. to 4 L and filter sterilize.

5.12.3l Coupling Buffer (0. 1M NaHCO3, 0.5 M NaCl)

Dissolve 0.84 g of $NaHCO_3$ and 2.92 g NaCl in 80 mL MilliQ H_2O and pH to 8.3 with HCl. Q.S. to 100 ml and filter sterilize.

5.12.3m Blocking Buffer

Can use either 0.1 M Tris-HCl, pH 8.0 or 1 M ethylamine, pH 8.0, filter sterilize

5.12.3n Washing Buffers of Alternate pH (0.1 M Acetate buffer with 0.5 M NaCl and 0.1 M Tris-HCl)

Dissolve 5.25 g sodium acetate in 850 ml dH_2O. Add 2.06 mL acetic acid. Dissolve 29.22 g NaCl and 15.76 g Tris-HCl. Adjust the pH using 1 M HCl or 1 M NaOH. Q.S. to 1 L.

5.12.3o Binding Buffer PBS, pH 7.5

Dissolve 8 g of NaCl, 0.2 g of KCl, 1.44 g of Na_2HPO_4 and 0.24 g of KH_2PO_4 in 800 ml of dH_2O; Adjust pH to 7.5 with HCl; QS to 1000 ml; Autoclave or filter sterilize and store at room temperature for up to 1 year.

5.12.3p Elution Buffer A

0.5 M sodium acetate, 0.15 M NaCl, adjust pH to 4.5

5.12.3q Elution Buffer B

0.5 M glycine, 0.15 M NaCl, adjust pH to 3.0

5.13 Commentary

5.13.1 Background Information

Rotaviruses (RV) are the major cause of severe, viral gastroenteritis in young children worldwide and are associated with sporadic outbreaks of diarrhea in elderly and immunocompromised patients (Estes, 2013). An established pathophysiologic mechanism by which RV induces diarrhea is malabsorption secondary to the destruction of infected enterocytes. Other mechanisms have been proposed including a reduction in epithelial surface area by replacing the absorptive enterocytes with immature, crypt-like, secretory cells; activation of the enteric nervous system; and villus ischemia. The enterotoxic activity of NSP4 represents another possible mechanism of RV-induced diarrhea (Ball et al., 1996). It is likely multiple mechanisms are responsible for the severe fluid loss associated with RV infections.

Rotaviruses are structurally complex with three concentric protein coats forming a capsid that encloses eleven double-stranded RNA segments. A spike protein composed of dimers of VP4 extend through the outermost layer, composed of 260 trimers of VP7, and interacts with the middle protein layer, which is composed of 260 trimers of VP6. The inner protein layer is primarily composed of 60 dimers of VP2 with VP1, a RNA-dependent polymerase and VP3, a guanyl and methyl transferase are located on the inner side of the channels. This inner layer also interacts with the genomic viral RNA (Estes, 2013).

The complete infectious virion is called a triple-layered particle (TLP). The double-layered rotaviral intermediates are called double-layered particles (DLPs). Due to the

calcium dependence of VP7, the outer coat is lost upon viral entry into the low-calcium environment of the cell cytosol forming DLPs, which are transcriptionally active but non-infectious. Transcription occurs within the confines of the DLPs once VP7 and VP4 are removed. RV contains 132 aqueous channels, spanning the outer two-capsid layers, which allow influx of molecules into the DLPs and efflux of newly formed viral mRNAs (Pesavento et al., 2001). Following translation of viral transcripts, newly formed core particles (single shelled) and DLP-like replication intermediates (RI) assemble into electron-dense, perinuclear, non-membrane-bound inclusions (viroplasms) adjacent to the ER. RNA replication occurs in concert with the packaging of the RNAs into the RI. Synthesis and packaging of the genomic dsRNAs are complex, tightly controlled, and described in detail in recent reviews (Patton et al., 2004; Trask et al., 2012). For more detailed background on the RV lifecycle, see Background Information in Unit 15C.3.

A unique step in RV morphogenesis is the budding of DLPs through the membrane of the ER, during which VP7 (outer layer), VP4 (spike protein), and a transient ER membrane is added to the immature particle. This budding event is mediated by the ER-localized nonstructural glycoprotein NSP4 (Estes, 2013), which functions as an intracellular receptor by binding VP6 (the outer layer of DLPs) (Taylor et al., 1996) and initiating translocation into the ER for addition of the outer protein layer. NSP4 contains a single transmembrane domain (residues 24-44) that traverses the ER bilayer such that the N-terminal 24 amino acids remain in the lumen of the ER and residues 45-175 form an extended, cytoplasmic domain. Two *N*-linked high mannose glycosylation sites are located within the short ER luminal domain at residues 8 and 18. Classical ER retention

signals are lacking in the NSP4 sequence and the mechanism of NSP4 retention in the ER remains unknown. NSP4 does not appear to be retrieved from the Golgi by retrograde transport since NSP4 carbohydrate moieties remain sensitive to endoglycosidase H digestion (oligosaccharide processing stops at $Man_8GlcNAc$).

Mutational analyses have revealed that the receptor activity of NSP4 is localized to the C-terminus of the fully-glycosylated 28 kD protein and has disclosed that only the C-terminal 20 aa are required for DLP binding (Taylor et al., 1996). Limited NSP4 proteolysis and mass spectroscopic analyses similarly reveal the NSP4 C-terminal residues as the binding domain for VP6 (O'Brien et al., 2000). To facilitate the addition of the outer coat and spike, NSP4 forms a complex with VP4 and VP7. The binding site for VP4 has been localized to NSP4 residues 112-148. Thus, maturation of infectious particles takes place in the ER lumen where the ER membrane and NSP4 are removed by an unknown mechanism and the outer layer and spike protein are added. There is some controversy as to where the spike protein is added to the TLP. Delmas et al. demonstrate that VP4 is added at the PM, and the discrepancy has not been resolved (Delmas et al., 2004).

RNA interference (RNAi) has revealed a 75% reduction in progeny RV when cells are transfected with $siRNA^{NSP4}$ or $siRNA^{VP7}$. This inhibition of virus production is specific, as $siRNA^{NSP4}$ fails to silence a RV strain with a four-nucleotide difference in the NSP4 gene sequence (Lopez et al., 2005). In cells transfected with $siRNA^{NSP4}$, there is a reduction in VP2 (20%), NSP2 (25%), VP7 (30%), VP4 (40%), and NSP5 (50%), and a two-fold increase in NSP3 (170%). Both DLPs and TLPs are reduced to

undetected levels in NSP4 silenced cells, and could explain the absence of defined viral particles and the condensed, sporadic viroplasms in cells with siRNA^{NSP4} (Lopez et al., 2005).

The results with siRNA^{VP7}-transfected cells are distinct from those of siRNA^{NSP4}. In addition to the altered accumulation of several RV-encoded proteins when only NSP4 is silenced, there is a redistribution of other RV proteins. Instead of localization to viroplasms, VP6 is extended to the periphery of the cell in filaments, likewise VP2 distributes throughout the cytoplasm rather than in viroplasms as in siRNA^{NSP4}-transfected cells. This is less surprising given the interactions of NSP4 with VP4 and VP7. The typically perinuclear and filamentous VP4 is found homogenously distributed in the cytoplasm and VP7 is no longer located at the ER in semicircular structures around viroplasms, but is perinuclear and more diffuse (Lopez et al., 2005). The relocalization of VP2, VP6, VP4 and VP7 can be explained by the protein associations with NSP4. NSP4 forms a complex with VP4 and VP7, directly interacts with VP4 and VP6, and VP6 interacts with VP2.

In contrast, alteration of the quantity and distribution of other RV proteins are not seen with siRNA^{VP7}, however a similar 75-80% reduction in progeny virus is noted with the silencing of VP7. In contrast to NSP4-silenced RV expression, DLPs and TLPs are not diminished with siRNA^{VP7}–transfected cells, but an accumulation of noninfectious, enveloped particles is seen within the lumen of the ER (Lopez et al., 2005). Notably in the absence of VP7 as well as VP4, NSP4 is sufficient for the budding of DLPs into the ER lumen (Lopez et al., 2005). Hence, NSP4 is critical to the late stages of RV

morphogenesis.

Full-length NSP4 and its active synthetic peptide, $NSP4_{114-135}$, induces Cl^- secretory currents across unstripped, mouse intestinal mucosa similar to carbachol, an endogenous Ca^{2+}-mobilizing agonist that potentiates cAMP-induced effects, as measured in Ussing chambers (Ball et al., 1996). To extend these observations, cystic fibrosis transmembrane conductance regulator (CFTR) gene knock out mice have been exploited since they are deficient in cAMP-mediated ion transport. In these studies, RV infection, NSP4 and $NSP4_{114-135}$ overcame the cAMP-promoted Cl^- secretion deficiency and induced an age-dependent diarrhea in the null mutation mouse pups. NSP4 also elicits iodide influx into isolated crypt cells from $CFTR^{+/+}$ wild type, $CFTR^{+/-}$ heterozygous, and $CFTR^{-/-}$ homozygous mouse pups, whereas both carbochol and forskolin fail to produce halide influx in the $CFTR^{-/-}$ genotype verifying the unique properties of NSP4 activity. NSP4 mobilizes $[Ca^{2+}]i$ in all regions of the crypt cells from all three RV genotypes (A-C). However, the crypt cell $[Ca^{2+}]i$ response is independent of cell maturity or the age of the mice from which the crypts are isolated. In contrast, the iodide influx is age-dependent, only occurring in crypts isolated from neonatal mice, and requires the presence of Ca^{2+}. Thus, NSP4-induced diarrhea may occur via the activation of an age- and Ca^{2+}-dependent, anionic halide permeability pathway.

RV infection directly inhibits Na^+-D-glucose (SGLT1) and Na^+-L-leucine symporter activity across young rabbit intestinal brush border membrane vesicles (Halaihel et al., 2000). This symporter inhibition is seen with NSP4 and $NSP4_{114-135}$ suggesting NSP4 is responsible for the inhibition of SGLT1 in intestinal brush border membrane vesicles

isolated from young rabbits (Halaihel et al., 2000). Because SGLT1 functions in the reabsorption of water, disruption of its activity would result in fluid accumulation in the lumen of the intestine and could contribute to the diarrheal disease caused by RV infection and/or NSP4. Hence, these data present another mechanism by which NSP4 could induce diarrhea.

Expression of NSP4 up-regulates the expression of cellular proteins, including the ER, Ca^{2+}-binding, host glucose-regulated chaperone proteins BiP (GRP78) and endoplasmin (GRP94), as well as the translationally controlled tumor protein (TCTP). Glycosylated NSP4 transiently associates with calnexin both *in vivo* and *in vitro* (Mirazimi et al., 1998). Calnexin is a trans-ER type I membrane chaperone that interacts with assembly intermediates of numerous membrane glycoproteins. The NSP4-calnexin association is lost upon complete enzymatic removal of the NSP4 glycan moieties.

NSP4 (i) has a microtubule-binding domain, (ii) functions as a microtubule-associated protein (MAP), and (iii) prevents ER-to-Golgi trafficking. Removal of the NSP4 C-terminal residues 140-175 results in loss of tubulin binding and NSP4 no longer redistributes ERGIC53 or β-COP to discrete structures in the cytoplasm that co-localize with NSP4 (Xu et al., 2000). Thus, the microtubule-binding domain has been localized to the C-terminus of NSP4 adjacent to the coiled-coil region. The authors postulate that by blocking the transport from the ER to the Golgi, NSP4 limits the activity of intestinal brush border disaccharidases in the plasma membrane and hence promotes the onset and/or the persistence of diarrheal disease (Xu et al., 2000).

There is compelling evidence that RV infection stimulates nerve reflexes in the ENS

to induce intestinal fluid losses (Lundgren et al., 2000). Given the activity of NSP4 in $[Ca^{2+}]i$ mobilization, it is reasonable to postulate that NSP4 also functions as an enteric nerve secretagogue. Thus, in addition to activating intracellular secretory pathways in enterocytes, NSP4 may activate the secretory reflexes of the ENS that are dependent on Ca^{2+} flux.

Other binding partners of NSP4 have been disclosed (Boshuizen et al., 2003). Genes encoding the extracellular matrix (ECM) proteins laminin-β3 and fibronectin consistently are bound in a yeast two-hybrid screen, and NSP4-ECM protein interactions have been confirmed by co-immunoprecipitation reactions. The NSP4 binding domain of the ECM proteins maps to residues 87-145 as determined by deletion analyses (Boshuizen et al., 2003). An intriguing finding in this study is the localization of NSP4 to the basement membrane of RV-infected and uninfected small intestinal epithelium in mice. These data suggest a basal release of NSP4 in agreement with our findings (Mitchell and Ball, 2004) and subsequent interaction with uninfected cells (Boshuizen et al., 2003).

The enterotoxin can be isolated with plasma membrane caveolae that lack ER markers (Storey et al., 2007), and the C-terminus of NSP4 interacts directly with caveolin-1. The binding domain has been mapped to 3 hydrophobic residues indicating a hydrophobic interaction between NSP4 and caveolin-1 (Parr et al., 2006; Storey et al., 2007). The C-terminus of NSP4 is exposed on the exofacial surface of the plasma membrane and the transport kinetics vary in cell lines of different origins (Gibbons et al., 2011). The mechanism by which NSP4 traffics to the plasma membrane via an

unconventional pathway remains unclear.

NSP4 purified from culture media of RV infected mammalian cells or rNSP4 expressed in insect cells shows strong enterotoxic activity when administered to neonatal mice or exogenously added to cultured intestinal cells. $NSP4_{112\text{-}175}$ induces an age- and dose-dependent diarrhea in young mouse pups equivalent to full-length NSP4 and in agreement with the 114-135 peptide. Moreover, $NSP4_{112\text{-}175}$ mobilizes $[Ca^{2+}]i$ when added exogenously to intestinal cells or expressed endogenously in insect cells (Zhang et al., 2000). NSP4 has recently been shown to act as a viroporin, inducing release of Ca^{2+} from ER stores and activating calcium/calmodulin-dependent kinase kinase β (CaMKK-β) signaling (Crawford et al., 2012; Hyser et al., 2010). Induction of the CaMKK-β pathway by NSP4 leads to induction of autophagy, which is vital to virus morphogenesis (Crawford et al., 2012).

We report that NSP4 traffics to the cell surface by a unique, Golgi-independent, unconventional pathway. Treatment of cells with brefeldin A has no effect on the release of NSP4, and the released NSP4 is sensitive to endoglycosidase H (EndoH) (Gibbons et al., 2011; Storey et al., 2007). Secretion of NSP4 into culture media is abolished by treatment with the cytoskeletal altering drugs nocodazole and cytochalasin D. We also have shown NSP4 secretion and binding to naïve cells in experimentally infected cells. Further, NSP4 binds microtubules, redistributes ER-Golgi intermediate compartment markers to structures that align along linear tracks and radiate through the cytoplasm, and co-localizes with ERGIC53 and β-COP when examined by confocal microscopy (Xu et al., 2000). Detailed studies are needed to fully elucidate the transport

pathway of a pool of NSP4 from the ER to the cell surface.

RV infections have been shown to cross species barriers, both animal-to-human and human-to-animal, and interspecies reassortment of RV genes can occur during co-infections producing novel RV strains (Iturriza-Gomara et al., 2001). Mixing of genes from different RV strains during a co-infection can lead to the packaging of genomic dsRNAs from different strains into subviral particles. This provides a mechanism for the production of genetic and antigenic reassortants.

Several studies suggest that interspecies transmission of RV may occur at a relatively high frequency, especially in developing countries, where mixed infections are more common and humans and animals live in close proximity (Jain et al., 2001). One study suggests that pigs are a reservoir of multiple species of RV and play a crucial role in newly adapted, emerging RV strains in other species (Parra et al., 2008). The unusual genotypes, vaccine evasion, and viruses with enhanced virulence in one or more species raises questions about the effectiveness of current live attenuated vaccines. Co-infection of simian strain SA11 and rhesus RV had 25% progeny virus reassortants as early as 12 hours post-infection, which increased to 80-100% by 72-96 hours post infection (Gombold and Ramig, 1986). With this in mind, there is a higher chance of interspecies reassortment than previously realized, which could result in enhanced RV virulence and vaccine failure.

5.13.2 Critical Parameters and Troubleshooting

5.13.2a Growth and Titering of RV and Generation of Reassortants

Plaque size is irregular or inconsistent-Adding 100 µg/ml of dextran in the primary overlay may help prevent plaquing inconsistencies. There are several other reasons that may cause a plaque assay to fail. For a helpful chart, refer to Table 2 in Arnold, et al. which lists common problems associated with plaque assays and how they can be managed.

Virus cannot be produced at high titer- Low passage virus may not be tissue-culture adapted, which can be problematic for viral growth in culture. Parental strains, especially those isolated from clinical specimens, likely will need to be passaged several times in culture before the titer will increase. For example, RV can be passaged every seven days in MA104 cells until there is evidence of tissue-culture adaptation by the presence of CPE.

Unable to generate the reassortant of interest- Addition of neutralizing monoclonal antibodies as a means of selection will eliminate packaging of the unwanted segment(s) (Gorrell and Bishop, 1997).

Acrylamide gel not polymerizing-It is imperative to degas the casting solutions properly. The solutions need to be room temperature before mixing together. APS must be made fresh daily for best results.

Gel solution solidifying too quickly-Be sure to add APS before adding TEMED. Once the APS is added, you must work quickly to ensure that the gel does not solidify too soon.

Rotavirus RNA contaminated with cellular RNA- The virus can be isolated on a cesium chloride gradient and then pelleted through a 35% sucrose cushion (Alternate Protocol 3 Unit 15C.3). TRIzol® can be added directly to this virus pellet, which will eliminate most cellular RNA contaminants. If the RNA on the PAGE gel looks smeared or bands are not visible, it is possible the RNA is degraded during or after the isolation process. The initial lysis buffer protects the RNA from degradation during extraction, but it is common that the RNA is contaminated with RNases during the isolation. Use of RNase inhibitors and sterile filter tips will reduce this problem. It is recommended to work in an RNA hood and use RNAse spray to reduce RNA degradation. Keep isolated RNA in the freezer at -20°C and when in use, keep RNA on ice at all times. The amount of time the RNA is left on ice should be limited to the time it takes to carry out the experiment.

Silver stain reveals no RNA nor DNA markers- Do not destain longer than 20 sec for 2 times before adding the developer solution. If the bands fail to be visible after the addition of developer, remove all of the developer from the gel by washing for 30 min with multiple changes of dH_2O. Start the process over starting from the sensitizing of the gel to staining and developing. If the bands are still not apparent the second time around, make a new 30% acrylamide solution and check the pH of the gel buffers. The pH of the gel buffers can significantly affect the way the RNA segments run and whether they stain well. Run a test gel with new 30% acrylamide with only markers to optimize your conditions.

5.13.2b Production and Purification of NSP4 from Cells

Low NSP4 production from infected cells-There is evidence showing that NSP4 production and release into the media is not only cell dependent, but also virus strain dependent. You can determine the maximum production time by testing media at different times post infection by dot blot. If the recovery of NSP4 remains low, the production scale may need to be increased by using roller bottles, or choose another cell line/viral strain combination.

Low recovery of NSP4 from the ConA column- It is critical that you run the concentrated media through the ConA column multiple times. Examine an aliquot of the flow through via dot blot each time the sample is passed through the column. This will ensure that additional NSP4 efficiently binds the column with each passage and that NSP4 is binding to the ConA ligand.

No plaques are formed in Sf9 plaque assays- Although it is common for baculovirus to replicate efficiently to form plaques in 4 or 5 days, some viruses may grow more slowly than others. In this case, extend the incubation time to 8 or 9 days and reexamine for plaques. If the plaques are still absent after 9 days of incubation, the titer is likely too low and requires concentration.

Sf9 cells die during the plaque assay - The titer of the virus may be too high, so dilute the virus prior to determining plaque forming units. Another cause of dead cells is not allowing the media/agarose mixture to sufficiently cool before adding the agarose to the cells. A good test is to test a drop on the inside of your wrist. It should be really warm but not scalding.

Low viability of SF9 suspension culture-Check the cell density. The cell suspension should contain 1 x 10^6 cells/ml. If they are too low, spin them down as in Alternate Protocol #3, Step 5 and resuspend in less media. Also ensure that there is adequate serum in the suspension. There should be at least 5% serum. 10% serum is ideal while expanding the cells.

Cells are clumping together in Sf9 spinner cultures-The suspension is too confluent or too old. If too confluent, split them down to 1 x 10^6 cell/ml. If they are too old, start new spinner cultures with fresh cells and media.

Absence of protein expression in Sf9 cells-The bacmid may be constructed incorrectly. Make sure that the bacmid contains a start codon (ATG) and is in the correct reading frame.

Low NSP4 expression in Sf9 cells-Make sure your reagents are fresh and stored properly. Old transfection reagent (Cellfectin II) can affect the transfection efficiency of the Sf9 cells. The Sf9 cells are best transfected in log phase growth (90%-95% viability) and are between 50%-70% confluent. The baculovirus infection should be completed at a high MOI. If inadequate baculovirus is used, the protein expression will be low.

Anti-NSP4 titer is low-This generally is seen when using peptides as the antigen. Even though the peptide is cross-linked to a larger protein, many of the antibodies are directed against the carrier protein, KLH for example. It may be necessary to set up a KLH affinity column in which KLH is used as the ligand. In this case, the antibody solution is added to the column and the anti-KLH is bound. The flow-through primarily is against

the target peptide. Concentration of IgG can be accomplished by dialysis using a volatile buffer such as ammonium sulfate and lyophilization.

Anti-NSP4 peptides fail to recognize the native protein-This is always a potential problem when working with synthetic peptides rather than the full protein. It is important to check the literature to determine the immune-dominant sites. You can use a mixture of synthetic peptides representing different regions of the protein to increase the possibility that the antisera will recognize the native protein. Alternatively you may have to use partially purified (~75%) protein as antigen. In addition, recognize that the peptide antibodies will have a lower titer for the protein than to the peptide. This can be overcome by concentrating and using a higher concentration of the purified IgG. Be cautious when selecting the peptide to be synthesized and ensure the quality and purity of the peptide sequence.

Purifying the antibody ligand for affinity chromatography- Polyclonal antibodies often are difficult to purify at a concentration greater than 2-3 mg/ml. In addition, the IgG can slowly precipitate at 4 °C. Storage in 50% glycerol in PBS is recommended to prevent this precipitation. Alternatively, the antibody remains very stable when lyophilized and stored under desiccation at -20 °C.

Preparation of the antibody affinity chromatography column-Unsuccessful coupling of the IgG can be due to the presence of amino groups in the sample or buffers. Typically it comes from the ammonium sulfate used to precipitate the antibody or the use of Tris buffers. Dialyze the IgG solution very carefully ensuring that multiple changes of large volumes are used. Be sure not to store buffers in plastic containers as

water may have amines that has leached from the plastic. When eluting with a low acid solution, elute quickly to avoid exposing the column to the acid for an extended length of time. The column should be regenerated for additional uses by washing the column several times with coupling buffer and store in sodium azide at 4 °C.

Dialysis- Because a solute's permeability is also dependent upon molecular shape, degree of hydration, ionic charge and polarity, it is recommended to select a MWCO that is half the size of the MW of the protein you want retained.

5.13.3 Time Considerations

Generation of rotavirus reassortants-Initially, 3 days are necessary to grow MA104 cells. Infection of the cells takes 2 hours and virus growth takes 1-3 days.

Plaque assay-Setting up the plaque assay generally will take about 3 h. Growth of the plaques will take 3-5 days, and staining with neutral red will take 4-24 h.

Viral RNA Isolation-RNA extraction takes 1- 2 hours, depending on the method is used.

PAGE-From beginning to end, PAGE and staining can be completed in one day. It takes generally takes 6-8 hours.

Purification of NSP4 from mammalian cells-The production of NSP4 takes several days. You will need a few days to grow the cell monolayers and after infection with RV, it may take 24-72 h for production and secretion of NSP4. Once the media is collected, purification is faster, generally taking 1-2 days.

Construction of Bacmid-The construction of the bacmid varies significantly depending on the method used. It should be expected to take at least a few days, unless the gene is

purchased already cloned into a vector. The construction will vary with the source of the components. It is best to follow manufacturer's instructions.

Production of recombinant baculovirus-The production of recombinant baculovirus should take 2-3 days if transfection efficiency is good. If transfection efficiency is lower, it will take longer.

Plaque assay for recombinant baculovirus-Setting up the baculovirus plaque assay will take 2-3 h. The plates need to incubate for 4-7 days to properly visualize the plaques. It is useful to check for plaques every 24 h.

Expression of NSP4 in Sf9 cells-The production of NSP4 will take ~36 hours, but may vary depending on the bacmid used.

NSP4 purification-It generally takes several days to purify any protein depending on the number of contaminants and the number of purification steps. If using antibody affinity chromatography, it will take at least a day to bind the ligand and complete the washes. The antibody must be purified before use, which also takes several days; and tested for specificity by ELISA and or Western blot, which takes one day.

6. SUMMARY AND CONCLUSIONS

6.1 Overview: Further Understanding the Role(s) of NSP4 Interactions with Cav-1, CyPA, CyP40, HSP56 and Cholesterol

This work began by building on the evidence that NSP4 interacts directly or indirectly with Cav-1, CyPA, CyP40, HSP56, and cholesterol. In this study, we showed that the silencing of the proteins fails to inhibit transport of NSP4 to the PM, but does change the intracellular distribution of NSP4 during RV infection. In addition, we presented evidence that the inhibition of cholesterol does impact NSP4 transport to the PM. We showed an interaction of NSP4 with HSP56 with FRET but not with yeast two-hybrid analysis, and presented evidence that expression of the cyclophilins are up-regulated during infection, while the expression of Cav-1 remains relatively consistent. Taking this study as a whole, we are left with many questions about the exact role of the interactions of NSP4 with Cav-1, the immunophilins and cholesterol.

6.1.1. Inhibition of Cav-1, CyPA, and CyP40 with siRNA Does Not Prevent NSP4 Transport to the PM

Silencing of Cav-1, CyPA, and CyP40 proved to be difficult in the cell lines we were working with (MDCK, MA104, and HT29.f8). However, as we moved forward with the project better reagents became available on the market for working with siRNA in difficult to transfect cell lines. Therefore, we were able to work not only with the much studied MA104 cell line but also with a more biologically-relevant, cloned human intestinal cell-line, HT29.f8. Since NSP4 displays different transport kinetics in a kidney

cell line (MDCK) when compared to the intestinal HT29.f8 cell line (Gibbons et al., 2011), we expected to see some influence of silencing on NSP4 transport to the cell surface albeit unique to each cell line. To our surprise, NSP4 was able to traffic to the cell surface upon silencing of Cav-1 and the cyclophilins in both MA104 and HT29.f8 cells.

Unpublished research in our lab showed that during RV infection of a cell line lacking Cav-1 (Fischer rat thyroid cells), NSP4 can bind to Cav-2 instead of Cav-1 and is transported to the cell surface. This indicated that certain proteins could compensate for others when one is not available. We determined that there was a good possibility that silencing only one of the proteins at a time would not inhibit NSP4 from trafficking to the PM, because the proteins could be compensating for each other. Therefore, we attempted to silence multiple proteins at a time, in combinations of two as well as all three. However, NSP4 still trafficked to the cell surface with the same kinetics, indicating that none of these proteins were necessary for NSP4 transport to the PM, alone or in combination.

6.1.2. Inhibition of Cav-1, CyPA, CyP40, and HSP56 with siRNA Altered the Intracellular Distribution of NSP4

Silencing of HSP56 could not be measured via Western blot due to limited antibody reactivity using this method. However, the silencing of HSP56 could be clearly seen by immunofluorescence. Therefore, we were able to evaluate the effect(s) of silencing Cav-1 and all three immunophilins on the intracellular distribution of NSP4. We determined that silencing of HSP56 had very little influence on intracellular NSP4 distribution.

However, there were significant intracellular changes in distribution of NSP4 and cellular proteins upon silencing of Cav-1 and CyPA.

It is known that a pool of intracellular Cav-1 localizes to the trans-Golgi network (TGN) (Fielding and Fielding, 2003). Upon silencing of Cav-1, NSP4 appears to co-localize with the Golgi protein, golgin-97. Therefore, silencing of Cav-1 may be altering intracellular distribution of NSP4 by reorganization of host-cell structures. The silencing of CyPA had a similar effect on the co-localization of NSP4 when compared to golgin-97. This increase of NSP4 co-localization with golgin-97 appeared to be due to a TGN re-distribution, rather than to localization of NSP4 to the Golgi, as NSP4 remained Endoglycosidase H sensitive upon silencing. There are reports of CyPA association with Golgi-associated vesicles (McDonald et al., 1992; Sarris et al., 1992), although most reports indicate that CyPA is a cytoplasmic protein with some nuclear localization (Krummrei et al., 1995; Zhu et al., 2007). The reason for perturbation of the Golgi complex upon silencing of Cav-1 and CyPA should be further investigated, but was beyond the scope of this project.

6.1.3. Expression of CyPA and CyP40 Are Up-regulated During Infection

During immunofluorescence studies, it was noted that the signal for CyP40 was much higher in infected cells than in uninfected cells. This led us to perform time course experiments to determine if protein expression of CyPA and CyP40 were up-regulated throughout RV infection. CypA and CyP40 did not increase until 3-4 hpi. The increase in expression of these two immunophilins could be due to an excess of unfolded non-native protein present in the cell later during infection since they are both important for

protein folding. It would be useful to determine whether the increase in protein expression occurs only in the presence of NSP4, or if RV infection as a whole increases expression.

CyPA plays a role in regulation of the IFN-β response during RV infection. Silencing of CyPA increases RV production and overexpression of CyPA causes a decrease in RV production (He et al., 2012). In addition, CyPA expression is increased during RV Wa infection and in intestines following RV infection of BALB/c mice (He et al., 2013). When CyPA is silenced, several viral mRNA levels are up-regulated including RV NSP4 (He et al., 2013). While these studies point to RV NSP1 activation of the PI3K/Akt pathway as a potential cause of up-regulation of CyPA expression, it is possible that NSP4 up-regulation of cytoplasmic [Ca^{2+}] may play a role as well. Interestingly, one study noted cell-type dependent differences in expression of CyPA during RV infection (He et al., 2013). This further supports our hypothesis that the interaction of NSP4 with immunophilins may be cell-type dependent.

CyPA plays a major role in many types of viral infections, including influenza, coronavirus, hepatitis C, and cytomegalovirus (Anderson et al., 2011; Keyes et al., 2012; Tanaka et al., 2013). Notably, in hepatitis B infection, CyPA is secreted from cells that is induced by viral infection (Tian et al., 2010). In vaccinia virus infection, CyPA is packaged into the virion and secreted from the cell (Castro et al., 2003). Although we showed that CyPA is not required for NSP4 transport to the PM, we did not investigate the role of CyPA in secretion of NSP4 nor did we explore whether CyPA is secreted during RV infection.

6.1.4. HSP56 Localized in Close Proximity to NSP4 Intracellularly, But May Not Directly Interact

Although it was determined that NSP4 and HSP56 localize within 10 nm of each other via intracellular FRET experiments, a direct interaction could not be confirmed by co-immunoprecipitation or yeast two-hybrid assay. Co-immunoprecipitation of HSP56 was not possible due to limited antibody reactivity, although it was attempted with antibodies from several sources. It is reasonable to propose that if NSP4 interacts with CyP40, it would be in close association with HSP56, since CyP40 and HSP56 both interact within the same protein complexes (Czar et al., 1994; Davies and Sanchez, 2005). A lack of interaction of HSP56 and NSP4 could explain why there was no alteration of intracellular NSP4 distribution upon silencing of HSP56.

6.2 Pitfalls

We set out to investigate a complex consisting of Cav-1, CyPA, CyP40, and HSP56, which was reported to transport cholesterol directly from the endoplasmic reticulum to the plasma membrane (Uittenbogaard et al., 2002; Uittenbogaard and Smart, 2000; Uittenbogaard et al., 1998). It seemed logical that NSP4 would utilize this complex for intracellular transport, since NSP4 interacts with several of the proteins as well as cholesterol. As we delved further into the research, it became apparent that the proteins did not affect the transport of NSP4 to the PM. Unfortunately, the studies describing the complex were retracted due to falsification of data (Office of the Secretary, 2012). Although we found that NSP4 interacts with several of these proteins, there are no other

reports that describe the complex, and our research did not focus on proving its existence, as it had been published for many years in top Journals.

The cost of the silencing RNAs led to another pitfall in our research. We set out to quantify the amount of NSP4 that reached the cell surface when Cav-1 and the immunophilins were inhibited. We ran into several problems when trying to quantitate NSP4 concentration at the exofacial PM. We initially tried to use sodium-potassium ATPase as a loading control for Western blot analysis. However, the amount of sodium-potassium ATPase varied significantly depending on the protein silenced and could not be used as an internal loading control. We tested a few other exofacially-expressed proteins, but they were either not expressed in the cell-lines we were using, or we had the same problem of getting consistent expression. Silencing of Cav-1 and the immunophilins or RV infection causes the distribution of PM-localized proteins to change and we therefore could not find a reliable internal loading control for our surface biotinylation assays.

We attempted to remedy this problem by quantifying protein at the cell surface. However, due to the cost of siRNA and the limitations of protein quantification kits, we were not able to scale up the reactions to a level high enough to acquire enough sample for both protein quantification and evaluation of NSP4 transport. We decided to overcome this by constructing a shRNA expression system using a lentivirus vector system. While this method would have overcome our inability to quantify NSP4 transport to the PM, sequencing of the shRNA segment was problematic and not successful.

Overall, the research presented in this work provided more questions than it did answers. While we now know that Cav-1, CyPA, CyP40, and HSP56 are not required for transport of NSP4 to the PM, the question remains, what is responsible for its unconventional transport? In addition, how are Cav-1 and the immunophilins involved in other intracellular transport pathways of NSP4? Elucidation of these other intracellular pathways may provide more insight into how NSP4 reaches the cell surface and is secreted.

6.3 Future Research

This research provided us with a few key findings: 1) Cav-1, CyPA, CyP40, and HSP56 are not required for NSP4 transport to the PM, 2) Cholesterol depletion does affect the amount of NSP4 that traffics to the PM, 3) Protein concentrations of the cyclophilins are up-regulated throughout RV infection, and 4) NSP4 is located in close proximity to HSP56, but may not be directly interacting. Details of the unconventional transport pathway that NSP4 utilizes to traffic to the PM still need to be explored.

6.3.1. Cholesterol, Lipid Bodies, and Caveolin

We found that lovastatin inhibition of *de novo* cholesterol synthesis decreased the amount of NSP4 that reached the PM using surface biotinylation. These studies cannot be performed with a PM-cholesterol depletion agent, such as methyl-β-cyclodextrin, since PM cholesterol is required for RV-infection. In addition, methyl-β-cyclodextrin treatment was toxic to MA104 cells when added 3 h after RV-infection (data not shown). At lower concentrations, methyl-β-cyclodextrin treatment did not lower cholesterol enough to affect NSP4 transport to the cell surface (data not shown).

NSP4 interacts directly with cholesterol (Schroeder, 2009) and cholesterol is important for NSP4 interaction with highly-curved membranes (Huang et al., 2001). However, the function of cholesterol in transport of NSP4 has yet to be evaluated. Our findings suggest that NSP4 may rely on cholesterol in order for transport to the PM. Lovastatin inhibition of cholesterol synthesis impacts the transport of free cholesterol to the PM (Cignarella et al., 1998). Upon RV infection of lovastatin-treated MA104 cells, there is a dramatic decrease of exofacial PM-localized NSP4. However, the decrease is less noticeable in HT29.f8 cells. This leads us to believe that NSP4 may rely on PM-directed cholesterol transport for its trafficking to the PM. The fact that the effect of lovastatin treatment on HT29.f8 cells is different than in MA104 cells further supports our hypothesis that NSP4 is trafficking via different pathways, which are cell-type dependent.

It is known that lipid droplets are important for RV replication in viroplasms (Cheung et al., 2010; Gaunt et al., 2013a; Gaunt et al., 2013b). In addition, autophagy plays a role in the breakdown of lipid droplets, and there is a known interaction of NSP4 with autophagy (Crawford et al., 2012). Whether this interaction is dependent upon lipid droplet formation is unknown. To investigate the possibility that lipid droplets play a role in NSP4 transport, small-molecule inhibitors of lipid droplet formation, such as compound C75 or TOFA (5-(Tetradecyloxy)-2-furoic acid) to inhibit the fatty acid synthase complex and acetyl-CoA carboxylase enzyme, respectively (Gaunt et al., 2013a), could be utilized. In addition, performing the cholesterol and lipid droplet inhibition studies on cells transfected with NSP4 only could be useful to distinguish their

roles in NSP4 transport without interference from other RV proteins.

The reason for studying the role of cholesterol in NSP4 transport becomes stronger when it is considered that cavolin-1 directly binds cholesterol in a 1:1 stoichiometry (Murata et al., 1995). Furthermore, Cav-1 is associated with lipid bodies, and this association may be part of caveolin-regulated cell signaling (Pol et al., 2004). We know NSP4 directly binds both caveolin-1 and cholesterol (Parr et al., 2006; Schroeder, 2009), and localizes to caveolae on the PM (Storey et al., 2007), which leads us to believe these molecules likely play a role in transport of NSP4 to distinct cell locations.

6.3.2. Cyclophilin 40 and Autophagy

In addition to its many other functions, cyclophilin 40 is a resident mitochondrial protein and is a component of the mitochondrial permeability transition pore (MTP) complex. This complex consists of voltage-dependent anion channel protein, adenine-nucleotide translocator, and CyP40, is activated under oxidative stress, and is Ca^{2+} regulated (Armstrong, 2006). In addition, the role of CyP40 in this complex is important for autophagy initiation for mitochondrial disposal. When CyP40 function is inhibited, autophagy is inhibited, which also inhibits cell death (Carreira et al., 2010; Chen et al., 2012). Therefore, CyP40 is necessary for the initiation of autophagic disposal of mitochondria.

We now know that RV NSP4 is also a regulator of autophagy. NSP4 initiates autophagy through calcium/calmodulin dependent kinase kinase-β signaling, which is required for virus maturation (Crawford et al., 2012). However, NSP4 prevents autophagic maturation and autophagy vesicle fusion with the lysosome for degradation.

In addition, this process is mediated through Ca^{2+} release following viroporin formation in the ER membrane (Crawford et al., 2012). It is not yet known if there is a connection between NSP4-induced autophagy and MTP-induced autophagy. Small molecule inhibitors (siRNA and CsA) to block CyP40 function and bafilomycin A1, chloroquine, or other autophagic inhibitors will be useful for examination of the possible role that CyP40 may play in autophagy during RV infection.

Autophagy also has been insinuated to play a role in unconventional transport of secretory proteins (Zhang and Schekman, 2013). A unique, chaperone-mediated autophagy pathway has been suggested to play a role in this type of transport through lysosomes (Kaushik and Cuervo, 2012). Chaperone-mediated transport into the lysosome is controlled through the cytosolic hsc70 family of heat-shock proteins, where proteins are loaded through a channel into the lysosome for degradation or secretion. It is known that CyP40 directly binds to hsc70 and may modulate its activity (Carrello et al., 2004). The known interactions of NSP4 with autophagy and CyP40 need to be further evaluated to determine if they play a role in transport of NSP4.

REFERENCES

Anderson, L.J., Lin, K., Compton, T., Wiedmann, B., 2011. Inhibition of cyclophilins alters lipid trafficking and blocks hepatitis C virus secretion. Virology Journal 8, 329.

Angel, J., Franco, M.A., Greenberg, H.B., 2007. Rotavirus vaccines: recent developments and future considerations. Nature Reviews: Microbiology 5, 529-539.

Arias, C.F., Romero, P., Alvarez, V., Lopez, S., 1996. Trypsin activation pathway of rotavirus infectivity. Journal of Virology 70, 5832-5839.

Arias, C.F., Silva-Ayala, D., Lopez, S., 2015. Rotavirus entry: a deep journey into the cell with several exits. Journal of Virology 89, 890-893.

Armstrong, J.S., 2006. Mitochondrial membrane permeabilization: the sine qua non for cell death. BioEssays : News and Reviews in Molecular, Cellular and Developmental Biology 28, 253-260.

Arnold, M., Patton, J.T., McDonald, S.M. 2009. Culturing, storage, and quantification of rotaviruses. Current Protocols in Microbiology 15C.3. 15C.3.1-15C.3.24

Axen, R., Porath, J., Ernback, S., 1967. Chemical coupling of peptides and proteins to polysaccharides by means of cyanogen halides. Nature 214, 1302-1304.

Ball, J.M., Mitchell, D.M., Gibbons, T.F., Parr, R.D., 2005. Rotavirus NSP4: a multifunctional viral enterotoxin. Viral Immunology 18, 27-40.

Ball, J.M., Tian, P., Zeng, C.Q., Morris, A.P., Estes, M.K., 1996. Age-dependent diarrhea induced by a rotaviral nonstructural glycoprotein. Science 272, 101-104.

Bergmann, C.C., Maass, D., Poruchynsky, M.S., Atkinson, P.H., Bellamy, A.R., 1989. Topology of the non-structural rotavirus receptor glycoprotein NS28 in the rough endoplasmic reticulum. The EMBO Journal 8, 1695-1703.

Berkova, Z., Crawford, S.E., Blutt, S.E., Morris, A.P., Estes, M.K., 2007. Expression of rotavirus NSP4 alters the actin network organization through the actin remodeling protein cofilin. Journal of Virology 81, 3545-3553.

Berkova, Z., Crawford, S.E., Trugnan, G., Yoshimori, T., Morris, A.P., Estes, M.K., 2006. Rotavirus NSP4 induces a novel vesicular compartment regulated by calcium and associated with viroplasms. Journal of Virology 80, 6061-6071.

Bhandari, N., Rongsen-Chandola, T., Bavdekar, A., John, J., Antony, K., Taneja, S., Goyal, N., Kawade, A., Kang, G., Rathore, S.S., Juvekar, S., Muliyil, J., Arya, A., Shaikh, H., Abraham, V., Vrati, S., Proschan, M., Kohberger, R., Thiry, G., Glass, R., Greenberg, H.B., Curlin, G., Mohan, K., Harshavardhan, G.V., Prasad, S., Rao, T.S., Boslego, J., Bhan, M.K., India Rotavirus Vaccine, G., 2014. Efficacy of a monovalent human-bovine (116E) rotavirus vaccine in Indian infants: a randomised, double-blind, placebo-controlled trial. Lancet 383, 2136-2143.

Black, R.E., Cousens, S., Johnson, H.L., Lawn, J.E., Rudan, I., Bassani, D.G., Jha, P., Campbell, H., Walker, C.F., Cibulskis, R., Eisele, T., Liu, L., Mathers, C., 2010. Global, regional, and national causes of child mortality in 2008: a systematic analysis. Lancet 375, 1969-1987.

Boschi Pinto, C., Bahl, R., Martines, J., 2009. Limited progress in increasing coverage of neonatal and child-health interventions in Africa and Asia. Journal of Health, Population and Nutrition 27, 755-762.

Boshuizen, J.A., Reimerink, J.H., Korteland-van Male, A.M., van Ham, V.J., Koopmans, M.P., Buller, H.A., Dekker, J., Einerhand, A.W., 2003. Changes in small intestinal homeostasis, morphology, and gene expression during rotavirus infection of infant mice. Journal of Virology 77, 13005-13016.

Boshuizen, J.A., Rossen, J.W., Sitaram, C.K., Kimenai, F.F., Simons-Oosterhuis, Y., Laffeber, C., Buller, H.A., Einerhand, A.W., 2004. Rotavirus enterotoxin NSP4 binds to the extracellular matrix proteins laminin-beta3 and fibronectin. Journal of Virology 78, 10045-10053.

Bowman, G.D., Nodelman, I.M., Levy, O., Lin, S.L., Tian, P., Zamb, T.J., Udem, S.A., Venkataraghavan, B., Schutt, C.E., 2000. Crystal structure of the oligomerization domain of NSP4 from rotavirus reveals a core metal-binding site. Journal of Molecular Biology 304, 861-871.

Bugarcic, A., Taylor, J.A., 2006. Rotavirus nonstructural glycoprotein NSP4 is secreted from the apical surfaces of polarized epithelial cells. Journal of Virology 80, 12343-12349.

Carreira, R.S., Lee, Y., Ghochani, M., Gustafsson, A.B., Gottlieb, R.A., 2010. Cyclophilin D is required for mitochondrial removal by autophagy in cardiac cells. Autophagy 6, 462-472.

Carrello, A., Allan, R.K., Morgan, S.L., Owen, B.A., Mok, D., Ward, B.K., Minchin, R.F., Toft, D.O., Ratajczak, T., 2004. Interaction of the Hsp90 cochaperone cyclophilin 40 with Hsc70. Cell Stress & Chaperones 9, 167-181.

Castro, A.P., Carvalho, T.M., Moussatche, N., Damaso, C.R., 2003. Redistribution of cyclophilin A to viral factories during vaccinia virus infection and its incorporation into mature particles. Journal of Virology 77, 9052-9068.

Chen, W., Feng, L., Nie, H., Zheng, X., 2012. Andrographolide induces autophagic cell death in human liver cancer cells through cyclophilin D-mediated mitochondrial permeability transition pore. Carcinogenesis 33, 2190-2198.

Cheung, W., Gill, M., Esposito, A., Kaminski, C.F., Courousse, N., Chwetzoff, S., Trugnan, G., Keshavan, N., Lever, A., Desselberger, U., 2010. Rotaviruses associate with cellular lipid droplet components to replicate in viroplasms, and compounds disrupting or blocking lipid droplets inhibit viroplasm formation and viral replication. Journal of Virology 84, 6782-6798.

Chevray, P.M., Nathans, D., 1992. Protein interaction cloning in yeast: identification of mammalian proteins that react with the leucine zipper of Jun. Proceedings of the National Academy of Sciences of the United States of America 89, 5789-5793.

Chua, C.E.L., Gan, B.Q., Tang, B.L., 2011. Involvement of members of the Rab family and related small GTPases in autophagosome formation and maturation. Cellular and Molecular Life Sciences 68, 3349-3358.

Chwetzoff, S., Trugnan, G., 2006. Rotavirus assembly: an alternative model that utilizes an atypical trafficking pathway. Curr Top Microbiol Immunol 309, 245-261.

Cignarella, A., Brennhausen, B., von Eckardstein, A., Assmann, G., Cullen, P., 1998. Differential effects of lovastatin on the trafficking of endogenous and lipoprotein-derived cholesterol in human monocyte-derived macrophages. Arteriosclerosis, Thrombosis, and Vascular Biology 18, 1322-1329.

Costes, S.V., Daelemans, D., Cho, E.H., Dobbin, Z., Pavlakis, G., Lockett, S., 2004. Automatic and quantitative measurement of protein-protein colocalization in live cells. Biophysical Journal 86, 3993-4003.

Crawford, S.E., Hyser, J.M., Utama, B., Estes, M.K., 2012. Autophagy hijacked through viroporin-activated calcium/calmodulin-dependent kinase kinase-beta signaling is required for rotavirus replication. Proceedings of the National Academy of Sciences of the United States of America 109, E3405-3413.

Crawford, S.E., Patel, D.G., Cheng, E., Berkova, Z., Hyser, J.M., Ciarlet, M., Finegold, M.J., Conner, M.E., Estes, M.K., 2006. Rotavirus viremia and extraintestinal viral infection in the neonatal rat model. Journal of Virology 80, 4820-4832.

Cuadras, M.A., Bordier, B.B., Zambrano, J.L., Ludert, J.E., Greenberg, H.B., 2006. Dissecting rotavirus particle-raft interaction with small interfering RNAs: insights into rotavirus transit through the secretory pathway. Journal of Virology 80, 3935-3946.

Cuadras, M.A., Feigelstock, D.A., An, S., Greenberg, H.B., 2002. Gene expression pattern in Caco-2 cells following rotavirus infection. Journal of Virology 76, 4467-4482.

Cuadras, M.A., Greenberg, H.B., 2003. Rotavirus infectious particles use lipid rafts during replication for transport to the cell surface in vitro and in vivo. Virology 313, 308-321.

Cubitt, W.D., Holzel, H., 1980. An outbreak of rotavirus infection in a long-stay ward of a geriatric hospital. Journal of Clinical Pathology 33, 306-308.

Czar, M.J., Owens-Grillo, J.K., Yem, A.W., Leach, K.L., Deibel, M.R., Jr., Welsh, M.J., Pratt, W.B., 1994. The hsp56 immunophilin component of untransformed steroid receptor complexes is localized both to microtubules in the cytoplasm and to the same nonrandom regions within the nucleus as the steroid receptor. Molecular Endocrinology 8, 1731-1741.

Davies, T.H., Sanchez, E.R., 2005. Fkbp52. The international Journal of Biochemistry & Cell Biology 37, 42-47.

Delmas, O., Gardet, A., Chwetzoff, S., Breton, M., Cohen, J., Colard, O., Sapin, C., Trugnan, G., 2004. Different ways to reach the top of a cell. Analysis of rotavirus assembly and targeting in human intestinal cells reveals an original raft-dependent, Golgi-independent apical targeting pathway. Virology 327, 157-161.

Didsbury, A., Wang, C., Verdon, D., Sewell, M.A., McIntosh, J.D., Taylor, J.A., 2011. Rotavirus NSP4 is secreted from infected cells as an oligomeric lipoprotein and binds to glycosaminoglycans on the surface of non-infected cells. Virology Journal 8, 551.

Dong, Y., Zeng, C.Q., Ball, J.M., Estes, M.K., Morris, A.P., 1997. The rotavirus enterotoxin NSP4 mobilizes intracellular calcium in human intestinal cells by stimulating phospholipase C-mediated inositol 1,4,5-trisphosphate production. Proceedings of the National Academy of Sciences of the United States of America 94, 3960-3965.

Du, W., Vidal, M., Xie, J.E., Dyson, N., 1996. RBF, a novel RB-related gene that regulates E2F activity and interacts with cyclin E in *Drosophila*. Genes & Development 10, 1206-1218.

Dunn, K.W., Kamocka, M.M., McDonald, J.H., 2011. A practical guide to evaluating colocalization in biological microscopy. American Journal of Physiology. Cell Physiology 300, C723-742.

Ericson, B.L., Graham, D.Y., Mason, B.B., Hanssen, H.H., Estes, M.K., 1983. Two types of glycoprotein precursors are produced by the simian rotavirus SA11. Virology 127, 320-332.

Estes, M.K., Graham, D.Y., Mason, B.B., 1981. Proteolytic enhancement of rotavirus infectivity: molecular mechanisms. Journal of Virology 39, 879-888.

Estes, M.K., Greenberg, H.B., 2013. Rotaviruses, Fields Virology, 6th ed. Lippincott-Raven Publishers, Philadelphia, Pa, pp. 1917-1974.

Fabbretti, E., Afrikanova, I., Vascotto, F., Burrone, O.R., 1999. Two non-structural rotavirus proteins, NSP2 and NSP5, form viroplasm-like structures in vivo. The Journal of General Virology 80 (Pt 2), 333-339.

Fang, Z.Y., Ye, Q., Ho, M.S., Dong, H., Qing, S., Penaranda, M.E., Hung, T., Wen, L., Glass, R.I., 1989. Investigation of an outbreak of adult diarrhea rotavirus in China. The Journal of Infectious Diseases 160, 948-953.

Fielding, C.J., Fielding, P.E., 2003. Relationship between cholesterol trafficking and signaling in rafts and caveolae. Biochimica et Biophysica Acta 1610, 219-228.

Fields, S., Song, O., 1989. A novel genetic system to detect protein-protein interactions. Nature 340, 245-246.

Fischer, G., Gallay, P., Hopkins, S., 2010. Cyclophilin inhibitors for the treatment of HCV infection. Current Opinion in Investigational Drugs 11, 911-918.

Fischer, G., Wittmann-Liebold, B., Lang, K., Kiefhaber, T., Schmid, F.X., 1989. Cyclophilin and peptidyl-prolyl cis-trans isomerase are probably identical proteins. Nature 337, 476-478.

Fruman, D.A., Burakoff, S.J., Bierer, B.E., 1994. Immunophilins in protein folding and immunosuppression. The FASEB Journal 8, 391-400.

Galigniana, M.D., Harrell, J.M., Murphy, P.J., Chinkers, M., Radanyi, C., Renoir, J.M., Zhang, M., Pratt, W.B., 2002. Binding of hsp90-associated immunophilins to cytoplasmic dynein: direct binding and in vivo evidence that the peptidylprolyl isomerase domain is a dynein interaction domain. Biochemistry 41, 13602-13610.

Galigniana, M.D., Morishima, Y., Gallay, P.A., Pratt, W.B., 2004. Cyclophilin-A is bound through its peptidylprolyl isomerase domain to the cytoplasmic dynein motor protein complex. The Journal of Biological Chemistry 279, 55754-55759.

Galigniana, M.D., Radanyi, C., Renoir, J.M., Housley, P.R., Pratt, W.B., 2001. Evidence that the peptidylprolyl isomerase domain of the hsp90-binding immunophilin FKBP52 is involved in both dynein interaction and glucocorticoid receptor movement to the nucleus. The Journal of Biological Chemistry 276, 14884-14889.

Gallegos, C.O., Patton, J.T., 1989. Characterization of rotavirus replication intermediates: a model for the assembly of single-shelled particles. Virology 172, 616-627.

Gaunt, E.R., Cheung, W., Richards, J.E., Lever, A., Desselberger, U., 2013a. Inhibition of rotavirus replication by downregulation of fatty acid synthesis. The Journal of General Virology 94, 1310-1317.

Gaunt, E.R., Zhang, Q., Cheung, W., Wakelam, M.J., Lever, A.M., Desselberger, U., 2013b. Lipidome analysis of rotavirus-infected cells confirms the close interaction of lipid droplets with viroplasms. The Journal of General Virology 94, 1576-1586.

Gibbons, T., 2007. Rotavirus NSP4 in extrareticular sites: support for its pathogenic role as an enterotoxin. Ph.D. Thesis Texas A&M University, Department of Veterinary Pathobiology.

Gibbons, T., Storey, S., Williams, C., McIntosh, A., Mitchel, D., Parr, R., Schroeder, M., Schroeder, F., Ball, J., 2011. Rotavirus NSP4: Cell type-dependent transport kinetics to the exofacial plasma membrane and release from intact infected cells. Virology Journal 8:278, 1-19.

Gombold, J.L., Ramig, R.F., 1986. Analysis of reassortment of genome segments in mice mixedly infected with rotaviruses SA11 and RRV. Journal of Virology 57, 110-116.

Gonzalez, R.A., Espinosa, R., Romero, P., Lopez, S., Arias, C.F., 2000. Relative localization of viroplasmic and endoplasmic reticulum-resident rotavirus proteins in infected cells. Arch Virol 145, 1963-1973.

Gorrell, R.J., Bishop, R.F., 1997. Production of reassortant viruses containing human rotavirus VP4 and SA11 VP7 for measuring neutralizing antibody following natural infection. Clinical and Diagnostic Laboratory Immunology 4, 509-514.

Gutierrez, M., Isa, P., Sanchez-San Martin, C., Perez-Vargas, J., Espinosa, R., Arias, C.F., Lopez, S., 2010. Different rotavirus strains enter MA104 cells through different endocytic pathways: the role of clathrin-mediated endocytosis. Journal of Virology 84, 9161-9169.

Halaihel, N., Lievin, V., Ball, J.M., Estes, M.K., Alvarado, F., Vasseur, M., 2000. Direct inhibitory effect of rotavirus NSP4(114-135) peptide on the Na(+)-D-glucose symporter of rabbit intestinal brush border membrane. Journal of Virology 74, 9464-9470.

Halvorsrud, J., Orstavik, I., 1980. An epidemic of rotavirus-associated gastroenteritis in a nursing home for the elderly. Scandinavian Journal of Infectious Diseases 12, 161-164.

He, H., Mou, Z., Li, W., Fei, L., Tang, Y., Zhang, J., Yan, P., Chen, Z., Yang, X., Shen, Z., Li, J., Wu, Y., 2013. Proteomic methods reveal cyclophilin a function as a host restriction factor against rotavirus infection. Proteomics 13, 1121-1132.

He, H., Zhou, D., Fan, W., Fu, X., Zhang, J., Shen, Z., Li, J., Li, J., Wu, Y., 2012. Cyclophilin A inhibits rotavirus replication by facilitating host IFN-I production. Biochemical and Biophysical Research Communications 422, 664-669.

Huang, H., Schroeder, F., Estes, M.K., McPherson, T., Ball, J.M., 2004. Interaction(s) of rotavirus non-structural protein 4 (NSP4) C-terminal peptides with model membranes. Biochem J 380, 723-733.

Huang, H., Schroeder, F., Zeng, C., Estes, M.K., Schoer, J.K., Ball, J.M., 2001. Membrane interactions of a novel viral enterotoxin: rotavirus nonstructural glycoprotein NSP4. Biochemistry 40, 4169-4180.

Huang, P., Xia, M., Tan, M., Zhong, W., Wei, C., Wang, L., Morrow, A., Jiang, X., 2012. Spike protein VP8* of human rotavirus recognizes histo-blood group antigens in a type-specific manner. Journal of Virology 86, 4833-4843.

Hyser, J.M., Collinson-Pautz, M.R., Utama, B., Estes, M.K., 2010. Rotavirus Disrupts Calcium homeostasis by NSP4 viroporin activity. Mbio 1, 1-11.

Hyser, J.M., Estes, M.K., 2009. Rotavirus vaccines and pathogenesis: 2008. Curr Opin Gastroenterol 25, 36-43.

Isa, P., Arias, C.F., Lopez, S., 2006. Role of sialic acids in rotavirus infection. Glycoconj J 23, 27-37.

Isa, P., Realpe, M., Romero, P., Lopez, S., Arias, C.F., 2004. Rotavirus RRV associates with lipid membrane microdomains during cell entry. Virology 322, 370-381.

Iturriza-Gomara, M., Isherwood, B., Desselberger, U., Gray, J., 2001. Reassortment in vivo: driving force for diversity of human rotavirus strains isolated in the United Kingdom between 1995 and 1999. Journal of Virology 75, 3696-3705.

Jain, S., Vashistt, J., Changotra, H., 2014. Rotaviruses: is their surveillance needed? Vaccine 32, 3367-3378.

Jain, V., Das, B.K., Bhan, M.K., Glass, R.I., Gentsch, J.R., Indian Strain Surveillance Collaborating, L., 2001. Great diversity of group A rotavirus strains and high prevalence of mixed rotavirus infections in India. Journal of Clinical Microbiology 39, 3524-3529.

Jayaram, H., Estes, M.K., Prasad, B.V., 2004. Emerging themes in rotavirus cell entry, genome organization, transcription and replication. Virus Res 101, 67-81.

Jourdan, N., Maurice, M., Delautier, D., Quero, A.M., Servin, A.L., Trugnan, G., 1997. Rotavirus is released from the apical surface of cultured human intestinal cells through nonconventional vesicular transport that bypasses the Golgi apparatus. Journal of Virology 71, 8268-8278.

Karpova, T.S., Baumann, C.T., He, L., Wu, X., Grammer, A., Lipsky, P., Hager, G.L., McNally, J.G., 2003. Fluorescence resonance energy transfer from cyan to yellow fluorescent protein detected by acceptor photobleaching using confocal microscopy and a single laser. Journal of Microscopy 209, 56-70.

Kaushik, S., Cuervo, A.M., 2012. Chaperone-mediated autophagy: a unique way to enter the lysosome world. Trends in Cell Biology 22, 407-417.

Kelkar, S.D., Zade, J.K., 2004. Group B rotaviruses similar to strain CAL-1, have been circulating in Western India since 1993. Epidemiology and Infection 132, 745-749.

Keyes, L.R., Bego, M.G., Soland, M., St Jeor, S., 2012. Cyclophilin A is required for efficient human cytomegalovirus DNA replication and reactivation. The Journal of General Virology 93, 722-732.

Krummrei, U., Bang, R., Schmidtchen, R., Brune, K., Bang, H., 1995. Cyclophilin-A is a zinc-dependent DNA binding protein in macrophages. FEBS Letters 371, 47-51.

Lab, H., RNAi Central. Cold Spring Harbor Laboratory. http://cancan.cshl.edu/RNAi_central/RNAi.cgi?type=shRNA

Laemmli, U.K., 1970. Cleavage of structural proteins during the assembly of the head of bacteriophage T4. Nature 227, 680-685.

Liakopoulou, E., Mutton, K., Carrington, D., Robinson, S., Steward, C.G., Goulden, N.J., Cornish, J.M., Marks, D.I., 2005. Rotavirus as a significant cause of prolonged diarrhoeal illness and morbidity following allogeneic bone marrow transplantation. Bone Marrow Transplantation 36, 691-694.

Lopez, T., Camacho, M., Zayas, M., Najera, R., Sanchez, R., Arias, C.F., Lopez, S., 2005. Silencing the morphogenesis of rotavirus. Journal of Virology 79, 184-192.

Lundgren, O., Peregrin, A.T., Persson, K., Kordasti, S., Uhnoo, I., Svensson, L., 2000. Role of the enteric nervous system in the fluid and electrolyte secretion of rotavirus diarrhea. Science 287, 491-495.

Maass, D.R., Atkinson, P.H., 1990. Rotavirus proteins VP7, NS28, and VP4 form oligomeric structures. Journal of Virology 64, 2632-2641.

Manders, E.M., Stap, J., Brakenhoff, G.J., van Driel, R., Aten, J.A., 1992. Dynamics of three-dimensional replication patterns during the S-phase, analysed by double labelling of DNA and confocal microscopy. J Cell Sci 103 (Pt 3), 857-862.

Manders, E.M., 1993. Measurement of co-localization of objects in dual-colour confocal images. Journal of Microscopy 169, 375-382.

Marrie, T.J., Lee, S.H., Faulkner, R.S., Ethier, J., Young, C.H., 1982. Rotavirus infection in a geriatric population. Archives of Internal Medicine 142, 313-316.

Martin, G.G., Atshaves, B.P., Landrock, K.K., Landrock, D., Schroeder, F., Kier, A.B., 2015. Loss of L-FABP, SCP-2/SCP-x, or both induces hepatic lipid accumulation in female mice. Archives of Biochemistry and Biophysics 580, 41-49.

McDonald, M.L., Ardito, T., Marks, W.H., Kashgarian, M., Lorber, M.I., 1992. The effect of cyclosporine administration on the cellular distribution and content of cyclophilin. Transplantation 53, 460-466.

Michelangeli, F., Ruiz, M.C., del Castillo, J.R., Ludert, J.E., Liprandi, F., 1991. Effect of rotavirus infection on intracellular calcium homeostasis in cultured cells. Virology 181, 520-527.

Mirazimi, A., Nilsson, M., Svensson, L., 1998. The molecular chaperone calnexin interacts with the NSP4 enterotoxin of rotavirus in vivo and in vitro. Journal of Virology 72, 8705-8709.

Mitchell, D.M., Ball, J.M., 2004. Characterization of a spontaneously polarizing HT-29 cell line, HT-29/cl.f8. In Vitro Cell Dev Biol Anim 40, 297-302.

Mizushima, N., Yoshimori, T., Ohsumi, Y., 2011. The role of Atg proteins in autophagosome formation. Annual Review of Cell and Developmental Biology 27, 107-132.

Mohan, K.V., Som, I., Atreya, C.D., 2002. Identification of a type 1 peroxisomal targeting signal in a viral protein and demonstration of its targeting to the organelle. Journal of Virology 76, 2543-2547.

Mori, Y., Borgan, M.A., Ito, N., Sugiyama, M., Minamoto, N., 2002. Sequential analysis of nonstructural protein NSP4s derived from Group A avian rotaviruses. Virus Res 89, 145-151.

Murata, M., Peranen, J., Schreiner, R., Wieland, F., Kurzchalia, T.V., Simons, K., 1995. VIP21/caveolin is a cholesterol-binding protein. Proceedings of the National Academy of Sciences of the United States of America 92, 10339-10343.

Nickel, W., 2003. The mystery of nonclassical protein secretion. A current view on cargo proteins and potential export routes. European Journal of Biochemistry / FEBS 270, 2109-2119.

Nickel, W., 2005. Unconventional secretory routes: direct protein export across the plasma membrane of mammalian cells. Traffic 6, 607-614.

Nickel, W., 2010. Pathways of unconventional protein secretion. Curr Opin Biotechnol 21, 621-626.

Nickel, W., Rabouille, C., 2009. Mechanisms of regulated unconventional protein secretion. Nat Rev Mol Cell Biol 10, 148-155.

Nickel, W., Seedorf, M., 2008. Unconventional mechanisms of protein transport to the cell surface of eukaryotic cells. Annual Review of Cell and Developmental Biology 24, 287-308.

O'Brien, J.A., Taylor, J.A., Bellamy, A.R., 2000. Probing the structure of rotavirus NSP4: a short sequence at the extreme C terminus mediates binding to the inner capsid particle. Journal of Virology 74, 5388-5394.

Office of the Secretary, H., 2012. Findings of Research Misconduct. Federal Register 77, 69627-69628. http://www.gpo.gov/fdsys/pkg/FR-2012-11-20/html/2012-28209.htm.

Padilla-Noriega, L., Paniagua, O., Guzman-Leon, S., 2002. Rotavirus protein NSP3 shuts off host cell protein synthesis. Virology 298, 1-7.

Parashar, U.D., Burton, A., Lanata, C., Boschi-Pinto, C., Shibuya, K., Steele, D., Birmingham, M., Glass, R.I., 2009. Global mortality associated with rotavirus disease among children in 2004. The Journal of Infectious Diseases 200 Suppl 1, S9-S15.

Parr, R.D., Storey, S.M., Mitchell, D.M., McIntosh, A.L., Zhou, M., Mir, K.D., Ball, J.M., 2006. The rotavirus enterotoxin NSP4 directly interacts with the caveolar structural protein caveolin-1. Journal of Virology 80, 2842-2854.

Parra, G.I., Vidales, G., Gomez, J.A., Fernandez, F.M., Parreno, V., Bok, K., 2008. Phylogenetic analysis of porcine rotavirus in Argentina: increasing diversity of G4 strains and evidence of interspecies transmission. Veterinary Microbiology 126, 243-250.

Patel, M.M., Parashar, U.D., Santosham, M., Richardson, V., 2013. The rotavirus experience in Mexico: discovery to control. Clin Infect Dis 56, 548-551.

Patton, J.T., Vasquez-Del Carpio, R., Spencer, E., 2004. Replication and transcription of the rotavirus genome. Curr Pharm Des 10, 3769-3777.

Pesavento, J.B., Lawton, J.A., Estes, M.E., Venkataram Prasad, B.V., 2001. The reversible condensation and expansion of the rotavirus genome. Proceedings of the National Academy of Sciences of the United States of America 98, 1381-1386.

Petrie, B.L., Greenberg, H.B., Graham, D.Y., Estes, M.K., 1984. Ultrastructural localization of rotavirus antigens using colloidal gold. Virus Res 1, 133-152.

Piron, M., Vende, P., Cohen, J., Poncet, D., 1998. Rotavirus RNA-binding protein NSP3 interacts with eIF4GI and evicts the poly(A) binding protein from eIF4F. The EMBO Journal 17, 5811-5821.

Pol, A., Martin, S., Fernandez, M.A., Ferguson, C., Carozzi, A., Luetterforst, R., Enrich, C., Parton, R.G., 2004. Dynamic and regulated association of caveolin with lipid bodies: modulation of lipid body motility and function by a dominant negative mutant. Molecular Biology of the Cell 15, 99-110.

Poncet, D., Aponte, C., Cohen, J., 1993. Rotavirus protein NSP3 (NS34) is bound to the 3' end consensus sequence of viral mRNAs in infected cells. Journal of Virology 67, 3159-3165.

Pratt, W.B., Morishima, Y., Murphy, M., Harrell, M., 2006. Chaperoning of glucocorticoid receptors. Handbook of Experimental Pharmacology, 111-138.

Prudovsky, I., Tarantini, F., Landriscina, M., Neivandt, D., Soldi, R., Kirov, A., Small, D., Kathir, K.M., Rajalingam, D., Kumar, T.K., 2008. Secretion without Golgi. J Cell Biochem 103, 1327-1343.

Rao, D.D., Vorhies, J.S., Senzer, N., Nemunaitis, J., 2009. siRNA vs. shRNA: similarities and differences. Advanced Drug Delivery Reviews 61, 746-759.

Ratajczak, T., Ward, B.K., Cluning, C., Allan, R.K., 2009. Cyclophilin 40: an Hsp90-cochaperone associated with apo-steroid receptors. The International Journal of Biochemistry & Cell Biology 41, 1652-1655.

Reynolds, A., Leake, D., Boese, Q., Scaringe, S., Marshall, W.S., Khvorova, A., 2004. Rational siRNA design for RNA interference. Nature Biotechnology 22, 326-330.

Ruiz, M.C., Cohen, J., Michelangeli, F., 2000. Role of Ca^{2+} in the replication and pathogenesis of rotavirus and other viral infections. Cell Calcium 28, 137-149.

Santos, N., Hoshino, Y., 2005. Global distribution of rotavirus serotypes/genotypes and its implication for the development and implementation of an effective rotavirus vaccine. Reviews in Medical Virology 15, 29-56.

Sarris, A.H., Harding, M.W., Jiang, T.R., Aftab, D., Handschumacher, R.E., 1992. Immunofluorescent localization and immunochemical determination of cyclophilin-A with specific rabbit antisera. Transplantation 54, 904-910.

Schroeder, M.E., 2009. Secondary structural and functional studies of rotavirus NSP4 and caveolin-1 peptide-peptide interactions. Thesis Texas A&M University, Department of Veterinary Pathobiology.

Silva-Ayala, D., Lopez, T., Gutierrez, M., Perrimon, N., Lopez, S., Arias, C.F., 2013. Genome-wide RNAi screen reveals a role for the ESCRT complex in rotavirus cell entry. Proceedings of the National Academy of Sciences of the United States of America 110, 10270-10275.

Silvestri, L.S., Tortorici, M.A., Vasquez-Del Carpio, R., Patton, J.T., 2005. Rotavirus glycoprotein NSP4 is a modulator of viral transcription in the infected cell. Journal of Virology 79, 15165-15174.

Spencer, E., Arias, M.L., 1981. In vitro transcription catalyzed by heat-treated human rotavirus. Journal of Virology 40, 1-10.

Staat, M.A., Rice, M.A., Donauer, S., Payne, D.C., Bresee, J.S., Mast, T.C., Curns, A.T., Cortese, M.M., Connelly, B., McNeal, M., Ward, R.L., Bernstein, D.I., Parashar, U.D., Salisbury, S., 2010. Estimating the rotavirus hospitalization disease burden and trends, using capture-recapture methods. The Pediatric Infectious Disease Journal 29, 1083-1086.

Storey, S.M., Gibbons, T.F., Williams, C.V., Parr, R.D., Schroeder, F., Ball, J.M., 2007. Full-length, glycosylated NSP4 is localized to plasma membrane caveolae by a novel raft isolation technique. Journal of Virology 81, 5472-5483.

Suguna, K., Rao, C.D., 2010. Rotavirus nonstructural proteins: a structural perspective. Current Science (00113891) 98, 352-359.

Tanaka, Y., Sato, Y., Sasaki, T., 2013. Suppression of coronavirus replication by cyclophilin inhibitors. Viruses 5, 1250-1260.

Tate, J.E., Burton, A.H., Boschi-Pinto, C., Steele, A.D., Duque, J., Parashar, U.D., 2012. 2008 estimate of worldwide rotavirus-associated mortality in children younger than 5 years before the introduction of universal rotavirus vaccination programmes: a systematic review and meta-analysis. Lancet Infect Dis 12, 136-141.

Taylor, J.A., Meyer, J.C., Legge, M.A., O'Brien, J.A., Street, J.E., Lord, V.J., Bergmann, C.C., Bellamy, A.R., 1992. Transient expression and mutational analysis of the rotavirus intracellular receptor: the C-terminal methionine residue is essential for ligand binding. Journal of Virology 66, 3566-3572.

Taylor, J.A., O'Brien, J.A., Yeager, M., 1996. The cytoplasmic tail of NSP4, the endoplasmic reticulum-localized non-structural glycoprotein of rotavirus, contains distinct virus binding and coiled coil domains. The EMBO Journal 15, 4469-4476.

Tian, P., 1995. The rotavirus nonstructural glycoprotein NSP4 mobilizes Ca^{2+} from the endoplasmic reticulum. Journal of Virology 69, 5763-5772.

Tian, P., Ball, J.M., Zeng, C.Q., Estes, M.K., 1996. The rotavirus nonstructural glycoprotein NSP4 possesses membrane destabilization activity. Journal of Virology 70, 6973-6981.

Tian, X., Zhao, C., Zhu, H., She, W., Zhang, J., Liu, J., Li, L., Zheng, S., Wen, Y.M., Xie, Y., 2010. Hepatitis B virus (HBV) surface antigen interacts with and promotes cyclophilin a secretion: possible link to pathogenesis of HBV infection. Journal of Virology 84, 3373-3381.

Torres-Flores, J.M., Silva-Ayala, D., Espinoza, M.A., Lopez, S., Arias, C.F., 2015. The tight junction protein JAM-A functions as coreceptor for rotavirus entry into MA104 cells. Virology 475, 172-178.

Trask, S.D., McDonald, S.M., Patton, J.T., 2012. Structural insights into the coupling of virion assembly and rotavirus replication. Nature Reviews Microbiology 10, 165-177.

Uittenbogaard, A., Everson, W.V., Matveev, S.V., Smart, E.J., 2002. Cholesteryl ester is transported from caveolae to internal membranes as part of a caveolin-annexin II lipid-protein complex. The Journal of Biological Chemistry 277, 4925-4931.

Uittenbogaard, A., Smart, E.J., 2000. Palmitoylation of caveolin-1 is required for cholesterol binding, chaperone complex formation, and rapid transport of cholesterol to caveolae. The Journal of Biological Chemistry 275, 25595-25599.

Uittenbogaard, A., Ying, Y., Smart, E.J., 1998. Characterization of a cytosolic heat-shock protein-caveolin chaperone complex. Involvement in cholesterol trafficking. The Journal of Biological Chemistry 273, 6525-6532.

Vidal, M., 1997. The Reverse Two-Hybrid System. Oxford University Press, New York, NY.

Vidal, M., Brachmann, R.K., Fattaey, A., Harlow, E., Boeke, J.D., 1996. Reverse two-hybrid and one-hybrid systems to detect dissociation of protein-protein and DNA-protein interactions. Proceedings of the National Academy of Sciences of the United States of America 93, 10315-10320.

Walker, J.M., 1996. The protein protocols handbook. Humana Press, Towota, N.J.

Walsh, C.T., Zydowsky, L.D., McKeon, F.D., 1992. Cyclosporin A, the cyclophilin class of peptidylprolyl isomerases, and blockade of T cell signal transduction. Journal of Biological Chemistry 267, 13115-13118.

Wines, B.D., Easterbrook-Smith, S.B., 1991. The Fab/c fragment of IgG produced by cleavage at cyanocysteine residues. Molecular Immunology 28, 855-863.

World Health Organization, 2009. Manual of rotavirus detection and characterization methods. World Health Organization, 1-146.

Xu, A., Bellamy, A.R., Taylor, J.A., 1998. BiP (GRP78) and endoplasmin (GRP94) are induced following rotavirus infection and bind transiently to an endoplasmic reticulum-localized virion component. Journal of Virology 72, 9865-9872.

Xu, A., Bellamy, A.R., Taylor, J.A., 2000. Immobilization of the early secretory pathway by a virus glycoprotein that binds to microtubules. The EMBO Journal 19, 6465-6474.

Yakshe, K.A., Franklin, Zachary D., Ball, Judith M. , 2015. Rotavirus: extraction and isolation of RNA, reassortant strains, and NSP4 protein. Current Protocols in Microbiology 37, 44.

Zambrano, J.L., Diaz, Y., Pena, F., Vizzi, E., Ruiz, M.C., Michelangeli, F., Liprandi, F., Ludert, J.E., 2008. Silencing of rotavirus NSP4 or VP7 expression reduces alterations in Ca2+ homeostasis induced by infection of cultured cells. Journal of Virology 82, 5815-5824.

Zambrano, J.L., Ettayebi, K., Maaty, W.S., Faunce, N.R., Bothner, B., Hardy, M.E., 2011. Rotavirus infection activates the UPR but modulates its activity. Virology Journal 8, 359.

Zhang, M., Schekman, R., 2013. Cell biology. Unconventional secretion, unconventional solutions. Science 340, 559-561.

Zhang, M., Zeng, C.Q., Morris, A.P., Estes, M.K., 2000. A functional NSP4 enterotoxin peptide secreted from rotavirus-infected cells. Journal of Virology 74, 11663-11670.

Zhu, C., Wang, X., Deinum, J., Huang, Z., Gao, J., Modjtahedi, N., Neagu, M.R., Nilsson, M., Eriksson, P.S., Hagberg, H., Luban, J., Kroemer, G., Blomgren, K., 2007. Cyclophilin A participates in the nuclear translocation of apoptosis-inducing factor in neurons after cerebral hypoxia-ischemia. The Journal of Experimental Medicine 204, 1741-1748.

Ziring, D., Tran, R., Edelstein, S., McDiarmid, S.V., Gajjar, N., Cortina, G., Vargas, J., Renz, J., Cherry, J.D., Krogstad, P., Miller, M., Busuttil, R.W., Farmer, D.G., 2005. Infectious enteritis after intestinal transplantation: incidence, timing, and outcome. Transplantation 79, 702-709.

APPENDIX A

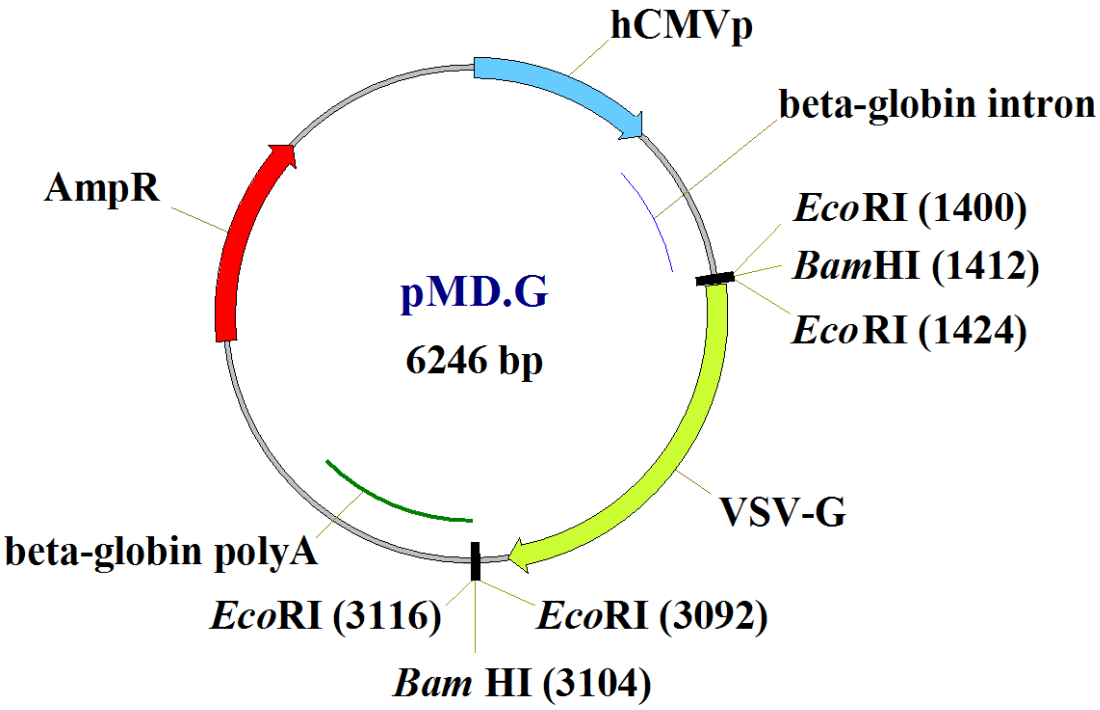

Figure A-1. Map of pMD.G. pMD.G is used in packaging of the pTripZ vector and expresses VSV-G for efficient entry into a wide variety of cell types. It possesses an Ampicillin resistance gene and an hCMV promoter for high expression of the VSV-G cDNA.

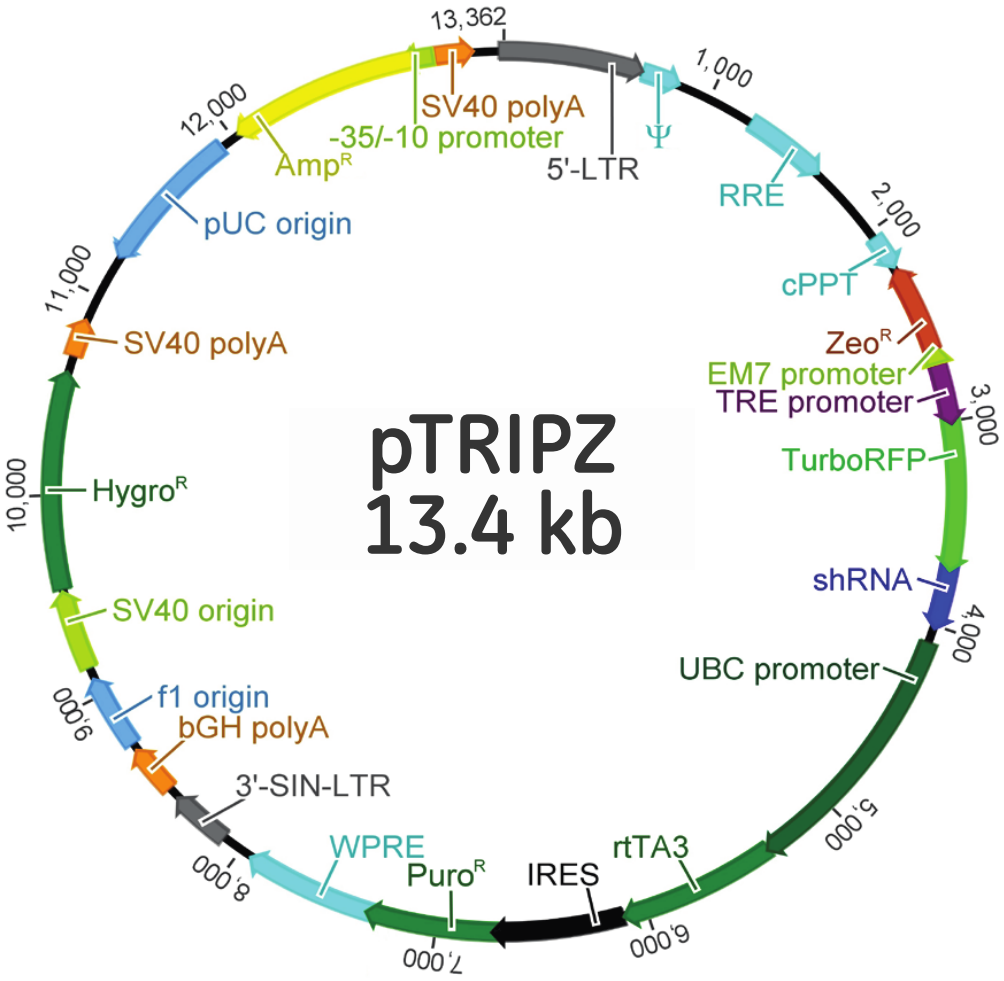

Figure A-2. Map of the pTripZ shRNA-expressing vector. The pTripZ contains several features that are listed in the table below (adapted from the pTripZ technical manual, Dharmacon).

Vector Element	Function
5' LTR	Long terminal repeat for incorporation into genomic DNA
3' SIN LTR	Self-inactivating long terminal repeat for incorporation into genomic DNA and to prevent lentiviral reproduction
RRE	Lentiviral packaging enhancer for production of lentivirus particles
TRE	Doxycycline inducible promoter
TurboRFP	Red fluorescent protein for analyzing induction and shRNA expression
shRNA	shRNA flanked by mir30 sequence for efficient gene knockdown
IRES	Internal ribosomal entry site for expression of rtTa3 and puromycin resistance genes
Zeocin Resistance	For bacterial selection inside the LTRs
Ampicillin Resistance	For bacterial selection outside the LTRs
Puromycin Resistance	For mammalian selection inside LTRs

Figure A-3. Map of pCMVΔR8.91. This vector contains the packaging genes for the production of lentivirus particles that will package the shRNA expressed within the LTRs of the shRNA insert. Additionally, it contains an Ampicillin resistance gene.